LIVING/CONTROLLED RADICAL POLYMERIZATION IN A CONTINUOUS TUBULAR REACTOR

by

THOMAS EDWARD ENRIGHT

A thesis submitted to the Department of Chemical Engineering

In conformity with the requirements for

the degree of Doctor of Philosophy

Queen's University

Kingston, Ontario, Canada

December, 2010

Abstract

Significant advances have been made in the understanding of living/controlled radical polymerization processes since their discovery in the early 1990's. These processes enable an unprecedented degree of control over polymer architecture that was previously not possible using conventional radical polymerization processes, and this has made possible the synthesis of many new and interesting materials. However, there has been only limited success in commercializing these new methods.

Recently there has been increased focus on the development of more industrially viable processes. Dispersed aqueous phase reactions have received much attention because these water-based processes have several technical, economic, and environmental benefits over the more common solution and bulk reactions that were originally developed. Likewise, there has been some investigation of using continuous reactors that have potential technical and economic benefits over the more commonly employed batch reactors.

This thesis presents an in-depth study that combines the three aforementioned technologies: living/controlled radical polymerization, dispersed phase aqueous reactions, and continuous reactors. Specifically, the system of interest is a nitroxide-mediated miniemulsion polymerization reaction in a continuous tubular reactor to produce polymer latex.

Design of the continuous tubular reactor is discussed in some detail with a focus on specific technical challenges that were faced in building a functional apparatus for this

system. Scoping experiments are described which identified a significant effect of temperature ramping rate that is critical to understand when moving to larger scale reactors for this system. The unexpected phenomenon of room temperature polymerization initiated by ascorbic acid is also described. There is demonstration for the first time that bulk and miniemulsion polymers can be produced in a tubular reactor under controlled nitroxide-mediated polymerization conditions, and copolymers can be produced. A detailed residence time distribution study for the tubular reactor is also shown, and several interesting phenomena are discussed that have implications on the practical operating conditions of the tubular reactor. This particular study makes it clear that one should experimentally verify the residence time distribution within a continuous system with the reactants of interest, and that model systems may not give an accurate picture of the real system.

Co-Authorship

Michael F. Cunningham (Queen's University) and Barkev Keoshkerian (Xerox Research Centre of Canada) were contributing co-authors of the following chapters in this thesis:

Chapter 5, externally published as: Enright, T. E.; Cunningham, M. F.; Keoshkerian, B. *Macromol. Rapid Commun.* **2005**, *26*, 221.

Chapter 6, externally published as: Enright, T. E.; Cunningham, M. F.; Keoshkerian, B. *Macromol. React. Eng.* **2010**, *4*, 186.

Acknowledgements

I would like to express my deepest gratitude to my supervisor Michael Cunningham for leading me along this road. He has been an inspirational mentor since the day I met him, and I thank him for the continued support and encouragement that he has shown over the years.

I also extend thanks to Xerox Research Centre of Canada for allowing me to pursue this dream and for their continued sponsorship. I am also indebted to my colleagues for their unwavering support and many helpful suggestions, particularly Barkev Keoshkerian who provided me with much insight along the way.

Most importantly I thank Rhonda, Jackson and Rachel who put up with my many absences (both figurative and literal) over this busy time. I could not have done this without their support, and to them this is dedicated.

Knowing is not enough; we must apply.

Willing is not enough; we must do.

- Johann Wolfgang von Goethe

Table of Contents

List of Figures

List of Tables

List of Schemes

Nomenclature

[C]	Concentration of component C
A	ATRP activator molecule or Cross-sectional area of tubular reactor
AA	Ascorbic acid
ATRP	Atom transfer radical polymerization
BPO	Benzoyl peroxide
C(t)	Concentration of tracer at time *t*
CRP	Controlled radical polymerization
CSA	Camphorsulfonic acid
CSTR	Continuous stirred tank reactor
D	Axial dispersion coefficient
D/uL	Vessel dispersion number
De	Dean number = Re*λ
$\mathbf{D_{eff}}$	Experimentally observed effective diffusion coefficient
DEPN (or SG1)	1-diethylphosphono-2, 2-dimethyl) propyl nitroxide
$d_{styrene}$; $d_{polystyrene}$	Density of styrene; Density of polystyrene
E or *E(t)*	Residence time distribution function
$\mathbf{E_{\theta,model}}$	Residence time distribution function for dispersion model
GC	Gas chromatography
GPC	Gel permeation chromatography

GSD	Graphical standard deviation
HPMA	2-hydroxypropyl methacrylate
$I^{\bullet}$	Initiator radical
I_2	Bimolecular initiator
K	Reversible activation equilibrium constant (k_{act}/k_{deact})
k_{act}	Activation rate constant for reversible activation
k_{deact}	Deactivation rate constant for reversible activation
k_{dim}	Rate constant for dimerization of styrene
k_{dis}	Alkoxyamine disproportionation rate constant
k_p	Propagation rate constant
k_{tc}	Termination by combination rate constant
k_{td}	Termination by disproportionation rate constant
L	Ligand, or Length of tubular reactor
λ	Ratio of tube diameter to coil diameter
L/CRP	Living/controlled radical polymerization
LRP	Living radical polymerization
M	Monomer
$M^{\bullet}$	Monomer radical
MADIX	Macromolecular Design via Interchange of Xanthates
MAH	Molecule assisted homolysis
MN or Mn	Number average molecular weight

Mt^z	Transition metal
MV	Mean volume diameter
MW or Mw	Weight average molecular weight
$N^\bullet$	Nitroxide radical controlling agent
nBA	n-butyl acrylate
N_c	Theoretical number of polymer chains
NMP	Nitroxide mediated polymerization
PDI	Polydispersity index of molecular weight distribution (MW/MN)
PEO	Poly(ethylene oxide)
P_n	Dead polymer chain
P-N	Dormant polymer chain (nitroxide-capped)
$P_n^\bullet$	Propagating polymer chain
PRE	Persistent radical effect
P-X	Dormant polymer chain (generic)
Q	Volumetric flow rate
θ	Dimensionless time (t/t_m)
QTRP	Quinone transfer radical polymerization
RAFT	Reversible addition-fragmentation chain transfer polymerization
Re	Reynolds number
RTD	Residence time distribution
σ	Variance of residence time distribution

SDBS	Dodecylbenzenesulfonic acid sodium salt
SFRP	Stable free radical polymerization
SFRP-BULK	Mixture of nitroxide-capped polymer in monomer
SME	Semi-miniemulsion
STY	Polystyrene latex sample
τ	Mean residence time in continuous reactor
TBEC	tert-butylperoxy 2-ethylhexyl carbonate
TEMPO	2,2,6,6-tetramethylpiperidine-1-oxyl
THF	Tetrahydrofuran
TIPNO	t-butylisopropylphenyl nitroxide
$t_{m,expt}$	Experimentally observed mean residence time
$t_{m,pf}$	Theoretical mean residence time for plug flow
u	Linear velocity of liquid in tubular reactor
V	Volume of tubular reactor
v	Volumetric flow rate
V_{active}	Active volume in tubular reactor
$V_{deadspace}$	Deadspace volume in tubular reactor
x	Monomer conversion
$X^{\bullet}$	Free radical polymerization controlling agent (generic)

Chapter 1

Introduction and Objectives

1.1 Introduction

In recent years, there has been a substantial amount of discovery and study in the area of living/controlled radical polymerization processes (L/CRP). These processes have enabled a significant degree of control over polymer architecture that is not possible using conventional free radical polymerization processes. Most research has focused on three primary mechanisms of L/CRP, namely nitroxide mediated polymerization (NMP) or stable free radical polymerization (SFRP), atom transfer radical polymerization (ATRP), and reversible addition-fragmentation chain transfer polymerization (RAFT). Each of these processes has its own unique attributes and drawbacks, and selection of a given process depends on the specific product that is desired.

Each of the three primary L/CRP processes has been commercialized to a limited degree, and one area of focus in recent years is development of more industrially viable process options. A significant amount of effort has been spent on developing dispersed phase aqueous L/CRP processes because these have technical, economical, and environmental advantages over bulk and solvent-based processes that were initially developed. There have also been some initial studies on the viability of using continuous reactors for L/CRP, because they also have several technical and economical advantages over batch reactors.

1.2 Objectives

The purpose of this research was to tie together the areas of L/CRP, dispersed phase aqueous polymerization, and continuous reactors. The specific system of study

was nitroxide mediated miniemulsion polymerization in a continuous tubular reactor. The primary goals were:

1. Design and build a viable continuous tubular reactor for this system.

2. Demonstrate that the initial bulk polymerization step and subsequent miniemulsion polymerization step could produce polymer under controlled conditions in the tubular reactor.

3. Demonstrate block copolymerization, an operation that is not possible using conventional radical polymerization, in the tubular reactor.

4. Develop an understanding of the residence time distribution in the reactor to help understand the operational requirements of the continuous system.

1.3 Thesis Outline

Chapters 2 and 3 present a literature overview of the areas that are of interest for this thesis. Chapter 2 gives a broad overview of L/CRP methods in general, along with details about how continuous reactor and microreactor systems have been used for these systems to date. Chapter 3 gives a more detailed overview of NMP reaction kinetics and how aqueous dispersed systems have been used for L/CRP.

Chapter 4 describes the development of the continuous tubular reactor and scoping experiments that were done to define reaction conditions that successfully achieved controlled radical polymerization. Details are given for the effect of ascorbic acid as a reaction accelerant, and the importance of temperature ramping profile for ensuring that controlled conditions are achieved. There is also some discussion about the unexpected phenomenon of room temperature polymerization due to initiation by ascorbic acid.

Chapter 5 describes a more detailed comparison of the differences between batch and continuous reactors for nitroxide-mediated miniemulsion homopolymerization, and chain extension is demonstrated for the first time in the continuous reactor. Chapter 6 develops the work further by demonstrating nitroxide-mediated bulk polymerization and copolymerization via miniemulsion for the first time in the tubular reactor.

Chapter 7 is a detailed residence time distribution (RTD) tracer study of the tubular reactor that compares the different flow profiles that are observed for an aqueous salt solution versus unreacted latex (monomer droplets in water) versus fully polymerized latex (polymer particles in water). Significant differences are observed between the systems and there is a comparison with the dispersed flow model.

Chapter 8 gives an overall summary of the work, and Chapter 9 makes some recommendations for future work that should be considered to advance the knowledge that was gained through this work.

1.4 Significant Contributions

This research was the first attempt at developing a continuous nitroxide-mediated polymerization process in miniemulsion, and it was successfully demonstrated. Bulk polymerization and miniemulsion polymerization of homopolymers and block copolymers were demonstrated under controlled polymerization conditions for the first time in a continuous tubular reactor. Several phenomena were identified during scoping experiments for which awareness will be critical as these NMP processes are moved towards commercialization (e.g., temperature ramp effect, ascorbic acid effect, surfactant effect). The residence time distribution study demonstrated a number of important

differences in the flow patterns for different systems, and this information will be important for long-term operation of the apparatus.

Chapter 2

Living Radical Polymerization

Published in Handbook of Micro Process Engineering (Chapter 3.1.2 in Volume 2)

2.1 Preface

The goal of this research was to develop a continuous tubular reactor for living/controlled radical polymerization processes. This chapter presents a background of the L/CRP field in general, along with some details about the three specific systems that have received the most research attention to date: nitroxide mediated polymerization (NMP), atom transfer radical polymerization (ATRP), and reversible addition-fragmentation chain transfer polymerization (RAFT). There is also an overview of initial work that has been done in adapting these systems to continuous reactor and microreactor systems.

2.2 Living Radical Polymerization

Free radical polymerization processes are used to produce approximately 50% of polymer products worldwide, and are therefore of great industrial importance.[1] However, many product properties cannot be controlled precisely using conventional free radical polymerization techniques due to the fundamental reaction mechanism. While general bulk properties of polymers can be controlled to some extent with conventional processes, structural control at the molecular level cannot be achieved.

Over the past fifteen years, new free radical polymerization techniques have been developed which enable significantly improved control over polymer structure at the molecular level. By using these techniques, customized polymeric materials can be produced which are not possible using conventional methods of the past. These new techniques are typically termed *living* or *controlled* free radical polymerization. There is some debate over the semantic use of these terms,[2,3] but the term 'living radical polymerization' (LRP) will be used here for simplicity.

The purpose of this discussion will be to give a basic overview of the living radical polymerization field, along with a survey of work that has been done specific to microreactors. First there will be a general definition of living polymerization processes and description of why they are useful. This will be followed by details of the mechanistic differences between conventional free radical polymerization and three general classes of living radical polymerization. A more detailed overview will then be given for the three most common living radical polymerization techniques: nitroxide mediated polymerization (NMP), atom transfer radical polymerization (ATRP), and reversible addition-fragmentation chain transfer (RAFT) polymerization. Finally, there

will be a discussion about living radical polymerization techniques that have been investigated in the microreactor field.

2.3 Living Polymerization

The term 'living' polymerization was coined by Szwarc in 1956 during development of the anionic polymerization process.[4,5] For a polymerization process to be considered living, it is necessary to suppress all chain breaking reactions such as termination and chain transfer.[6] In other words, a living polymer chain should always have the ability to grow further under appropriate circumstances.

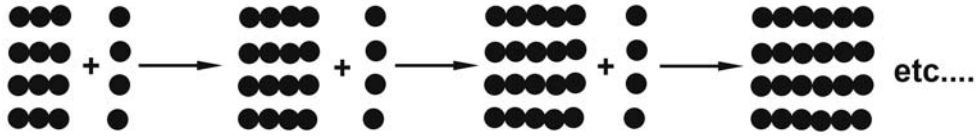

Figure 2-1. Idealized living polymerization: One monomer unit adds to the end of each polymer chain during each reaction step. Each black dot is a single monomer molecule and a string of black dots is a polymer chain.

An *ideal* living polymerization process would consist of the following conditions (see Figure 2-1):

1. Each polymer chain in a system starts growing at the same time.
2. A monomer unit is added to every polymer chain endgroup in the system during each growth (propagation) step of the reaction.
3. No unwanted side reactions occur.

In addition to the above, there are two further requirements for an ideal living polymerization process:

1. The reaction only stops when there is no more monomer present in the system, or when the conditions are adjusted to force the reaction to stop.

2. The polymerization reaction can be restarted at any time. One interesting aspect of this condition is that a block copolymer can be formed if a different monomer is added to the system before restarting the reaction (see Figure 2-2).

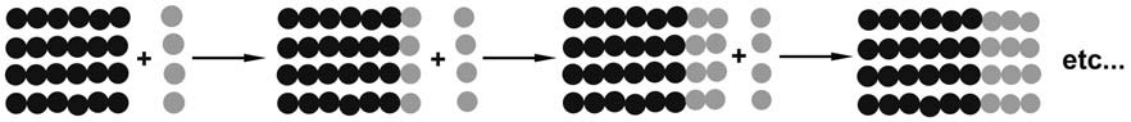

Figure 2-2. Idealized living polymerization: Reaction can be restarted using a different monomer, thus creating a block copolymer.

Note that the term 'living' arises from the fact that the polymer chain never 'dies' via a termination reaction or other side reaction, and it can start growing again if new monomer 'food' is added to the system.[4] In principle one should be able to stop and restart the process at will, and polymers can be tailored to any molecular weight and structure desired for a given application.[7] (see Figure 2-3 for examples).

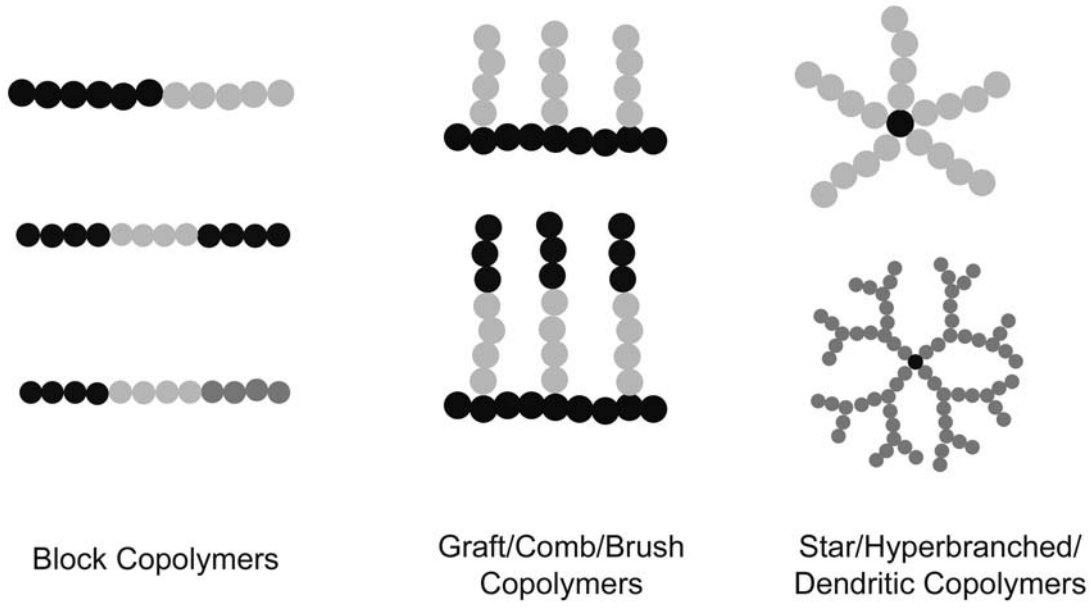

Figure 2-3. Examples of structures that have been prepared by LRP.

This idealized process is not possible using current methods, but there has been much progress towards approaching the ideal. Until the early 1990's, the most successful living polymerization work was in the area of anionic, cationic and group transfer polymerization processes.[8] However, while these techniques have been studied heavily in academia, they have not been implemented in industry as widely as conventional processes due to a number of drawbacks such as sensitivity to impurities, inability to react in the presence of water, and undesirably low reaction temperatures.[9] Free radical polymerization processes are not affected by these issues to the same degree, so there has always been interest in developing living polymerization techniques that work for free radical systems.

Studies as early as 1955 hinted at methods by which living radical polymerization (LRP) could be done,[10] and a number of studies over the years also suggested that it

should be feasible.[11] One of the first major breakthroughs occurred in 1982 when Otsu demonstrated the concept of the 'iniferter' (*ini*tiator-trans*fer* agent-*ter*minator) and first used the term *living* radical polymerization.[12-14] Some living polymer characteristics were demonstrated at this time (i.e., linear increase of molecular weight with time), but non-living characteristics were also observed (i.e., broad molecular weight distribution). Other promising results were shown in 1986, but only low molecular weight materials could be obtained.[15] Major breakthroughs began in the early 1990's when several techniques were demonstrated that clearly approached the concept of a living radical polymerization process. Since this time, three general LRP mechanisms have been developed into practical processes that improve control significantly compared to conventional processes. The next sections will describe how these new processes differ mechanistically from conventional free radical processes, and how they control the polymerization reaction.

2.4 Free Radical Polymerization Mechanism

All conventional free radical polymerization processes contain three basic mechanistic steps, along with various potential side reactions. Living radical polymerization processes share the first two steps, and aim to eliminate the third step and side reactions.

Step 1. *Initiation* (start of a polymer chain): An initiator molecule (I_2) decomposes into two primary free radicals ($2I^{\bullet}$). The primary free radicals can then react with the double bond of a monomer molecule (M). This forms the initiating radical which is the first unit in a polymer chain ($IM^{\bullet}$).

$I_2 \longrightarrow 2I^{\bullet}$

$I^{\bullet} + M \longrightarrow IM^{\bullet}$

Scheme 2-1. Initiation.

Step 2. *Propagation* (growth of a polymer chain): The initiating radical reacts with the double bond of another monomer molecule creating a new free radical, and this process repeats in a chain reaction to create a polymer chain (P_n).

$IM^{\bullet} + M \longrightarrow P_n^{\bullet}$

$P_n^{\bullet} + M \longrightarrow P_{n+1}^{\bullet}$ (Reaction repeats until termination occurs)

Scheme 2-2. Propagation.

Step 3. *Termination* (end of polymer chain growth): The radical endgroups of two growing chains meet and termination of the chains occur via a combination or disproportionation reaction.

$P_n^{\bullet} + P_m^{\bullet} \longrightarrow P_{n+m}$ (Combination)

OR

$P_n^{\bullet} + P_m^{\bullet} \longrightarrow P_n + P_m$ (Disproportionation)

Scheme 2-3. Termination.

This initiation/propagation/termination cycle occurs within about 0.1 to 1 second during a conventional free radical polymerization, resulting in a long polymer chain which cannot react further (i.e., it is 'dead').[16] Initiation occurs throughout the reaction,

so that new polymer chains are continually growing and 'dying' over the course of the reaction. The polymer chains grow to different lengths throughout the reaction depending on factors such as monomer concentration, termination mechanism, viscosity, etc. The molecular weight and polymer structure are also affected by number of side reactions, particularly chain transfer to monomer, solvent, or impurities. This overall process results in a mixture of polymer chains of varying length and structure (e.g., linear, branched, etc.).

There are two main changes to this mechanism that are required for an ideal living radical polymerization process.

1. Initiation should only occur at the start of the reaction so that all chains start growing at the same time. This is not achievable in practice, but it is approached by applying fast initiation at the start of the reaction and minimizing initiation throughout the remainder of the reaction.

2. Termination and side reactions must be eliminated completely. This is also not achievable in practice, but these reactions can be minimized to an acceptable level and this is the key to the different LRP mechanisms.

In practice, the termination reactions are minimized by reducing the overall concentration of free radicals in the system at any given time, which reduces the probability of two radicals meeting and terminating. In basic terms, this is done by placing removable 'caps' on the ends of the polymer chains. When the cap is present on the chain endgroup, the polymer is 'dormant' and it does not propagate. The cap can be released from the chain endgroup for a short period of time during which the polymer becomes 'active' and a few monomer units are added to the chain, then the cap is

replaced. Most of the polymer chains are in the dormant state at any given time during the reaction. Therefore, relatively few active chains are growing at a given time, which in turn results in a low probability that two chains will meet and terminate. The process of reverting between dormant and active states is termed 'reversible activation' or 'activation-deactivation', and it is the basis for all current successful living radical polymerization techniques. The type of cap, or *controlling agent*, that is used dictates the reversible activation mechanism that will occur.

2.5 Living Radical Polymerization General Mechanisms

There are three general classifications of living radical polymerization based on differences in the reversible activation reaction step described in the previous section. These three mechanisms are termed dissociation-combination, atom transfer, and degenerative chain transfer respectively.[17,18]

(1) Dissociation-Combination

$$P\text{-}X \rightleftharpoons P^{\bullet} + X^{\bullet}$$

Scheme 2-4. Reversible activation step for dissociation-combination reactions.

In this case, the controlling species (X) is released from the endgroup of the dormant polymer chain (P-X). When this occurs, the polymer becomes activated ($P^{\bullet}$), and the radical at the end of the polymer chain can propagate in the presence of monomer. The propagating radical readily deactivates back to the dormant state (P-X) by reacting with the controlling species ($X^{\bullet}$) after only a short period of propagation. Nitroxide-mediated polymerization (NMP) is the most extensively studied example of

dissociation-combination, and this will be discussed in more detail in the next section. Other examples of this mechanism involve the use of quinones[19] and boroxyls[20] as the controlling species.

(2) Atom Transfer

$$P\text{-}X + A \rightleftharpoons P^{\bullet} + AX$$

Scheme 2-5. Reversible activation step for atom transfer reactions.

This is similar to the dissociation-combination scheme, but the release and return of the controlling species (X) is catalyzed by an activator (A) which is a transition metal complex. The controlling species is a halide radical in the most common form of this reaction, atom transfer radical polymerization (ATRP), and this technique will be described further in section 2.7. It is also possible to use of a quinone instead of a halide as the controlling species in atom transfer reactions, in a process termed quinone transfer radical polymerization (QTRP).[21]

(3) Degenerative Chain Transfer

$$P\text{-}X + P'^{\bullet} \rightleftharpoons P^{\bullet} + P'X$$

Scheme 2-6. Reversible activation step for degenerative chain transfer reactions.

Degenerative transfer is the third general LRP mechanism. In this case, activation and deactivation occur as the controlling agent (X) is exchanged between an active and dormant polymer chain (P and P') thus activating one chain and deactivating the other. The most commonly studied type of this reaction is the reversible activation-

fragmentation transfer (RAFT) method, which will be described in more detail in section 2.8 along with a variant that has been named MADIX. Other examples of degenerative chain transfer include the use of controlling agents such as1,1-diphenylethylene (DPE)[22], alkyl iodides,[23-25] and organotellurium (TERP) and organostibine (STBP).[26]

The next three sections will describe in more detail the three most common examples of the above general mechanisms.

2.6 Nitroxide-Mediated Polymerization

Since its discovery in 1993,[27] nitroxide mediated polymerization (NMP) has been the most extensively studied technique from the dissociation-combination class of LRP mechanisms. This method is also commonly termed *stable free radical polymerization* (SFRP). NMP reactions are distinguished by the use of stable free radical nitroxide molecules ($N^{\bullet}$) as the controlling agent (e.g., 2,2,6,6-tetramethylpiperidine-1-oxyl (TEMPO), (1-diethylphosphono-2, 2-dimethyl) propyl nitroxide (DEPN), etc.):

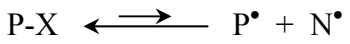

Scheme 2-7. Reversible activation step for NMP reactions.

Many different nitroxide molecules can be used successfully for NMP reactions, and the reaction conditions and kinetics have been studied extensively.[28] Nitroxide selection is important in determining the specific conditions under which the NMP reaction will control the polymerization successfully.[29] Numerous tailored structures can be prepared using the NMP method, and general strategies for achieving various structures have been developed.[30]

NMP reactions are not usually done by simply adding a nitroxide molecule to a conventional free radical polymerization formulation and running under conventional conditions. Usually, NMP reactions are run at elevated temperatures (e.g., 115-135°C), compared to conventional systems which are done at temperatures well below 100°C. Progress has been made in this area though, and controlled NMP reactions have been demonstrated below 100°C by using nitroxides that have been designed for lower temperature reactions.[31]

Most polymerization schemes can easily be performed using NMP (e.g., bulk, solution, miniemulsion, etc.), with a notable exception being emulsion polymerization. In fact, none of the LRP techniques are easily done via emulsion polymerization, and it is common to observe colloidal instability and loss of polymerization control in all cases. The general cause for these problems involves mass transfer limitations of the controlling species which are usually not soluble in water, and recent reviews describe in detail the mechanisms that cause these problems.[32-35] However, some recent progress has been made in developing emulsion systems for NMP reactions, typically by using water soluble nitroxides.[36,37]

NMP is somewhat limited in the selection of monomers that can be polymerized under controlled conditions compared to the other LRP techniques. Most work to date has been done in the area of styrene, acrylates, and their copolymers. A number of other monomers have been demonstrated, but there are some monomers that cannot be easily polymerized controllably by NMP, notably methacrylates. However, there has been some recent progress in preparing copolymers of styrene with methyl methacrylate[38,39] and butyl methacrylate,[40] and research remains active in this area.

2.7 Atom Transfer Radical Polymerization

In terms of the atom transfer reversible activation mechanism, the most actively studied method is *atom transfer radical polymerization* (ATRP) which was first demonstrated in 1995.[41-43] ATRP reactions use a halogenated initiator (e.g., alkyl halide) to start the polymerization and the halide becomes the removable controlling agent on the polymer chain endgroup. A transition metal complex is present in the formulation to mediate the removal of the halide radical from the polymer chain. The general atom transfer reversible activation scheme shown previously can be represented in more detail for ATRP by the following reaction:

$$P\text{-}X + Mt^{z}L \rightleftharpoons P^{\bullet} + X\,Mt^{z+1}L$$

Scheme 2-8. Reversible activation step for ATRP reactions.

In this case, X is a halide, Mt^{z} is a transition metal ion in oxidation state z, and L is a ligand that is complexed with the metal to impart solubility in the polymerization medium. Numerous transition metals, halide initiators, and ligands can be used to facilitate ATRP reactions, and the reaction conditions are more similar to conventional systems than in NMP reactions, particularly in terms of reaction temperature.[44,45] Similar to NMP however, ATRP reactions cannot be done easily in emulsion polymerization systems, although specialized techniques have been developed using modified emulsion methods.[46,47]

Monomer selection for ATRP reactions is somewhat more flexible than with NMP reactions. Specifically, methacrylate monomers are significantly easier to

polymerize, and homopolymers can be synthesized readily.[48] However, polymerization of protic monomers such as acrylic acid can be problematic.[49]

One of the primary drawbacks of ATRP involves residual catalysts in the final product which can be toxic and/or can cause discoloration issues. However, recent progress has been made in this area through several different strategies such as improving catalyst removal and recycling techniques, and reduction of catalyst concentration by improving activity.[50]

2.8 Reversible Addition-Fragmentation Chain Transfer

Reversible addition-fragmentation chain transfer (RAFT) polymerization is the third LRP method which has been developed to a relatively mature state since its first demonstration in 1998.[51] RAFT is a specialized case of the degenerative transfer LRP mechanism in which the controlling agent (X) is a thiocarbonylthio molecule (e.g., dithioesters, dithiocarbamates, trithiocarbonates, etc.).

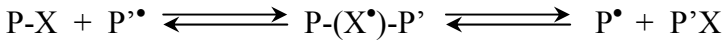

Scheme 2-9. Reversible activation step for RAFT reactions.

The generic structure for thiocarbonylthio RAFT agents is Z-C(=S)SR, where C and S are carbon and sulphur molecules respectively, Z is a functional group which dictates the reactive properties of the agent, and R is the free radical leaving group (a polymer chain once the reaction is up and running). Numerous different initiators and controlling agents can be used for RAFT reactions, and the reaction conditions are similar to those used for conventional systems.[52,53] One specific subclass of RAFT is

Macromolecular Design via Interchange of Xanthates (MADIX), where the controlling agent is a xanthate molecule.[54]

Similar to NMP and ATRP, emulsion polymerization reactions are challenging for RAFT systems. Recently however, techniques have been developed that enable this type of reaction.[55-59]

2.9 NMP, ATRP, and RAFT Summary

NMP, ATRP, and RAFT currently are the most commercially promising LRP techniques, and many of the fundamental kinetic mechanisms and issues have been elucidated.[60-66] These processes are now at the stage where companies are actively pursuing commercial applications and building larger scale production capabilities.[67] Each of the processes have certain advantages and limitations which must be considered when choosing which method is best for a particular application.[68] Recent demonstrations have shown that it is useful to use various combinations of NMP, ATRP, and RAFT reactions to capitalize on the specific advantages of each process.[69-72]

2.10 Living Radical Polymerization in Tubular Reactors

Most of the foundation research for LRP reactions has been done using batch processes. As development of these methods progresses towards commercialization, some scoping work has been done to investigate using continuous reactors which could offer some economic benefits. A number of these studies have been done in continuous tubular reactors which approach the size scale of microreactors.

Homogeneous bulk ATRP of methyl methacrylate homopolymer and block copolymers can be done with some success in a continuous packed bed tubular reactor

using a supported catalyst.[73-75] The metal catalyst can be adsorbed onto the silica gel column packing material instead of dissolving the catalyst in the bulk of the reaction medium. Some control can be achieved, but it is not as effective as more typical reactions using soluble catalysts. This is typical of ATRP systems that use supported catalysts, and it is attributed to inefficient reaction of the propagating radicals with the supported deactivator.[76] Also, it has been speculated that the activation/deactivation reaction does not actually occur at the supported catalyst site, but rather occurs with a trace amount of free catalyst that is present in the system.[77]

RAFT miniemulsion reactions can be done successfully in a continuous tubular reactor.[78,79] In the reported experiments, the tubing inner diameter was 1.6 mm, which is slightly larger than the typical microreactor size regime. Stable latexes can be produced in the tubular reactor and the polymerization exhibits living nature. However, the tubular reactor produces polymer with slightly higher molecular weight distribution than comparable samples produced in a batch reactor. This is attributed to back-mixing or axial dispersion effects in the tubular reactor that would broaden the residence time distribution of particles within the reactor.

Nitroxide mediated miniemulsion polymerization reactions can also be done successfully in a tubular reactor.[80] The demonstrated case used a tubular reactor with an inner diameter of 2 mm and a length of 170 m. Samples prepared in the tubular reactor are comparable to those made in a batch reactor in terms of kinetics and molecular weight characteristics.

2.11 Living Radical Polymerization in Microreactors

A fairly limited number of studies have been done to date using LRP reactions in microreactors, but it seems that interest in this area is starting to grow.

Before discussing LRP reactions *within* microreactors, it is interesting to point out that LRP methods can be used to *fabricate* microfluidic devices. Surface-bound iniferters can be used to graft polymers onto surfaces in directed micropatterns using a degenerative transfer living radical polymerization method.[81-83] This method can be used to pattern and build microfluidic devices that have varying grafted functionalities on the surface. Different physical and chemical properties can therefore be patterned on the surface, such as varying hydrophobicity. These devices have been demonstrated for uses such as direction of fluid flow, and surface-assisted cell patterning applications.[84] The same technique can be used in conjunction with a salt leaching process to build macroporous polymer networks within microfluidic devices. These porous networks can be used for applications such as static mixers, high surface-to-volume reactors, and rapidly responding hydrogel valves.[85]

Several recent studies have demonstrated ATRP reactions within microfluidic devices. An initial study demonstrates the use of a thiolene polymer based reactor with rectangular microchannels (500μm X 600μm).[86] The device consists of two inlet channels, an active mixing chamber containing a magnetic stir bar, and one outlet channel. Homopolymerization of 2-hydroxypropyl methacrylate (HPMA) by ATRP was demonstrated in this device, and it was shown that kinetics and product properties were similar to experiments done in a batch reactor. This technique provides a fast way of screening various ATRP reaction conditions while using a minimum of raw materials.

The above study was expanded to investigate block copolymerization via ATRP in a similar device containing three inlet channels.[87] Block copolymers of poly(ethylene oxide-block-2-hydroxypropyl methacrylate) (PEO-b-PHPMA) were successfully demonstrated with varying block lengths. This technique provides a rapid method for screening various block copolymer compositions.

ATRP can also be used to graft polymer chains onto surfaces within microchannels.[88] The surface of a microreactor channel can be functionalized with the ATRP initiator, then polymer grafts form and grow from the surface initiator sites as reactants flow through the reactor. Gradients form based on the exposure time to reactants, with the longest grafts at the inlet of the reactor and shortest grafts at the outlet. This demonstrates the unique topologies that can be built within devices using these techniques.

Initial work with NMP reactions in microreactors has shown some promise for product improvements due to the improved heat transfer characteristics of the reactor. It is well known that molecular weight of polymers is affected by the reaction temperature. This can be problematic when exothermic polymerization reactions cause the temperature within the reactor to drift, thus causing deviations from the desired molecular weight. Since microreactors improve heat removal due to the large surface-to-volume ratio, they should theoretically enable improvements in molecular weight control for exothermic polymerization reactions. Living radical polymerization of n-butyl acrylate in a microtube reactor of 900 μm inner diameter does indeed show significantly narrower polydispersity than comparable reactions in a batch reactor.[89] Similar experiments with

styrene do not show the same degree of polydispersity improvement which is expected since it is significantly less exothermic.

Micromixers in conjunction with serial microreactors can also be used effectively for LRP reactions, particularly for mixing viscous living polymer melts with non-viscous monomer for block copolymer production. For example, poly(n-butyl acrylate) can be synthesized in a microtube reactor via a NMP reaction, then the viscous homopolymer melt can be efficiently mixed with low viscosity styrene monomer via a micromixer[90]. This can then be followed by NMP of the styrene onto the poly(n-butyl acrylate) chains in a second microtube reactor, thus creating a block copolymer. This technique gives narrower molecular weight distribution product than comparable batch reactions.

2.12 Conclusions

Living radical polymerization has seen much research activity over the past fifteen years, and it has reached the point where commercialization activities are in progress. The fundamental mechanisms of three different LRP techniques (NMP, ATRP, and RAFT) are well understood, and many different unique materials can be prepared using these methods. While these three processes are developed to the commercial scale, newer LRP techniques are being discovered and investigated in the hopes of developing even better processes and materials.

The use of LRP methods in the area of microprocessing and microreactors is in the very early stages. It has been shown that LRP techniques can be used to fabricate unique microreactor devices, and controlled structures can be grown within microreactors. Also, microreactors have been demonstrated as an interesting tool for rapid screening of different LRP structures such as block copolymers. Finally, there has

been some indication that the improved heat transfer characteristics of microreactors can enable a further improvement in polymerization control for LRP reaction, particularly for more exothermic reactions.

Overall, the combined area of living radical polymerization and microreactors remains a fairly wide open field. Presumably more activity will be seen over the next few years and into the future as microreactor technology is introduced into more LRP-based research groups and the inherent benefits of this technology become better known.

2.13 References

1. Studer, A.; Schulte, T. *The Chemical Record* **2005**, *5*, 27.
2. Darling, T. R.; Davis, T. P.; Fryd, M.; Gridnev, A. A.; Haddleton, D. M.; Ittel, S. D.; Matheson Jr., R. R.; Moad, G.; Rizzardo, E. *J. Polym. Sci., Part A: Polym. Chem.* **2000**, *38*, 1706.
3. Szwarc, M. *J. Polym. Sci., Part A: Polym. Chem.* **2000**, *38*, 1710.
4. Szwarc, M.; Levy, M.; Milkovich, R. M. J. *J. Am. Chem. Soc.* **1956**, *78*, 2656.
5. Szwarc, M. *Nature* **1956**, *178*, 1168.
6. Matyjaszewski, K. *Macromolecules* **1993**, *26*, 1787.
7. Matyjaszewski, K. *Prog. Polym. Sci.* **2005**, *30*, 858.
8. Rudin, A. *The Elements of Polymer Science and Engineering*, 2nd ed., Academic Press, San Diego, **1999**, pp. 301-333.
9. Webster, O. W. *Science* **1991**, *251*, 887.
10. Ferington, T. E.; Tobolsky, A. V. *J. Am. Chem. Soc.* **1955**, *77*, 4510.
11. Matyzaszewski, K. *ACS Symp. Ser*. **1998**, *685*, 13.

12. Otsu, T.; Yoshida, M. *Makromol. Chem. Rapid Commun.* **1982**, *3*, 127.

13. Otsu, T.; Yoshida, M.; Tazaki, T. *Makromol. Chem. Rapid Commun.* **1982**, *3*, 133.

14. Otsu, T. *J. Polym. Sci., Part A: Polym. Chem.* **2000**, *38*, 2121.

15. Solomon, D. H.; Rizzardo, E.; Cacioli, P. *U.S. Patent 4,581,429* **1986**, assigned to Commonwealth Scientific and Industrial Research Organization.

16. Moad, G.; Solomon, D. H. *The Chemistry of Radical Polymerization, 2nd Edition*; Elsevier Science: Oxford, 2006.

17. Fukuda, T.; Yoshikawa, C.; Kwak, Y.; Goto, A.; Tsuji, Y. *ACS Symp. Ser*. **2003**, *854*, 24.

18. Fukuda, T.; Goto, A.; Tsuji Y. in *Handbook of Radical Polymerization* (Eds.: K. Matyjaszewski, T. P Davis); John Wiley and Sons: New Jersey, 2002, p. 409.

19. Debuigne, A.; Caille, J.-R.; Jerome, R. *J. Polym. Sci., Part A: Polym. Chem.* **2006**, *44*, 1233.

20. Chung, T. C. M. Boroxyl-Mediated Living Radical Polymerization and Applications, *Polymer News* **2003**, *28*, 238.

21. Caille, J.-R.; Debuigne, A.; Jerome, R. *Macromolecules* **2005**, *38*, 27.

22. Wieland, P. C.; Nuyken, O.; Heischkel, Y.; Raether, B.; Strissel, C. *ACS Symp. Ser*. **2003**, *854*, 619.

23. Goto, A.; Ohno, K.; Fukuda, T. *Macromolecules* **1998**, *31*, 2809.

24. David, G.; Boyer, C.; Tonnar, J.; Ameduri, B.; Lacroix-Desmazes, P.; Boutevin, B. *Chem. Rev.* **2006**, *106*, 3936.

25. Matyjaszewski, K.; Gaynor, S.; Wang, J.-S. *Macromolecules* **1995**, *28*, 2093.

26. Yamago, S. *J. Polym. Sci. Part A: Polym. Chem.* **2006**, *44*, 1.

27. Georges, M. K.; Veregin, R. P. N.; Kazmaier, P. M.; Hamer, G. K. *Macromolecules* **1993**, *26*, 2987.

28. Hawker, C. J.; Bosman, A. W.; Harth, E. *Chem. Rev.* **2001**, 101, 3661.

29. Nilsen, A.; Braslau, R. *J. Polym. Sci., Part A: Polym. Chem.* **2006**, *44*, 697.

30. Malmstrom, E. E.; Hawker, C. J. *Macromol. Chem. Phys.* **1998**, *199*, 923.

31. Farcet, C.; Lansalot, M.; Charleux, B.; Pirri, R.; Vairon, J. P. *Macromolecules* **2000**, *33*, 8559.

32. Charmot, D.; Corpart, P.; Adam, H.; Zard, S. Z.; Biadatti, T.; Bouhadir, G. *Macromol. Symp.* **2000**, *150*, 23.

33. Cunningham, M. F. *Prog. Polym. Sci.* **2002**, *27*, 1039.

34. Save, M.; Guillaneuf, Y.; Gilbert, R. C. *Aust. J. Chem.* **2006**, *59*, 693.

35. Cunningham, M.F. *C. R. Chimie* **2004**, *6*, 1351.

36. Nicolas, J.; Charleux, B.; Guerret, O.; Magnet, S. *Macromolecules* **2005**, *38*, 9963.

37. Nicolas, J.; Charleux, B.; Magnet, S. *J. Polym. Sci., Part A: Polym. Chem.* **2006**, *44*, 4142.

38. Charleux, B.; Nicolas, J.; Guerret, O. *Macromolecules* **2005**, *38*, 5485.

39. Nicolas, J.; Dire, C.; Mueller, L.; Belleney, J.; Charleux, B.; Marque, S. R. A.; Bertin, D.; Magnet, S.; Couvreur, L. *Macromolecules* **2006**, *39*, 8274.

40. Burguiere, C.; Dourges, M.-A.; Charleux, B.; Vairon, J.-P. *Macromolecules* **1999**, *32*, 3883.

41. Wang, J.-S.; Matyjaszewski, K. *J. Am. Chem. Soc.* **1995**, *117*, 5614.

42. Wang, J.-S.; Matyjaszewski, K. *Macromolecules* **1995**, *28*, 7901.

43. Kato, M.; Kamigaito, M.; Sawamoto, M.; Higashimura, T. *Macromolecules* **1995**, *28*, 1721.

44. Matyjaszewski, K.; Xia, J. *Chem. Rev.* **2001**, *101*, 2921.

45. Kamigaito, M.; Ando, T.; Sawamoto, M. *Chem. Rev.* **2001**, *101*, 3689.

46. Chan-Seng, D.; Georges, M. K. *J. Polym. Sci., Part A: Polym. Chem.* **2006**, *44*, 4027.

47. Min, K.; Gao, H.; Matyjaszewski, K. *J. Am. Chem. Soc.* **2006**, *128*, 10521.

48. Mittal, A.; Baskaran, D.; Sivaram, S. *Macromol. Symp.* **2006**, *240*, 238.

49. Storey, R. F.; Scheuer, A. D.; Achord, B. C. *Polymer* **2005**, *46*, 2141-2152.

50. Tsarevsky, N. Y.; Matyjaszewski, K. *J. Polym. Sci., Part A: Polym. Chem.* **2006**, *44*, 5098.

51. Chiefari, J.; Chong, Y. K.; Ercole, F.; Krstina, J.; Jeffery, J.; Le, T. P. T.; Mayadunne, R.T.A.; Meijs, G. F.; Moad, C. L.; Moad, G.; Rizzardo, E.; Thang, S. H. *Macromolecules* **1998**, *31*, 5559.

52. Moad, G.; Rizzardo, E.; Thang, S. H. *Aust. J. Chem.* **2005**, *58*, 379.

53. Moad, G.; Rizzardo, E.; Thang, S. H. *Aust. J. Chem.* **2006**, *59*, 669.

54. Charmot, D.; Corpart, P.; Adam, H.; Zard, S. Z.; Biadatti, T.; Bouhadir, G. *Macromol. Symp.* **2000**, *150*, 23.

55. Prescott, S. W.; Ballard, M. J.; Rizzardo, E.; Gilbert, R. G. *Macromolecules* **2002**, *35*, 5417.

56. Apostolovic, B; F. Quattrini, F.; Butte, A.; Storti, G.; Morbidelli, M. *Helvetica Chimica Acta.* **2006**, *89*, 1641.

57. Urbani, C. N.; Nguyen, H. N.; Monteiro, M. J. *Aust. J. Chem.* **2006**, *59*, 728.

58. Freal-Saison, S.; Save, M.; Bui, C.; Charleux, B.; Magnet, S. *Macromolecules* **2006**, *39*, 8632.

59. Nozari, S.; Tauer, K.; Ali, A. M. I. *Macromolecules* **2005** , *38*, 10449.

60. Johnson, C. H. J.; Moad, G.; Solomon, D. H.; Spurling, T. H.; Vearing, D. J. *Aust. J. Chem.* **1990**, *43*, 1215.

61. Matyjaszewski, K.; Patten, T. E.; Xia, J. *J. Am. Chem. Soc.* **1997**, *119*, 674.

62. Shi, A.-C.; Georges, M. K.; Mahabadi, H. K. *Polym. React. Eng.* **1999**, *7*, 283.

63. Butte, A.; Storti, G.; Morbidelli, M. *Chem. Eng. Sci.* **1999**, *54*, 3225.

64. Fukuda, T.; Goto, A.; Ohno, K. *Macromol. Rapid Commun.* **2000**, *21*, 151.

65. Fischer, H. *Chem. Rev.* **2001**, *101*, 3581.

66. Goto, A.; Fukuda, T. *Prog. Polym. Sci.* **2004**, *29*, 329.

67. Matyjaszewski, K.; Spanswick, J. *Materials Today* **2005**, *8*,26.

68. Matyjaszewski, K. in *Handbook of Radical Polymerization* (Eds: K. Matyjaszewski, T. P. Davis); John Wiley and Sons: New Jersey, **2002**, pp. 397-399.

69. Higaki, Y.; Otsuka, H.; Takahara, A. *Macromolecules* **2004**, *37*, 1696.

70. Durmaz, H.; Karatas, F.; Tunca, U.; Hizal, G. *J. Polym. Sci., Part A: Polym. Chem.* **2006**, *44*, 499.

71. Zhao, B. *Polymer* **2003**, *44*, 4079.

72. Percec, V.; Barboiu, B.; Grigoras, C.; Bera, T. K. *J. Am. Chem. Soc.* **2003**, *125*, 6503.

73. Shen, Y.; Zhu, S.; Pelton, R. *Macromol. Rapid Commun*. **2000**, *21*, 956.

74. Shen, Y.; Zhu, S.; Zeng, F.; Pelton, R. H. *Macromolecules* **2000**, *33*, 5427.

75. Shen, Y.; Zhu, S. *AIChE J.* **2002**, *48*, 2609.

76. Tsarevsky, N. Y.; Matyjaszewski, K. *J. Polym. Sci. Part A: Polym. Chem.* **2006**, *44*, 5098.

77. Faucher, S.; Zhu, S. *Macromolecules* **2006**, *39*, 4690.

78. Russum, J. P.; Jones, C. W.; Schork, F. J. *Macromol. Rapid Commun*. **2004**, *25*, 1064.

79. Russum, J. P.; Jones, C. W.; Schork, F. J. *Ind. Eng. Chem. Res.* **2006**, *44*, 2484.

80. Enright, T.; Cunningham, M.F.; Keoshkerian, B. *Macromol. Rapid Commun.* **2005**, *26*, 221.

81. Luo, N.; Hutchinson, J. B.; Anseth, K. S.; Bowman, C. N. *J. Polym. Sci. Part A: Polym. Chem.* **2002**, *40*, 1885.

82. Luo, N.; Metters, A. T.; Hutchinson, J. B.; Bowman, C. N.; Anseth, K. S. *Macromolecules* **2003**, *36*, 6739.

83. Hutchison, J. B.; Haraldsson, K. T.; Good, B. T.; Sebra, R. P.; Luo, N.; Anseth, K. S.; Bowman, C. N. *Lab on a Chip* **2004**, *4*, 658.

84. Sebra, R. P.; Anseth, K. S. *J. Polym. Sci. Part A: Polym. Chem.* **2006**, *44*, 1404.

85. Simms, H. M.; Brotherton, C. M.; Good, B. T.; Davis, R. H.; Anseth, K. S.; Bowman, C. N. *Lab on a Chip* **2005**, *5*, 151.

86. Wu, T.; Mei, Y.; Cabral, J. T.; Xu, C.; Beers, K. L. *J. Am. Chem. Soc*. **2004**, *126*, 9880.

87. Wu, T.; Mei, Y.; Xu, C.; Byrd, H. C. M.; Beers, K. L. *Macromol. Rapid Commun.* **2005**, *26*, 1037.

88. Xu., C.; Wu, T.; Drain, C.M.; Batteas, J.D.; Beers, K.L. *Macromolecules* **2005**, *38*, 6.

89. Rosenfeld, C.; Serra, C.; Brochon, C.; Hadziioannou, G. *Chem. Eng. Sci*. **2007**, *62*, 5245.

90. Rosenfeld, C.; Serra , C.; Brochon C.; Hadziioannou, G. *Chem. Eng. J*. **2008**, *135S*, S242-S246.

Chapter 3

Nitroxide Mediated Polymerization and Aqueous Dispersed Systems

3.1 Preface

The previous chapter presented a broad overview of L/CRP research with some additional detail given to NMP, ATRP, and RAFT, plus an overview of work that has been done with these systems in continuous and microreactor systems. This study was interested specifically in adapting an aqueous-based NMP system into a continuous tubular reactor. To set the stage for this work, this chapter presents a more detailed background of work that has been done specific to NMP reactions along with an overview of research that has been done to date in L/CRP reactions done in aqueous dispersed systems.

3.2 Nitroxide Mediated Polymerization

3.2.1 Chemical Reaction and Kinetics Overview

Knowledge of kinetics is essential for all chemical processes. Well defined rate equations and rate constants enable process simulation which can predict product properties under various reaction conditions. Determination of optimum process conditions is also aided by such knowledge. Kinetics of homogeneous NMP systems have been studied extensively and the following is a brief summary of the knowledge to date.

All of the reaction steps in NMP are similar to those found in conventional free radical polymerization, with the inclusion of the reversible activation step described in the previous chapter. Therefore, the reactions shown in Scheme 3-1 must be considered in the NMP process.[1]

Reaction Step	Reaction Detail	Reaction Rate Expression
	$I \xrightarrow[k_d]{\Delta} 2R_0^{\bullet}$	Initiator Decomposition: $k_d[I]$
Initiation	$R_0^{\bullet} + M \xrightarrow[k_i]{} P_1^{\bullet}$	Primary Radical Initiation: $k_i[R_0^{\bullet}][M]$
	$3M \xrightarrow[k_{thermal}]{} M_2^{\bullet} + M_1^{\bullet}$	Thermal Initiation: $k_{thermal}[M]^3$
Reversible Activation	$NP_i \underset{k_{deact}}{\overset{k_{act}}{\rightleftharpoons}} N^{\bullet} + P_i^{\bullet}$	Forward: $k_{act}[NP]$ Reverse: $k_{deact}[N^{\bullet}][P^{\bullet}]$ $\quad K = k_{act}/k_{deact}$
Propagation	$P_i^{\bullet} + M \xrightarrow{k_p} P_{i+1}^{\bullet}$	$k_p[P^{\bullet}][M]$
Termination	$P_i^{\bullet} + P_j^{\bullet} \xrightarrow{k_{tc}} D_{i+j}$	Combination: $k_{tc}[P^{\bullet}]^2$
	$P_i^{\bullet} + P_j^{\bullet} \xrightarrow{k_{td}} D_i + D_j$	Disproportionation: $k_{td}[P^{\bullet}]^2$
	$NP_i \xrightarrow{k_{dis}} NH + D_i$	Alkoxyamine Disproportionation: $k_{dis}[NP]$
		where $[P^{\bullet}] = \sum_{i=0}^{\infty}[P_i^{\bullet}]$ and $[NP] = \sum_{i=0}^{\infty}[NP_i]$

Scheme 3-1. Nitroxide Mediated Polymerization

A number of detailed models have been developed to simulate the NMP reaction under different conditions. Kinetic models, simulation and parameter estimates have been extensively developed for styrene NMP reaction systems,[2-7] and rigorous experimental studies have been done recently for the styrene-BPO-TEMPO reaction system to create a parameter database over the full conversion range.[8,9]

3.2.2 Initiation

The first two reactions shown in Scheme 3-1 exemplify a standard *bimolecular* initiation process in which I is an initiator such as a peroxide or azo compound. This initiator decomposes into two primary radicals (R_0) by thermal or photochemical stimulus, or by a redox process. The primary radical can then react with monomer (M) to form a unimer radical ($P_1^{\bullet}$). Up until this point, the process is equivalent to a conventional free radical polymerization process and the initiation rate constants (k_d and k_i) will depend on the type of initiator used and reaction conditions. Values for these rate constants are readily available in the literature.[10] In NMP processes, the unimer radical ($P_1^{\bullet}$) ideally is capped next by the nitroxide control agent ($N^{\bullet}$) to create a dormant molecule (NP_1), and this is the point at which the controlled radical process mechanism diverges from a conventional radical system.

In an ideal living process, the unimer radicals should all be formed at the same instant, and each of these radicals then should be capped with a nitroxide radical. This ensures that all polymer chains are formed at the same time, and they will grow at the same rate to give a monodisperse molecular weight distribution. In reality, initiation occurs over a period of time until the initiator has been fully consumed, so this leads to some polymer chains being born earlier than others. Also, initiators are not 100%

efficient as they can be lost due to cage reaction, primary radical termination, transfer to initiator, and various side reactions.[11] This leads to deviations from ideal living behavior.

One solution to this nonideality is to use a *unimolecular* initiation technique.[12,13] In this scheme, an initiator is synthesized which has nitroxide functionality (NP_1). This is then used in the NMP process, starting at the reversible activation step which will be discussed in the next section. This procedure ensures that one initiator molecule initiates one polymer chain, and the problem of initiator inefficiency is eliminated.

Finally, thermal self-initiation is present during polymerization of styrene which is the most common monomer used in NMP currently. The most widely accepted mechanism for styrene thermal initiation is the molecule assisted homolysis (MAH) reaction first proposed by Mayo.[14] This involves a Diels-Alder reaction in which two styrene molecules form a dimer, and this can then react with a third styrene monomer to form a dimer radical and monomer radical (Scheme 3-2). The rate coefficient for the dimerization reaction (k_{dim}) has been estimated to be 3×10^{-8} $mol^{-1}\cdot L\cdot s^{-1}$, while the rate coefficient for the radical formation step (k_i') is estimated at 5×10^{-8} $mol^{-1}\cdot L\cdot s^{-1}$ (both at 120°C).[15]

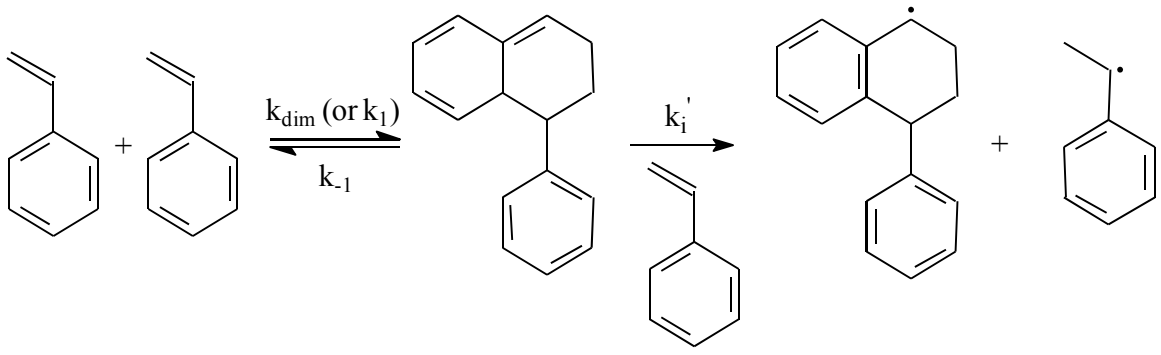

Scheme 3-2. Thermal Initiation of Styrene Monomer.

Since most NMP reactions occur above 110°C, this self-initiation reaction is present throughout the reaction. This has significant implications on the polymerization kinetics which will be discussed below, and the phenomenon has been examined in some detail for NMP reaction systems.[16-18]

3.2.3 Reversible Activation

The reversible activation step is the basis of the NMP process, and the success of the process depends on achieving the proper balance between activation and deactivation. As mentioned above, newly initiated unimer radicals ($P_1^{\bullet}$) should be deactivated immediately by being capped with the nitroxide controlling agent ($N^{\bullet}$) and this becomes a dormant molecule (NP_1). Dormant molecules are activated into propagating chains every $1/k_{act}$ seconds and they deactivate back to dormant polymer every $1/[N^{\bullet}]k_{deact}$ seconds as the nitroxide molecule leaves the end of the molecule and then returns (or is replaced by another). Typically, successful NMP processes require $1/k_{act}$= 10 to 10^3 s and $1/[N^{\bullet}]k_{deact}$ = 0.1 to 1 ms.[19] The equilibrium constant for the reversible activation reaction ($K=k_{act}/k_{deact}$) has been estimated to be somewhere around 10^{-11} to 2.1×10^{-11} mol L^{-1} for NMP of styrene with TEMPO at 125°C.[5,15] Deactivation clearly occurs much faster than activation at this high temperature, so the equilibrium is shifted strongly towards the dormant polymer state. This ensures that relatively few radicals are present in the overall system at any time, and this reduces the probability of termination reactions.

A number of different nitroxides have been studied for controlling the reversible activation step in NMP reactions, and three of the most thoroughly tested ones are 2,2,6,6-tetramethylpiperidine-1-oxyl (TEMPO), t-butylisopropylphenyl nitroxide

(TIPNO), and 1-diethylphosphono-2, 2-dimethyl) propyl nitroxide (DEPN, also known as SG1) (Figure 3-1) and various analogues of these molecules. Reviews have been published that summarize the various studies[20] and strategies that can be used for nitroxide selection and functionalization for use under various conditions[21,22], and recent studies demonstrate a variety of functionalized nitroxides for different applications.[23-26]

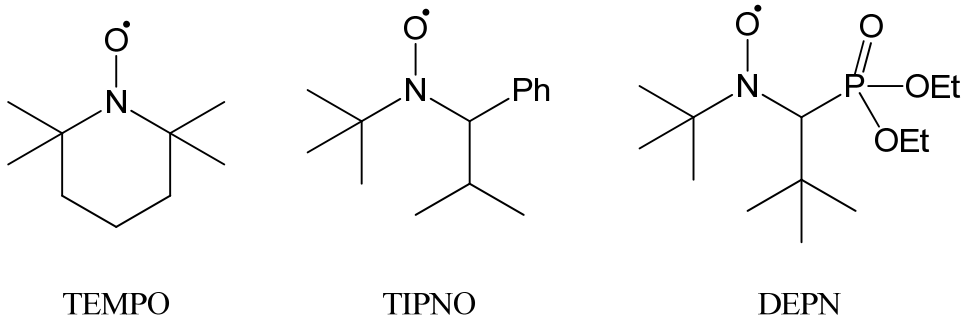

Figure 3-1. Common nitroxides for NMP reactions.

3.2.4 Propagation

While the radical polymer chains ($P_i^{\bullet}$) are active, they propagate with monomer (M). It is has been shown that the propagation rate in controlled radical polymerization processes is the same as that in conventional radical processes, and independent of the concentration of controlling nitroxide.[5,27] In the case of styrene at 120°C, the propagation rate coefficient (k_p) has been estimated to be 2300 $M^{-1}s^{-1}$.[28]

3.2.5 Termination

Chain termination does not occur in an ideal living polymerization, and early NMP modeling studies assumed that termination reactions were insignificant.[29,30] However, termination does inevitably occur in NMP and other controlled radical

polymerization processes. Polymer chains that terminate are considered to be 'dead', because they cannot be reacted further in the same manner as a 'living' chain. Therefore, it is of great interest to understand the termination mechanisms and rates so that one can determine methods of minimizing such undesirable reactions.

Conventional radical polymerization and NMP share the same mechanisms and rate constants for biradical termination reactions by combination and disproportionation. These termination reactions are minimized in the NMP process by minimizing the concentration of radicals in the system at any given time. The actual rate constants will depend on viscosity, temperature, and polymer chain length, but simplified model systems have been considered using $k_{tc} = 4\times10^8$ $M^{-1}s^{-1}$ and $k_{td}=0.01k_{tc}$ at 135°C.[31] This study suggested that termination by combination and disproportionation contributed to only 15% of dead polymer chains in a typical NMP system. A technique has been developed to measure the extent of chain-chain coupling reactions by reacting chromophore-labelled linear polymers with unlabelled multifunctional star polymers.[32] After reaction, the resulting star polymers are isolated and analyzed for chromophore incorporation which would result from radical-radical combination between star and linear polymer. This work also indicates that termination by combination contributes only a small fraction of dead polymer chain, 1.7% for an n-butyl acrylate system and 1.2% for a styrene system.

Alkoxyamine disproportionation has been found to contribute to more dead polymer chains than the previously discussed biradical termination mechanisms.[15,27,33] This is a first-order reaction with respect to the total living chain population, thus proceeding at a nearly constant rate throughout the reaction.[34] This means that reaction

time should be minimized to reduce the amount of dead polymer due to alkoxyamine disproportionation.

3.2.6 Persistent Radical Effect

The above described reactions lead to a phenomenon that has been termed the 'persistent radical effect' (PRE).[4,35,36] The nitroxide controlling agent is classified as a persistent radical while the growing polymer chains are transient radicals. The persistent radicals will not react amongst themselves to self-terminate, and they will only react with the transient radicals. Transient radicals not only react with persistent radicals, but can also react amongst themselves in termination reactions as described above. Therefore, the transient radical concentration will decrease while persistent radical concentration increases in an ideal case where there are no persistent radical losses or newly initiated transient radicals. This in turn will drive the reversible activation reaction equilibrium towards the dormant species, thus lowering the reaction rate.

Real systems become more complex than that described above due to the various side reactions that have been described previously. For example, new transient radicals are constantly formed during NMP of styrene due to the thermal self-initiation reaction, and this helps to counterbalance transient radical losses due to termination. Also, persistent radical does disappear from the reaction due to the alkoxyamine disproportionation reaction, and this has been accounted for in some PRE modeling work.[37]

3.2.7 Rate Enhancement

The main goal of NMP is to prepare a well defined polymer with high degree of livingness in a reasonable time frame. There are several competing factors defined above

that need to be balanced in order to achieve these goals. First, biradical termination must be minimized. This can be done by reducing the number of active radicals, but this results in a longer reaction. Second, alkoxyamine disproportionation must be minimized, and this can be done by reducing the reaction time. Since this reaction is predominant over biradical termination, the best strategy seems to involve running the reaction in the shortest time possible. There seem to be two main strategies for increasing the reaction rate:[38] (1) Reduce the persistent radical concentration by scavenging with some type of additive, and (2) Add extra conventional initiator throughout the reaction. Both of these techniques shift the reversible activation reaction towards the active radical state, thus increasing the reaction rate.

Several additives have been studied for increasing the reaction rate. For example, camphorsulfonic acid (CSA) has been shown to increase the rate of NMP significantly.[39-42] It was shown that the level of free nitroxide was lowered in the presence of CSA, thus shifting the reversible activation reaction away from the dormant state and increasing the reaction rate. However, it also has been shown that CSA reduces the rate of styrene thermal initiation by deactivating the dimer shown in Scheme 3-2 above, so this must be considered in the kinetic scheme.[43] Acetic anhydride and benzoyl chloride have shown a similar effect[44-46], as well as reducing agents,[47] pyridinium salts,[48] and ascorbic acid.[34,49,50]

A different approach to rate enhancement involves the addition of extra initiator to offset the reaction rate reduction that occurs as chains terminate, similar to the effect of styrene thermal self-initiation as described above. This has been demonstrated using *tert*-butyl hydroperoxide[51] dicumyl peroxide[52], and tert-butylperoxy 2-ethylhexyl carbonate

(TBEC).[53] It has also been shown that continuous addition of initiator throughout the reaction significantly increases this rate enhancing effect compared to batch addition.[54]

3.2.8 Monomer Conversion Equations

Several rate equations have been developed based on the above information, each corresponding to specific ideal cases. Power law expressions have been developed for the case where there is no conventional initiation or self-initiation (i.e., only unimolecular initiation occurs and rate of initiation R_i=0). Originally, the power law expression was developed for a specific case in which no excess nitroxide radicals are present at the start of reaction ($[N^\bullet]_0$=0).[4,35,55,56] The resulting monomer conversion expression is shown in Equation 3-1, and this equation has been shown to match some experimental data.[57]

$$\ln\left(\frac{[M]_0}{[M]}\right) = \frac{3}{2}k_p\left(\frac{KI_0}{3k_t}\right)^{1/3} t^{2/3} \qquad (R_i=0,\ [N^\bullet]_0=0) \qquad (3\text{-}1)$$

Another special case is for a large excess of nitroxide radicals present in the formulation at the start of reaction ($[N^\bullet]_0 >> (3k_tK^2I_0^2t)^{1/3}$). The resulting monomer conversion expression is shown in equation 3-2.[55]

$$\ln\left(\frac{[M]_0}{[M]}\right) = \left(\frac{k_pKI_0}{[N^\bullet]}\right)t \qquad (R_i=0,\ [N^\bullet]_0 >> 0) \qquad (3\text{-}2)$$

Another treatment of NMP kinetics has been developed which does include the effects of conventional initiation and self-initiation. This approach has been termed the 'stationary state' method, and the assumption is made that $[N^\bullet]$ and $[P^\bullet]$ reach a steady state soon after the reaction begins. This is achievable if the rate of initiation balances

the radical losses due to termination and other side-reactions. The resulting monomer conversion expression for this case is shown in equation 3-3.[5,55]

$$\ln\left(\frac{[\mathrm{M}]_0}{[\mathrm{M}]}\right) = k_\mathrm{p}\left(\frac{R_\mathrm{i}}{k_\mathrm{t}}\right)^{1/2} t \qquad (3\text{-}3)$$

The work discussed in this section has been focused primarily on homogeneous reaction systems such as bulk and solution processes. However, heterogeneous systems such as emulsion polymerization processes are widely used in industry, so it is of great interest to achieve controlled radical polymerization processes in a similar system.

3.3 Aqueous Dispersed Polymerization

3.3.1 Introduction

Water-based processes offer numerous advantages over bulk and solution processes including improved heat transfer and flow properties, and environmental benefits due to reduced solvent requirements. Industry has widely adopted emulsion polymerization for these reasons, so it is important to enable NMP reactions in a similar water-based system to achieve these benefits. Several comprehensive reviews have been published recently around this topic[58-61] and some of the highlights are described below.

3.3.2 Emulsion Polymerization

Emulsion polymerization formulations consist of water, surfactant, initiator, monomer, and optional additives such as chain transfer agent and buffer. Surfactant is present in a concentration above its critical micelle concentration (CMC) to ensure that micelles are present for particle nucleation. The initial state of the reaction mixture

contains monomer droplets (1-20μm) stabilized with surfactant, monomer-swollen surfactant micelles (10-20nm), and water-dissolved initiator, surfactant, and monomer as dictated by their respective water solubility's. The reaction begins by introducing radicals into the system, typically by thermal homolysis of the water-borne initiator. These radicals react with dissolved monomer to form short chain radical molecules, typically 2-3 monomer units in length.[62] These radicals can then nucleate polymer particles by one of three mechanisms: (1) Heterogeneous or micellar nucleation in which the short chain radical enters a monomer-swollen micelle, (2) Homogeneous nucleation where the short chain radical continues to propagate in the aqueous phase until it becomes insoluble and precipitates thus forming a new particle, and (3) Droplet nucleation where the short chain radical enters a monomer droplet. The latter is unlikely however, because the surface area of the relatively large monomer droplets is much lower than the micelles in the system. Therefore most particles are formed by either heterogeneous/micellar or homogeneous nucleation, and the specific reaction system will determine the prevailing nucleation mechanism.

Propagation occurs within the nucleated particles, and monomer is continually fed to the growing particles by diffusion through the aqueous phase from the monomer droplets until the monomer droplets have been completely depleted. Water solubility of monomer obviously has a strong influence on this mechanism, and very hydrophobic monomers pose a challenge as mass transfer through the aqueous phase is difficult due to diffusional limitations.

During propagation within a given polymer particle, only one radical entity is present in the particle. Propagation continues until another radical enters the particle

from the aqueous phase, at which point termination occurs almost instantaneously. This leads to a phenomenon termed compartmentalization, which refers to the fact that radical species within particles are segregated from radicals outside of the particles and in other particles. This is not the case in homogeneous polymerization processes where radicals are all present in the same phase. This leads to the fact that termination reactions do not occur as frequently in emulsion systems compared to homogeneous systems. This generally results in higher molecular weight and broader molecular weight distribution in emulsion systems.

Unfortunately, there have been many difficulties in developing successful NMP reactions in emulsion, with most attempts showing problems with colloidal stability or loss of livingness.[63-65] These problems have been attributed to the fact that there is a lack of compartmentalization in controlled free radical processes compared to their conventional free radical emulsion counterparts,[66,67] coupled with monomer droplet polymerization.[68] The polymerization rate is much higher in polymer particles compared to monomer droplets in conventional free radical emulsion processes due to the compartmentalization effect discussed above. However, the NMP mechanism makes the polymerization rate the same in monomer droplets and polymer particles because of the capping mechanism of the nitroxide control agent. This results in droplets and particles containing equal concentration of polymer, and this removes the thermodynamic driving force that causes diffusion from droplets to particles.

There has been some progress in development of emulsion-based NMP reactions, notably through the use of water soluble SG1-based alkoxyamines[69-73] that can also be created in-situ thus eliminating the need to synthesize a macroinitiator in a separate

step.[74] Another technique that has shown some promise is to selectively inhibit polymerization in the monomer droplets.[75]

Because of the limitations of emulsion polymerization with the NMP process, an alternative heterogeneous approach has been studied in some detail. Miniemulsion polymerization processes have been much more successful for NMP processes. Miniemulsion processes have not been adopted in industry to the degree of emulsion polymerization, but it is hoped that this research will help to demonstrate the unique attributes of this technology.

3.3.3 Miniemulsion Polymerization

Miniemulsion polymerization is different from emulsion polymerization in that the initial monomer droplets are driven down to a much smaller size, for example 0.05-0.5 μm compared to 1-20 μm. Also, the surfactant is present in a concentration such that there is complete surface coverage of monomer droplets and the droplets are stable, but no micelles are present. Because of the much higher droplet surface area and lack of micelles, monomer droplet nucleation becomes the primary particle nucleation process. This fact makes the process much more suitable for NMP because the requirement for mass transfer between particles is removed.

Miniemulsion polymerization was first demonstrated in the early 1970's,[76] and the actually term 'miniemulsion' was coined in 1980.[77] One critical requirement for a successful miniemulsion process is that the latex remains stable, at least for the duration of the polymerization. There are two primary mechanisms of latex destabilization: coalescence and Ostwald ripening.[78]

Coalescence occurs when particles collide and adhere due to van der Walls forces. This is prevented through the use of ionic surfactants that enable an electrostatic barrier, and/or non-ionic surfactants that enable a steric barrier to coalescence.

Ostwald ripening is a diffusional degradation mechanism that occurs if the droplet size distribution is polydisperse. A hydrophobic costabilizer is added to the miniemulsion formulation to prevent Ostwald ripening. Typical additives include hexadecane, cetyl alcohol, dodecyl mercaptan, alkyl methacrylates, and others. It has also been shown that dissolved polymer can be used to stabilize against Ostwald ripening effects,[79,80] although with less effectiveness than smaller hydrophobes.[81] Ostwald ripening occurs because smaller droplets have a higher Laplace pressure than larger droplets, and this creates a thermodynamic driving force for monomer diffusion from small to large droplets.[78] Addition of hydrophobic costabilizer builds an osmotic pressure throughout the droplets that counterbalances the Laplace pressure, thus preventing Ostwald ripening.

To form the miniemulsion, all of the components are mixed together and then some form of high energy mixing is applied to break down the droplet size. Typically this is done using a high pressure homogenizer or microfluidizer,[82] ultrasonification,[83] or rotor-stator device.[84,85] Ultimately, one would prefer that one polymer particle forms out of every single monomer droplet that is formed during the initial droplet formation, and this has been termed to as a "one-to-one copy". This does not occur in reality as some droplets are invariably lost due to Ostwald ripening or coalescence. Also, new particles can be formed due to homogeneous nucleation caused by monomer that may react in the aqueous phase.

The mixture is heated to the reaction temperature after particle formation is complete. If there is a true one-to-one copy, the reaction proceeds within each monomer droplet as described in section 3.2 above. However, kinetics typically differ from bulk systems due to two phenomena: reactant partitioning and compartmentalization.

Partitioning refers to the fact that, after particle formation, the various reaction components (initiator, monomer, etc.) are dispersed between the organic and aqueous phases according to the water and monomer solubility of the respective components. This will have a significant effect on kinetics. For example, systems with highly water soluble components will have very different concentrations and ratios of monomer/initiator/etc in a miniemulsion system compared to a bulk system as the hydrophilic components partition towards the aqueous phase.

Compartmentalization refers to effects that occur because reactants are separated from one another into small droplets within an aqueous medium. There are actually two specific effects that occur due to the compartmentalization phenomenon: the *segregation effect* and the *confined space effect*.[86] The segregation effect refers to the fact that reacting species are separated in separate particles and therefore cannot react with one another. The confined space effect refers to the fact that the rate of reaction between two species is higher in a small particle compared to a larger particle, since the reacting species are closer together on average than in a bulk system. These effects have specific implications in NMP systems which will be discussed in the next section.

3.3.4 NMP in Miniemulsion

NMP in miniemulsion was first demonstrated in the late 1990's,[87-90] and advances have been summarized in the aqueous dispersed phase reviews mentioned earlier[58-61] along with a review that is specific to this topic.[91]

Kinetic treatment in miniemulsion is not straightforward due to the compartmentalization and partitioning phenomena described previously. Initially, theoretical treatments of NMP in miniemulsion came to different conclusions regarding compartmentalization effects, depending on the assumptions that were used. One analysis suggested that polymerization rate will decrease and molecular weight distribution should become narrower as particle size decreases, due to compartmentalization effects.[92] Another analysis suggests the opposite, that polymerization rate will increase at the expense of broader molecular weight distribution as particle size decreases.[93] The conflicting results seem to be due to different assumptions regarding the presence of thermal autopolymerization, which creates differences between bulk and miniemulsion NMP systems,[94] and the way in which termination was treated. Experimentally, it has been shown that some NMP miniemulsion systems do not display compartmentalization effects, and there is little difference between the materials produced in bulk versus miniemulsion systems.[66,91]

Further experimental[95-97] and theoretical[86,98-100] investigations have clarified the compartmentalization effect to some degree, and it seems that there are specific regimes where different effects are observed. This is based on the competing segregation and confined space effects, each of which can become dominant depending on the conditions of the system. When the confined space effect is dominant, rate of polymerization is

faster, polydispersity is broader, and livingness is higher than bulk systems. When the segregation effect is dominant, the rate of polymerization is slower, polydispersity is narrower, and livingness is higher than in bulk. The particle size range for the dominant effect is also dependent on the type and amounts of reactants that are present, particularly the nitroxide. It has also been shown that the compartmentalization effect cannot be mimicked by dilution or increasing nitroxide concentration in bulk systems, so the effect is unique to dispersed phase systems.[101]

Understanding of miniemulsion NMP kinetics is further complicated by the partitioning of the various reactants between the aqueous and organic phases[102] and at the interface.[103] Particle nucleation becomes very complex as the reaction components are distributed between two phases. A delicate balance is required between nitroxide and initiator to maintain reaction control, and this can be disrupted by partitioning effect.

A series of studies of styrene NMP with TEMPO-based nitroxides has been presented by Cunningham et al. which includes discussion of partitioning[104] and interfacial transfer[105] of components between phases, along with a comprehensive model of the system.[31,106] These studies included some discussion about optimizing reaction conditions to maximize polymer livingness while minimizing polydispersity[107,108] primarily by identifying conditions that enable the minimizing total reaction time while maintaining control of the polymerization.

The crosslinking polymerization reaction of styrene and divinylbenzene has also been studied in an NMP miniemulsion system using a bimolecular[109,110] initiation method. It was found that pendant reactivity was lower, and thus there was lower crosslink density compared to equivalent bulk systems. A similar study using a

unimolecular[111] initiation method showed that crosslink density and gel formation could be controlled by varying the amount of hydrophobe used.

3.4 Summary

Great strides have been made in recent years towards understanding controlled radical polymerization processes. The kinetics and mechanisms of CRP processes are starting to be well understood, heterogeneous processes have been demonstrated and the corresponding mechanisms are being elucidated, and there have been some initial forays in continuous CRP processes. However, more research is required to put these three areas together into a package that will enable further development into commercial processes. The research described in the following chapters is aimed at being one more piece in the puzzle that will develop NMP into a viable industrial technology.

3.5 References

1. Cunningham, M. F. *Prog. Polym. Sci.* **2002**, *27*, 1039.
2. Bonilla, J.; Saldivar, E.; Flores-Tlacuahuac, A.; Vivaldo-Lima, E.; Pfaendner, R.; Tiscareno-Lechuga, *F. Polym. React. Eng.* **2002**, *10*, 227.
3. Belincanta-Ximenes, J.; Mesa, P. V. R.; Lona, L. M. F.; Vivaldo-Lima, E.; McManus, N. T.; Penlidis, A. *Macromol. Theory Simul.* **2007**, *16*, 194.
4. Fischer, H. *J. Polym. Sci., Part A: Polym. Chem.* **1999**, *37*, 1885.
5. Fukuda, T.; Terauchi, T.; Goto, A.; Ohno, K.; Tsuji, Y.; Miyamoto, T., Kobatake, S.; Yamada, B. *Macromolecules* **1996**, *29*, 6393.
6. Greszta, D.; Matyjaszewski, K. *Macromolecules* **1996**, *29*, 7661.

7. Roa-Luna, M.; Nabifar, A.; Diaz-Barber, M. P.; McManus, N. T.; Vivaldo-Lima, E.; Lona, L. M. F.; Penlidis, A. J. *Macromol. Sci. A: Pure Appl. Chem.* **2007**, *44*, 337.

8. Nabifar, A.; McManus, N. T.; Vivaldo-Lima, E.; Lona, L. M. F.; Penlidis, A. *Can. J. Chem. Eng.* **2008**, *86*, 879.

9. Zhou, M.; McManus, N.T., Vivaldo-Lima, E.; Lona, L. M.; Penlidis, A. *Macromol. Symp.* **2010**, *289*, 95.

10. Masson, J. C. in *Polymer Handbook, Third Edition*; Brandrup, J., Immergut, E. H. Eds.; John Wiley and Sons: New York, **1989**; pp. II-1 to II-66.

11. Moad, G.; Solomon, D. H. *The Chemistry of Free Radical Polymerization*; Elsevier Science: Tarrytown, NY, **1995**; p. 50

12. Hawker, C. J. *J. Am. Chem. Soc.* **1994**, *116*, 11185.

13. Hawker, C. J.; Barclay, G. G.; Orellana, A.; Dao, J.; Devonport, W. *Macromolecules* **1996**, *29*, 5245.

14. Mayo, F. R. *Polym. Prepr. (Am. Chem. Soc., Div. Polym. Chem.)* **1961**, *2*, 55.

15. Grezsta, D.; Matyjaszewski, K. *Macromolecules* **1996**, *29*, 7661.

16. Boutevin, B.; Bertin, D. *Eur. Polym. J.* **1999**, *35*, 815.

17. Nabifar, A.; McManus, N. T.; Vivaldo-Lima, E.; Lona, L. M. F.; Penlidis, A. *Chem. Eng. Sci.* **2009**, *64*, 304.

18. Bonilla-Cruz, J.; Caballero, L.; Albores-Velasco, M.; Saldivar-Guerra, E.; Percino, J.; Chapela, V. *Macromol. Symp.* **2007**, *248*, 132.

19. Goto, A.; Fukuda, T. *Prog. Polym. Sci.* **2004**, *29*, 329.

20. Hawker, C. J.; Bosman, A. W.; Harth, E. *Chem. Rev.* **2001**, *101*, 3661.

21. Nilsen, A.; Braslau, R. *J. Polym. Sci., Part A: Polym. Chem.* **2006**, *44*, 697.

22. Malmstrom, E. E.; Hawker, C. J. *Macromol. Chem. Phys.* **1998**, *199*, 923.

23. Fleischmann, S.; Komber, H.; Appelhans, D.; Voit, B. I. *Macromol. Chem. Phys.* **2007**, *208*,1050.

24. Nicolay, R.; Marx, L.; Hemery, P.; Matyjaszewski, K. *Macromolecules* **2007**, *40*, 6067.

25. Debuigne, A.; Chan-Seng, D.; Li. L.; Hamer, G. K.; Georges, M. K. *Macromolecules* **2007**, *40*, 6224.

26. Ruehl, J.; Ningnuek, N.; Thongpaisanwong, T.; Braslau, R. *J. Polym. Sci., Part A: Polym. Chem.* **2008**, *46*, 5049.

27. Catala, J. M.; Bubel, F.; Hammouch, S. O. *Macromolecules* **1995**, *28*, 8441.

28. Gilbert, R. G. *Pure Appl. Chem.* **1996**, *68*, 1491.

29. Veregin, R. P. N.; Georges, M. K.; Hamer, G. K.; Kazmaier, P. M. *Macromolecules*, **1995**, *28*, 4391.

30. Veregin, R. P. N.; Odell, P. G.; Michalak, L. M.; Georges, M. K. *Macromolecules* **1996**, *29*, 3346.

31. Ma, J. W.; Smith, J. A.; McAuley, K. B.; Cunningham, M. F.; Keoshkerian, B.; Georges, M. K. *Chem. Eng. Sci.* **2003**, *58*, 1163.

32. Pyun, J.; Rees, I.; Frechet, J. M. J.; Hawker, C. J. *Aust. J. Chem.* **2003**, *56*, 775.

33. Li, I.; Howell, B. A.; Matyjaszewski, K.; Shigemoto, T.; Smith, P. B.; Priddy, D. B. *Macromolecules* **1995**, *28*, 6692.

34. Lin, M.; Cunningham, M. F.; Keoshkerian, B. *Macromol. Symp.* **2004**, *206*, 263.

35. Fischer, H. *Macromolecules* **1997**, *30*, 5666.

36. Fischer, H. *Chem. Rev.* **2001**, *101*, 3581.

37. Souaille, M.; Fischer, H. *Macromolecules* **2001**, *34*, 2830.

38. Souaille, M.; Fischer, H. *Macromolecules* **2002**, *35*, 248.

39. Georges, M. K.; Veregin, R. P. N.; Kazmaier, P. M.; Hamer, G. K.; Saban, M. *Macromolecules* **1994**, *27*, 7228.

40. Odell, P. G.; Veregin, R. P. N.; Michalak, L. M.; Brousmiche, D.; Georges, M. K. *Macromolecules* **1995**, *28*, 8453

41. Veregin, R. P. N.; Odell, P. G.; Michalak, L. M.; Georges, M. K. *Macromolecules* **1996**, *29*, 4161.

42. Baldovi, M. V.; Mohtat, N.; Scaiano, J. C. *Macromolecules* **1996**, *29*, 5497.

43. Buzanowski, W. C.; Graham, J. D.; Priddy, D. B.; Shero, E. *Polymer* **1992**, *33*, 3055.

44. Malmstrom, E. E.; Hawker, C. J. *Macromol. Chem. Phys.* **1998**, *199*, 923.

45. Baumann, M.; Schmidt-Naake, G. *Macromol. Chem. Phys.* **2001**, *202*, 2727.

46. Goto, A.; Tsujii, Y,; Fukuda, T. *Chem. Lett.* **2000**, *29*, 788.

47. Keoshkerian, B.; Georges, M.; Quinlan, M.; Veregin, R.; Goodbrand, B. *Macromolecules* **1998**, *31*, 7559.

48. Odell, P. G.; Veregin, R. P. N.; Michalak, L. M.; Georges, M. K. *Macromolecules* **1997**, *30*, 2232.

49. Georges, M. K.; Lukkarila, J. L.; Szkurhan, A. R. *Macromolecules* **2004**, *37*, 1297.

50. Cunningham, M. F.; Ng, D. C. T.; Milton, S. G.; Keoshkerian, B. *J. Polym. Sci., Part A: Polym. Chem.* **2006**, *44*, 232.

51. Goto, A.; Fukuda, T. *Macromolecules* **1997**, *30*, 4272.

52. Greszta, D.; Matyjaszewski, K. *J. Polym. Sci., Part A: Polym. Chem.* **1997**, *35*, 1857.

53. Nogueira, T. R.; Goncalves, M. C.; Lona, L. M. F.; Vivaldo-Lima, E.; McManus, N.; Penlidis, A. *Adv. Polym. Tech.* **2010**, *29*, 11.

54. He, J.; Chen, J.; Li, L.; Pan, J.; Li, C.; Cao, J.; Tao, Y.; Hua, F.; Yang, Y.; McKee, G. E.; Brinkmann, S. *Polymer* **2000**, *41*, 4573.

55. Fukuda, T.; Goto, A.; Ohno, K. *Macromol. Rapid Commun.* **2000**, *21*, 151.

56. Ohno, K.; Tsujii, Y.; Miyamoto, T.; Fukuda, T.; Goto, M.; Kobayashi, K.; Akaike, T. *Macromolecules* **1998**, *31*, 1064.

57. Yoshikawa, C.; Goto, A.; Fukuda, T. *Macromolecules* **2002**, *35*, 5801.

58. Qiu, J.; Charleux, B.; Matyjaszewski, K. *Prog. Polym. Sci.* **2001**, *26*, 2083.

59. Cunningham, M. F. *Prog. Polym. Sci.* **2002**, *27*, 1039.

60. Cunningham, M. F. *Prog. Polym. Sci.* **2008**, *33*, 365.

61. Zetterlund, P. B.; Kagawa, Y.; Okubo, M. *Chem. Rev.* **2008**, *108*, 3747.

62. Gilbert, R. G. *Emulsion Polymerization: A Mechanistic Approach*; Ottewill, R.H., Rowell, R.L. Eds.; Academic Press: San Diego, **1995**.

63. Bon, S. A. F.; Bosveld, M.; Klumperman, B.; German, A. L. *Macromolecules* **1997**, *30*, 324.

64. Marestin, C.; Noel, C.; Guyot, A.; Claverie, J. *Macromolecules* **1998**, *31*, 4041.

65. Cao, J.; He, J.; Li, C.; Yang, Y. *Polym. J.* **2001**, *33*, 75.

66. Pan, G.; Sudol, E. D.; Dimonie, V. L.; El-Aasser, M. S. *Macromolecules* **2001**, *34*, 481.

67. Cunningham, M. F.; Xie, M.; McAuley, K. B.; Keoshkerian, B.; Georges, M. K. *Macromolecules* **2002**, *35*, 59.

68. Pohn, J.; Buragina, C.; Georges, M. K.; Keoshkerian, B.; Cunningham, M. F. *Macromol. Theory Simul.* **2008**, *17*, 73.

69. Nicolas, J.; Charleux, B.; Guerret, O.; Magnet, S. *Macromolecules* **2005**, *38*, 9963.

70. Delaittre, G.; Nicolas, J.; Lefay, C.; Save, M.; Charleux, B. *Chem. Commun.* **2005**, 614.

71. Nicolas, J.; Charleux, B.; Magnet, S. *J. Polym. Sci., Part A: Polym. Chem.* **2006**, *44*, 4142.

72. Charleux, B.; Nicolas, J. *Polymer* **2007**, *48*, 5813.

73. Nicolas, J.; Ruzette, A.-V.; Farcet, C.; Gerard, P.; Magnet, S.; Charleux, B. *Polymer* **2007**, *48*, 7029.

74. Simms, R. W.; Hoidas, M. D.; Cunningham, M. F. *Macromolecules* **2008**, *41*, 1076.

75. Maehata, H.; Liu, X.; Cunningham, M.; Keoshkerian, B. *Macromol. Rapid Commun.* **2008**, *29*, 479.

76. Ugelstad, J.; El-Aasser, M. S.; Vanderhoff, J. W. *J. Polym. Sci. Lett. Ed.* **1973**, *11*, 503.

77. Chou, Y. J.; El-Aasser, M. S.; Vanderhoff, J. W. *J. Dispersion Sci. Technol.* **1980**, *1*, 129.

78. Antonietti, M.; Landfester, K. *Prog. Polym. Sci.* **2002**, *27*, 689.

79. Miller, C. M.; Blythe, P. J.; Sudol, E. D.; Silebi, C. A.; El-Aasser, M. S. *J. Polym. Sci. Part A: Polym. Chem.* **1994**, *32*, 2365.

80. Reimers, J.; Schork, F. J. *J. Appl. Polym. Sci.* **1996**, *59*, 1833.

81. Asua, J. M. *Prog. Polym. Sci.* **2002**, *27*, 1283.

82. Manea, M.; Chemtob, A.; Paulis, M.; della Cal, J. C.; Barandiaran, M. J.; Asua, A. M. *AIChE J.* **2008**, *54*, 289.

83. Landfester, K.; Eisenblätter, J.; Rothe R. *JCT Research* **2004**, *1*, 65.

84. El-Jaby, U.; McKenna, T. F. L.; Cunningham, M. F. *Macromol. Symp.* **2007**, *259*, 1.

85. El-Jaby, U.; Cunningham, M.; Enright, T.; McKenna, T. F. L. *Macromol. React. Eng.* **2008**, *2*, 350.

86. Zetterlund, P. B.; Okubo, M. *Macromolecules* **2006**, *39*, 8959.

87. Prodpran, T.; Dimonie, V. L.; Sudol, E. D.; El-Aasser, M. S. *Polym. Mater. Sci. Eng.* **1999**, *80*, 534.

88. Prodpran, T.; Dimonie, V. L.; Sudol, E. D.; El-Aasser, M. S. *Macromol. Symp*. **2000**, *155*, 1.

89. MacLeod, P. J.; Keoshkerian, B.; Odell, P. G.; Georges, M. K. *Polym. Mater. Sci. Eng.* **1999**, *80*, 539.

90. MacLeod, P. J.; Barber, R.; Odell, P. G.; Keoshkerian, B.; Georges, M. K. *Macromol. Symp.* **2000**, *155*, 31.

91. Cunningham, M. F. *C. R. Chimie* **2003**, *6*, 1351.

92. Butte, A.; Storti, G.; Morbidelli, M. *Macromolecules* **2000**, *33*, 3485.

93. Charleux, B. *Macromolecules* **2000**, *33*, 5358.

94. Pan, G.; Sudol, D.; Dimonie, V. L.; El-Aasser, M. S. *J. Polym. Sci., Part A: Polym. Chem.* **2004**, *42*, 4921.

95. Nakamura, T.; Zetterlund, P. B.; Okubo, M. *Macromol. Rapid Commun.* **2006**, *27*, 2014.

96. Maehata, H.; Buragina, C.; Cunningham, M.; Keoshkerian, B. *Macromolecules* **2007**, *40*, 7126.

97. Zetterlund, P. B.; Nakamura, T.; Okubo, M. *Macromolecules* **2007**, *40*, 8663.

98. Tobita, H. *Macromol. Theory Simul.* **2007**, *16*, 476.

99. Tobita, H.; Yanase, F. *Macromol. Theory Simul.* **2007**, *16*, 810.

100. Zetterlund, P. B.; Okubo, M. *Macromol. Theory Simul.* **2009**, *18*, 277.

101. Zetterlund, P. B. *Aust. J. Chem.* **2010**, *63*, 1195.

102. Zetterlund, P. B.; Okubo, M. *Macromol. Theory Simul.* **2005**, *14*, 415.

103. Zetterlund, P. B. *Macromol. Theory Simul.* **2010**, *19*, 11.

104. Ma, J. W.; Cunningham, M. F.; McAuley, K. B.;Keoshkerian, B.; Georges, M. K. *J. Polym. Sci., Part A: Polym. Chem.* **2001**, *39*, 1081.

105. Ma, J. W.; Cunningham, M. F.; McAuley, K. B.; Keoshkerian, B.; Georges, M. K. *Macromol. Theory Simul.* **2002**, *11*, 953.

106. Ma, J. W.; Cunningham, M. F.; McAuley, K. B.; Keoshkerian, B.; Georges, M. K. *Chem. Eng. Sci.* **2003**, *58*, 1177.

107. Ma, J. W.; Cunningham, M. F.; McAuley, K. B.; Keoshkerian, B.; Georges, M. K. *Macromol. Theory Simul.* **2003**, *12*, 72.

108. Cunningham, M. F.; Lin. M.; Milton, S.; Ng, D.; Hsu, C. C.; Keoshkerian, B. *Polymer*, **2005**, *46*, 1025.

109. Zetterlund, P. B.; Alam, M. N.; Minami, H.; Okubo, M. *Macromol. Rapid Commun.* **2005**, *26*, 955.

110. Alam, M. N.; Zetterlund, P. B.; Okubo, M. *Macromol. Chem. Phys.* **2006**, *207*, 1732.

111. Saka, Y.; Zetterlund, P. B.; Okubo, M. *Polymer* **2007**, *48*, 1229.

Chapter 4

Continuous Reactor Design and Scoping Experiments

4.1 Preface

When this research project was started, continuous L/CRP reactions had not yet been reported and NMP miniemulsion processes were just beginning to be reported and understood. This chapter starts out by describing the development of the first continuous tubular reactor for NMP miniemulsion, along with the technical challenges that were overcome. Scoping experiments are then described which identified several phenomena that are unique to the NMP miniemulsion system, and it will be important to be aware of these phenomena as this technology advances. The end result of this chapter is that controlled NMP miniemulsion reactions were demonstrated in the tubular reactor, and the reaction was understood well enough to move on to a more detailed comparison between batch and continuous reactions.

4.2 Introduction

4.2.1 Continuous Tubular Reactor Apparatus – Design Considerations

The general objective of this project was to feed unreacted miniemulsion latex through a heated tube and obtain a stable polymer latex that has 'living' characteristics. The initial apparatus concept involved immersing a length of tube in a heated oil bath and feeding the latex through either by pressure or using a pump. Several iterations were required before a properly functioning tubular reactor was achieved, and these will be discussed in the following sections. There were several issues encountered that made the task more challenging than originally anticipated:

1) The reaction takes several hours, which meant that the residence time within the reactor was fairly long. This required either very long tube length or very low feed rate for the reactor, and this lead to practical difficulties.

2) The process is run at relatively high temperature (120-135°C) and under moderate pressure (400-650 kPa), and this limited the choices for materials of construction and metering devices.

A brief summary of the above issues is given in the following sections, while full details are given in Section 4.4 which describes the different reactor designs that were tested.

4.2.2 Reactor Residence Time

When this work was initiated, a typical NMP miniemulsion reaction required approximately four to five hours to achieve high monomer conversion in a batch reactor.

This meant that the NMP latex needed to reside within the tubular reactor for this amount of time. The average residence time in a reactor is calculated using Equation 4.1.

$$\tau = V/Q \qquad (4\text{-}1)$$

where τ is the average residence time, V is the volume of the heated portion of the reactor tube, and Q is the volumetric flow rate of latex through the tube. The volume of the reactor can be calculated with Equation 4-2.

$$V = A \cdot L = (\pi D^2/4) \cdot L \qquad (4\text{-}2)$$

where A is the tube cross-sectional area, L is tube length, and D is the tube diameter. Obviously, as tubing diameter decreases, the length must increase significantly to achieve the same residence time. This becomes a problem spatially within a lab environment where the tube must fit inside a relatively small oil bath. Alternative to increasing length of the reactor, flow rate can be reduced to increase the residence time. However, controlling low flow rates for this system was also a challenge.

4.2.3 Metering Devices

Metering the latex at a consistent feed rate was one of the biggest initial challenges of this project. The flow rate must be fairly low to achieve the desired reaction residence time, with typical flow rates between 0.4 to 4.0 mL/minute. This in itself is not a problem, because there are many different types of precision low flow pumps available. However, the reaction is run under moderate pressure (e.g., 400-650kPa), and this eliminated many of the potential pump options. Of the few low flow

pumps that are pressurizable, several were found to be incompatible with the polymer latex.

Metering valves were also considered for controlling the latex feed rate. However, it was found that the polymer latex tends to clog the valves over time, leading to inconsistent flow rates.

These issues will be described in more detail throughout the following sections that describe the various tubular reactor designs that were tested.

4.2.4 Materials of Construction

Since the NMP reaction is run under pressure and at relatively high temperature, it was decided that metal tubing would be used for safety reasons. The tubing also had to be relatively easy to bend so that it could be coiled up to fit in the confines of the relatively small oil bath. For this reason, copper tubing was originally chosen, due to its malleability. However, it was later decided that stainless steel was a more suitable material for this reaction. In order to be easily bendable, the stainless steel tubing had to have a smaller diameter than the copper tubing. As discussed above, this meant that the length had to be increased substantially to maintain the desired residence times within the reactor.

4.3 Experimental

4.3.1 Modified NMP Miniemulsion Procedure ("Semi-miniemulsion")

A modified miniemulsion polymerization process, also called semi-miniemulsion (SME), was used for all of the experiments in this study. This process had been developed previously using batch polymerization methods, and was one of the first

successful methods of producing controlled free radical polymers in a dispersed phase.[1,2] This process involved the following three steps:

Step 1: Partial bulk polymerization to low conversion, resulting in a solution of ~10 wt% polymer dissolved in 90 wt% monomer.

Step 2: Dispersion of the above monomer/polymer mixture in water to produce a latex of monomer/polymer droplets in water.

Step 3: Miniemulsion polymerization of the above dispersion to produce a polymer latex consisting of polymer particles dispersed in water.

The step one partial bulk polymerization and step two dispersion were run only in batch for all of the experiments described in this chapter of the study, while the step three miniemulsion was run both in batch and continuous modes for comparison. To run the experiments head-to-head, a large batch of unreacted latex was prepared and then split between the batch and continuous reactors. The reactions were then run concurrently using the same unreacted latex. The general procedure for batch and continuous reactions is described in the following sections.

4.3.1.1 Step 1: Partial Bulk Polymerization (NMP Batch Reaction)

TEMPO (10.2 g; Z.D. Chemipan) and benzoyl peroxide (16.2 g Luperox A75FP; Aldrich) were dissolved in styrene (1473.6 g; StanChem) by mixing with a six-bladed pitch blade impeller in a 4-litre stainless steel beaker. This mixture was charged into a 2-litre stainless steel Buchi reactor which was fitted with a condenser, and mixing was started at 450 rpm. The mixture was deoxygenated by bubbling nitrogen through the monomer solution for 20 minutes during reactor heating. The reactor was heated to 135°C over a period of 2.5 hours, held at 135°C for 60 minutes, and cooled to room

temperature in 90 minutes. The reactor was discharged yielding a monomer/polymer solution hereafter referred to as *bulk prepolymer solution*.

4.3.1.2 Step 2: Dispersion to Prepare Unreacted Latex

Dodecylbenzenesulfonic acid sodium salt (SDBS) (61 g; Aldrich) and ascorbic acid (5.1 g; Aldrich) were dissolved in deionized water (3076g) by mixing at 500 rpm with a six-bladed pitch blade impeller in a 4-L Nalgene jar. 696 g bulk prepolymer solution (from above procedure) was added to the mixture and mixed for 1 minute. The mixture was homogenized by flowing through a Niro Soavi piston homogenizer at 400-600 bar pressure. This unreacted latex was then divided, with one portion used for a batch reaction and the other used for a continuous reaction. Both reactions were done on the same day.

4.3.1.3 Step 3a: Miniemulsion in Batch Reactor

1500 g of unreacted latex (from Section 4.3.1.2 above) was charged into a 2-L stainless steel Buchi reactor. Mixing was started at 550 rpm and the reactor was sealed. The reactor was deoxygenated with three pressure/vacuum cycles using nitrogen at 500 kPa pressure. The reactor was heated to 135°C over a period of 2.5 hours and held at 135°C for 2 to 4 hours depending on the experiment. Periodically, samples were removed through a reactor dip tube and cooled under cold water (~20 g samples). When the reaction was complete, the reactor was cooled to room temperature over 90 minutes and was then discharged yielding the final latex product. The reactor was dropped after product discharge to observe if reactor fouling occurred during the reaction.

A typical batch miniemulsion experiment time/temperature profile is shown in Figure 4-1 below. Note the relatively slow heating profile, as this turned out to have a significant impact on the reaction kinetics and is discussed further in Section 4.6.3.

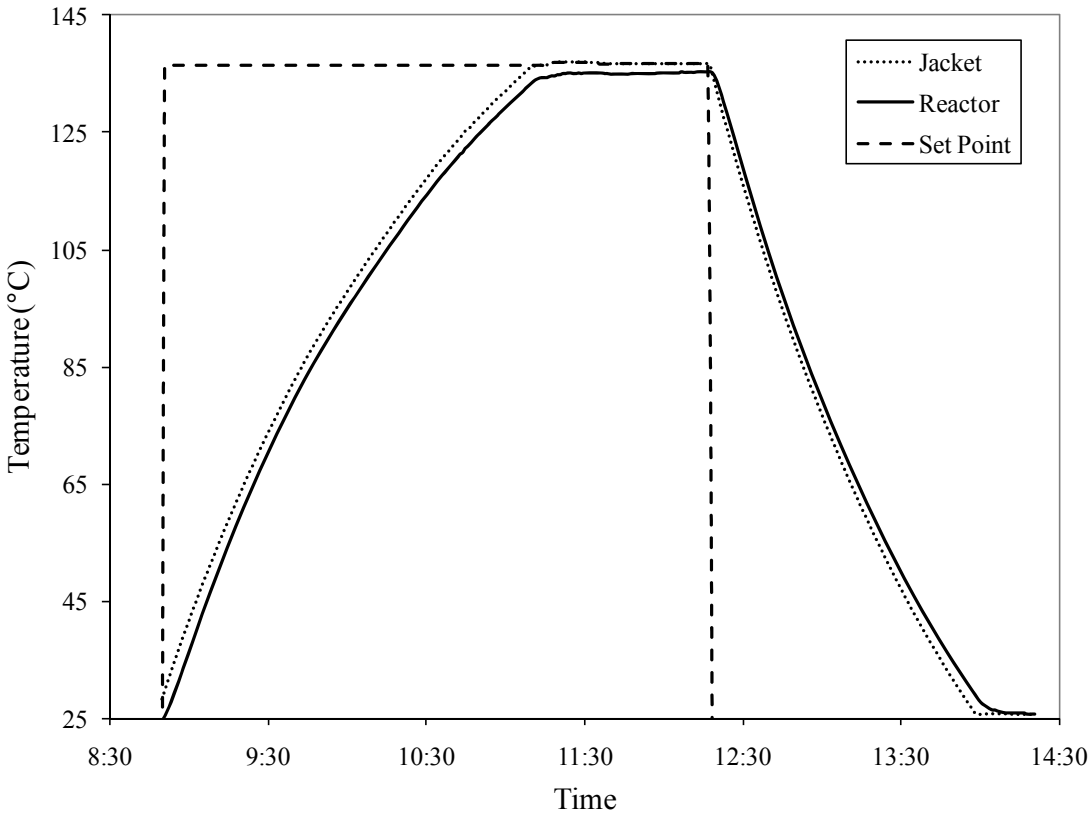

Figure 4-1. NMP Miniemulsion Time-Temperature Profile (Batch Reaction).

The time at which the reactor reached 110°C was arbitrarily designated as time-zero for the reaction. This is because the NMP reaction rate starts to become significant around this temperature, and the rate increases as the temperature slowly increases to 135°C over the period of ~1 hour. This obviously impacts the kinetic analysis, and the true results in comparison to the continuous reactor are likely shifted somewhat from the results that are shown.

4.3.1.4 Step 3b: Miniemulsion in Continuous Tubular Reactor

A number of different continuous tubular reactor apparatuses were tested and are described in detail in the following sections. However, all of them had a few common elements that can be used to describe the general reaction procedure. In all cases a tube was immersed in a heated oil bath, and this constituted the reaction section of the apparatus. A holding vessel was installed at the inlet of the tube, ahead of the heated section, and unreacted latex was charged into this vessel to be fed through the heated tube. Various methods were tested for feeding the reactants at a controlled rate, and these methods are described in the following sections. Finally, a beaker was positioned on an electronic balance at the outlet of the reactor tube to capture the final product and monitor the rate of collection.

To run a reaction, the oil bath in which the reactor tube was immersed was heated to 135°C. The unreacted latex from Section 4.3.1.2 above was charged into the holding vessel(s). The unreacted latex was then deoxygenated by a series of nitrogen pressurization followed by vacuum, and was fed through the continuous reactor at the desired feed rate using the methods that are described in the following sections.

4.3.2 Analytical

Weight average molecular weight (MW), number average molecular weight (MN) and polydispersity (PDI) for bulk and miniemulsion polymerized samples were measured by gel permeation chromatography (GPC) using a Waters/Millipore liquid chromatograph equipped with a Waters model 510 pump, Ultrastyragel columns of pore size 10^5 Å, 10^4 Å, and 10^3 Å in series with a Styragel HR0.5 column, a Waters model 410 differential refractometer (RI), and a Waters model 486 tunable absorbance detector

(UV). Polystyrene standards were used for calibration. Tetrahydrofuran (THF) was used as the eluant at a flow rate of 1.0 mL min^{-1}. Reproducibility analysis for the GPC measurement was done by running six repeat analyses of the same sample at various times over the period of a week with other samples tested in-between. Based on the results, 95% confidence interval was calculated for number average molecular weight (± 1360), weight average molecular weight (± 1880), and polydispersity (± 0.02). Confidence interval will not be the same for all samples, but it is assumed that they will be of similar magnitude since the molecular weights are all within the same general range. Conversion for bulk polymerization experiments was analyzed gravimetrically by drying samples overnight at room temperature, then vacuum drying at 50°C for eight hours. Solids analysis for miniemulsion polymerization samples was analyzed gravimetrically by drying latex samples overnight at room temperature, then vacuum drying at 50°C for eight hours. Conversion was calculated for miniemulsion polymerization experiments after measuring residual monomer by gas chromatography (GC) using a Perkin-Elmer XL Autosystem GC equipped with a flame ionization detector and Supelcowax 10 column (15m x 0.53 mm ID; 0.5 μm film). Particle size analysis for miniemulsion polymerized particles was done on wet latex samples by dynamic light scattering using a NICOMP model 370 submicron particle sizer.

4.4 Continuous Tubular Reactor Apparatus Development

4.4.1 Iteration #1 – Pump at Reactor Inlet

The initial tubular reactor consisted of a 9 metre coil of ¼" copper tubing immersed in a small oil bath. A piston pump was used to meter latex into the reactor, and

a needle valve was positioned at the exit of the reactor to control the latex flow. A schematic is shown in Figure 4-2:

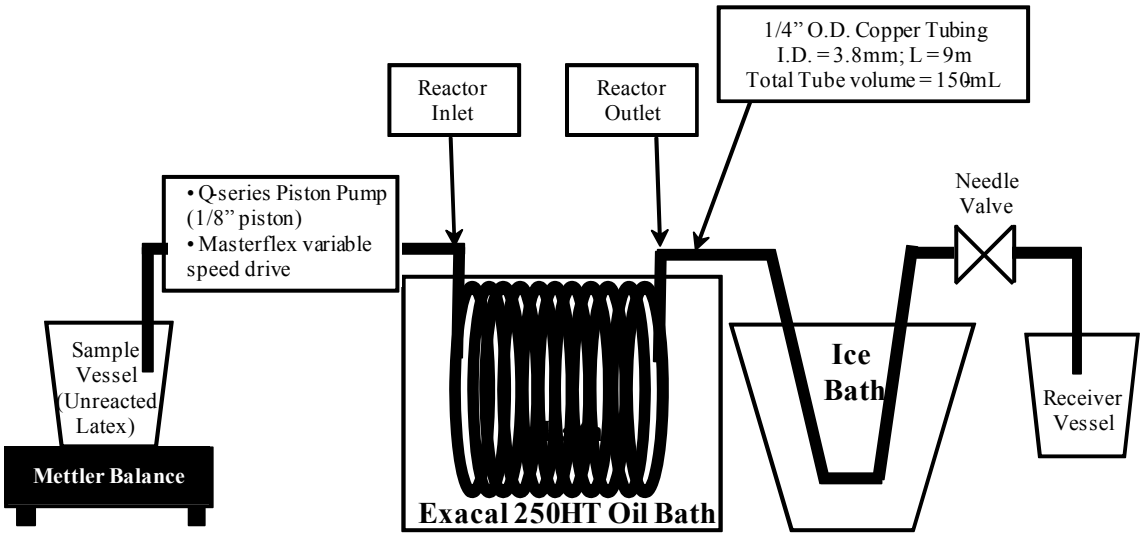

Figure 4-2. Continuous Tubular Reactor - Iteration #1.

A series of experiments were run with this apparatus with no promising results. The primary problem with this setup was inconsistent flow rate. Large air pockets appeared to be present in the reactor, and backflow through the piston pump was observed due to the pressure in the reactor. Also, the latex did not flow consistently through the metering valve, but instead pulsed significantly. Therefore the reactor was redesigned to enable more consistent flow.

4.4.2 Iteration #2 – Pump at Reactor Outlet

The second design iteration involved positioning the metering pump at the exit of the tubular reactor, and pressurizable stainless steel sample cylinders were positioned at the inlet of the reactor as holding vessels. A schematic of the apparatus is shown in Figure 4-3:

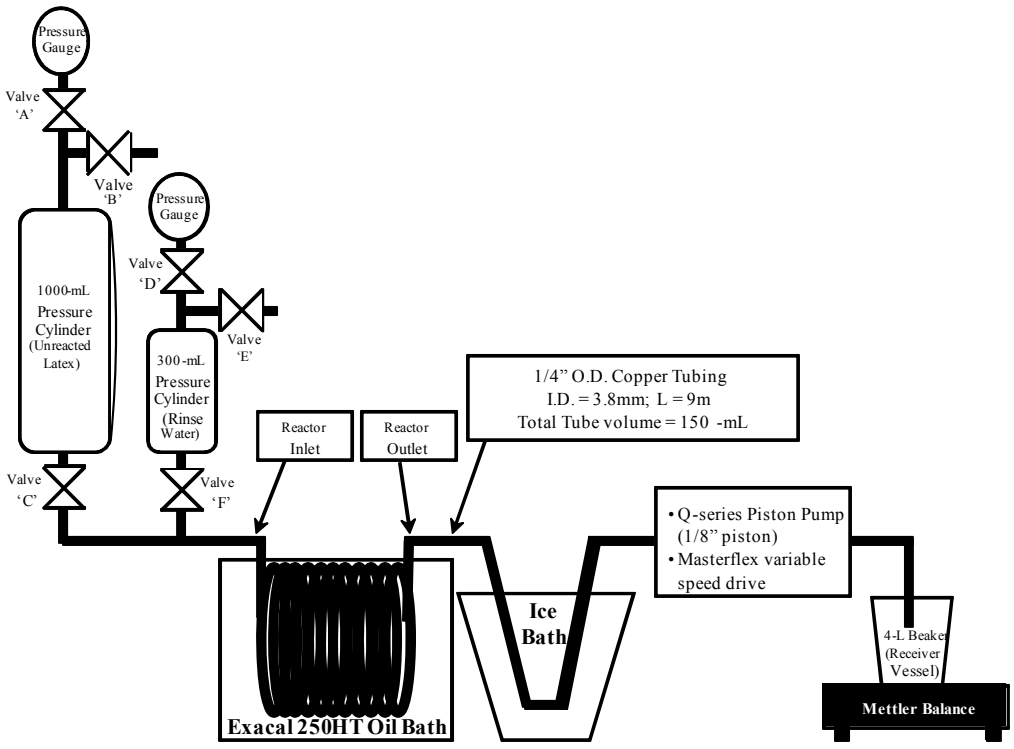

Figure 4-3. Continuous Tubular Reactor - Iteration #2.

In this case, the unreacted latex was charged into the 1-L pressure cylinder that was positioned upstream of the reactor inlet. The cylinder was then pressurized to 400 kPa with nitrogen to provide a backpressure to eliminate the backflow problems that were encountered in the original reactor design. The piston pump was used to control latex feed rate.

Several unsuccessful experiments were run with this apparatus, with two significant problems encountered:

1) The piston pump seized several times, and it was found that this was caused by latex particles. Unreacted latex was compatible with the pump, but the piston would jam once the latex started to react and form solid particles. This resulted in bent or broken pistons that were scrapped.

2) All of the experiments produced broad molecular weight distribution polymer, signifying that the NMP mechanism was not working as desired. The cause for the loss of polymerization control was unclear during these initial experiments, although it was likely caused by startup of the reaction with water filling the reactor (see discussion in next section).

4.4.3 Iteration #3 – Stainless Steel Tubing and Metering Valve at Reactor Outlet

One theory for the loss of livingness in the initial experiments was that the copper tubing was somehow affecting the NMP mechanism. Therefore, a stainless steel tube reactor was built. To facilitate in the bending of the tubing, a smaller diameter tube (1/8") was used. Longer tubing length was required due to the reduced diameter, and the first stainless steel reactor was 30 metres in length (two 15 metre coil sections joined by a union).

A high pressure metering pump could not be identified for the low flow rates that were required for this process, so a metering valve was used instead. The apparatus details are shown in Figure 4-4:

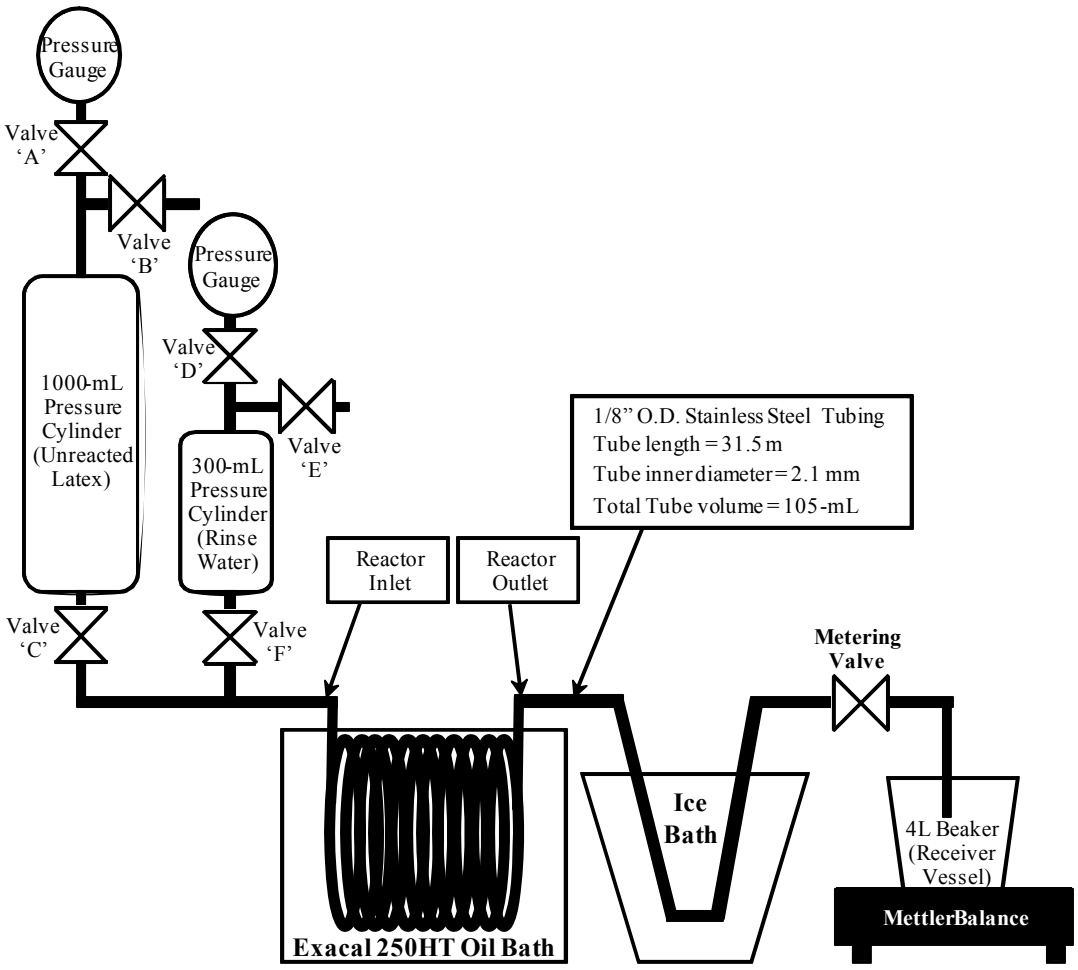

Figure 4-4. Continuous Tubular Reactor - Iteration #3.

Several unsuccessful experiments were run initially using this apparatus, with broad molecular weight distribution polymer forming in all cases. At the time, the tubular reactor was heated, and then pre-filled with deionized water prior to the reaction. The unreacted latex was then fed through the reactor following the water. It was postulated that the water was diluting the system such that free-nitroxide concentration was reduced to a point that the NMP mechanism became uncontrolled. Therefore, it was decided to prefill the reactor with unreacted latex instead of water before the reaction to

avoid any dilution effect. This was the change in operating procedure that enabled the first successful NMP reaction in the tubular reactor.

At this stage in the process development, the continuous reactor operating procedure was fairly well established. The operating procedure for the first successful continuous NMP semi-miniemulsion reaction using the apparatus in Figure 4-4 is described in the next section. Subsequent experiments also followed this general procedure with minor changes noted when appropriate.

4.4.4 NMP Miniemulsion in Continuous Tubular Reactor – Detailed Procedure

Step 1 partial bulk polymerization was done as described previously in Section 4.3.1.1. The bulk reaction went to 17% conversion, meaning that the final product was a solution containing approximately 17% polystyrene (TEMPO-capped) dissolved in 83% styrene monomer, along with free TEMPO. Molecular weight characteristics of the polymer (MN = 3126, MW = 3645, and PDI = 1.17) indicated that the NMP reaction was controlled due to the narrow PDI.

Step 2 dispersion was done as described in Section 4.3.1.2 to prepare the unreacted latex, and the tubular reactor oil bath was heated to 135°C. The unreacted latex was charged by vacuum into the 1-L sample cylinder of the tubular reactor apparatus. Oxygen was purged out of the unreacted latex by pressurizing/evacuating the cylinder five times with nitrogen at 400 kPa. The cylinder was pressurized through valve 'B' with 400 kPa nitrogen and the cylinder was sealed. Once the oil bath reached 135°C, the continuous reactor was filled with latex by opening Valve 'C' followed by opening the metering valve at the end of the reactor. When latex was observed exiting the reactor, the metering valve was closed. Latex flow rate was set by monitoring product collection

on the Mettler balance and adjusting the metering valve to achieve the desired flow rate for the experiment. The first 210 mL of material (two reactor residence times) collected at the reactor outlet was discarded as waste during these experiments, and product collection was started.

Feed rate was set based on the desired mean residence time distribution in the reactor (Table 1). The actual feed rate was very inconsistent (stop-and-go) due to difficulties with metering valve clogging, and the overall average flow rate and mean residence time is reported in the table.

Table 4-1. Initial NMP Experiments in Tubular Reactor. Effect of Residence Time.

Experiment Number	Flow Rate (mL/min)	Mean Residence Time (hours)	% Solids	Mn	Mw	PDI	ppm Styrene (Residual)
1	0.58	3	16.2%	22537	32316	1.43	< 50
2	0.87	2	14.8%	17739	24837	1.40	< 50
3	1.73	1	14.7%	18033	24307	1.35	2973

Relatively narrow PDI indicated that the NMP reaction was controlled in all of these experiments. Full conversion was achieved using as low as a two hour residence time, while unreacted monomer was present using a one hour residence time. The reaction occurred relatively quickly due to the presence of ascorbic acid in the formulation, and this will be further explored in following sections. Since a controlled NMP reaction had now been successfully demonstrated in the tubular reactor for the first

time, the next step was to do some more structured experiments with more detailed analysis of the process and product. However, there were still some issues with metering the reactants in the existing apparatus, so some final modifications were made before embarking on further experiments.

4.5 Tubular Reactor Optimization

Problems with latex metering were encountered during the previously described experiments. The metering valves tended to clog over time during the experiments, causing significant fluctuations in feed rate. Several different types of metering valve were tested, but all of them showed the same clogging problem. A new type of 'high-pressure' peristaltic pump was identified at this time, and was tested as an alternative. This pump is capable of withstanding a backpressure of 690 kPa which is above the NMP miniemulsion reaction pressure, and the minimum flow rate is around 2.0 mL/minute. In order to achieve acceptable residence time at this flow rate, the reactor had to be lengthened considerably. This involved using a larger oil bath and adding nine more stainless steel coils to the original two coils, all connected with Swagelok unions. Also, a second 1-litre holding cylinder was added to the front-end of the reaction apparatus. This enabled long-term continuous reactions, because there was an ability to switch back and forth between the cylinders as they ran out of unreacted latex. The final reactor apparatus schematic is shown in Figure 4-5. This reactor apparatus has been used for all experiments described in the rest of this document, with minor modifications (e.g., removal or addition of additional tube coils). This apparatus design was also adapted for a separate study of ATRP in a tubular reactor.[3]

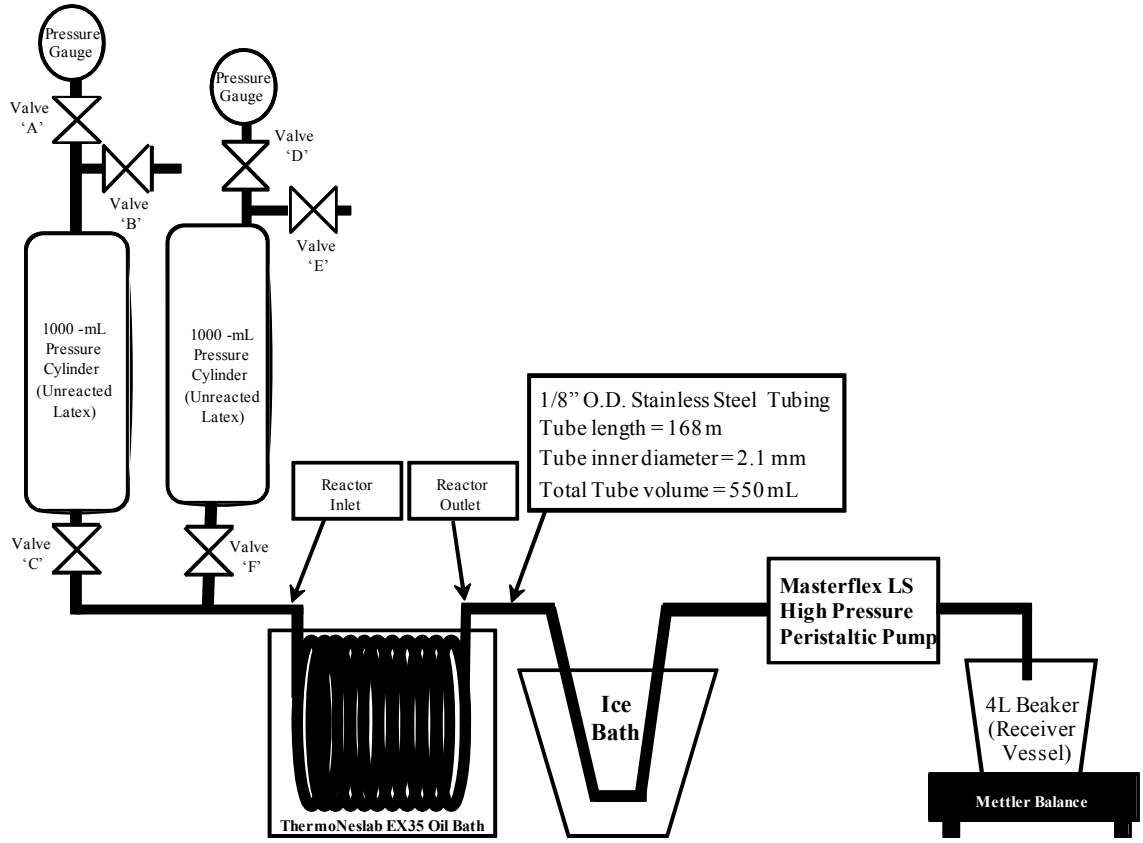

Figure 4-5. Final Optimized Tubular Reactor Apparatus.

4.6 Scoping Experiments

At this point in the investigation, NMP miniemulsion latexes had successfully been demonstrated in a continuous tubular reactor for the first time. The remainder of this chapter describes some further scoping experiments that were done to probe the reaction space that was under investigation and to begin preliminary comparison with materials produced in a batch reactor. The main purpose of the scoping experiments was to ensure that the proper reaction conditions and experimental techniques were being used to compare the batch and continuous reactions.

Comparison of results between a continuous tubular reactor and batch reactor are somewhat difficult, since it is not as easy to remove batch samples at specific time

intervals during the reaction in a tubular reactor. One possible solution for this problem would be to add 'T-junctions' at various intervals along the reactor for sample removal. However, it was felt that this would disrupt the flow pattern significantly in the reactor and have an effect on the kinetic results. In this work, samples were removed for analysis at intervals during the start-up of the continuous reactor. When the experiment first started, the latex immediately at the reactor outlet was sampled and had not yet started to react (i.e., this sample would represent time-zero of the reaction). Samples that were then collected from the reactor outlet over time had reacted to a higher conversion until the initial charge of unreacted latex had been fed through the reactor. During start-up, samples were collected at an 8-minute interval around the desired point of interest. For example, if a sample was desired after 60-minutes of reaction, latex was collected from the reactor outlet between 56 minutes and 64 minutes. When one full residence time had been completed, the collected latex should be consistently reacted to the same conversion (i.e., this represents the final product). At this point, larger samples were collected as final product and steady state was assumed. This assumption was tested and is discussed further in Chapter 5.

4.6.1 Initial Experiments – Ascorbic Acid vs. No Ascorbic Acid / Batch vs. Continuous

The starting point for more detailed experimentation was to investigate the kinetics of reactions with and without ascorbic acid present, and to run head-to-head experiments in a batch reactor and the continuous tubular reactor. Four experiments were initially done both with and without ascorbic acid (AA), and in batch and continuous reaction mode.

Partial bulk prepolymer solution was prepared as described in Section 4.3.1.1. The bulk reaction went to 9.7 % conversion, meaning that the final product was a solution containing approximately 9.7 % polystyrene (TEMPO-capped) and 90.3 % styrene monomer, along with free TEMPO. Molecular weight characteristics of the polymer (Mn = 1870, Mw = 2165, and PDI = 1.16) indicated that the NMP reaction was controlled due to the narrow PDI.

Step 2 dispersion was done as described in Section 4.3.1.2 to prepare the unreacted latex, and the tubular reactor oil bath was set at 135°C. In these experiments, the latex was prepared using three passes through the piston homogenizer during dispersion of the unreacted latex. Average residence time was 4 hours for all of the experiments which corresponded to 2.33 mL/minute in the continuous reactor. Analytical results for the final product are shown in Table 4-2, while conversion results over time are shown in Figure 4-6.

Table 4-2. Batch versus Continuous NMP Miniemulsion. Effect of Ascorbic Acid. Three Homogenizer Passes.

Experiment Number	% Solids	GPC Analysis			GC Analysis		Particle Size	
		Mn	Mw	PDI	ppm Styrene (Residual)	% Conversion (Calculated)	Vol. Mean (nm)	Num. Mean (nm)
4 (Batch; AA)	17.1%	37549	55341	1.47	248	99.8	64.8	56.8
5 (Cont.; AA)	14.0%	21722	27802	1.28	<100	>99.9	66.1	54.0
6 (Batch; No AA)	18.0%	28625	73072	2.55	5906	96.4	67.1	46.8
7 (Cont.; No AA)	13.1%	16912	21004	1.24	2832	98.3	53.8	32.6

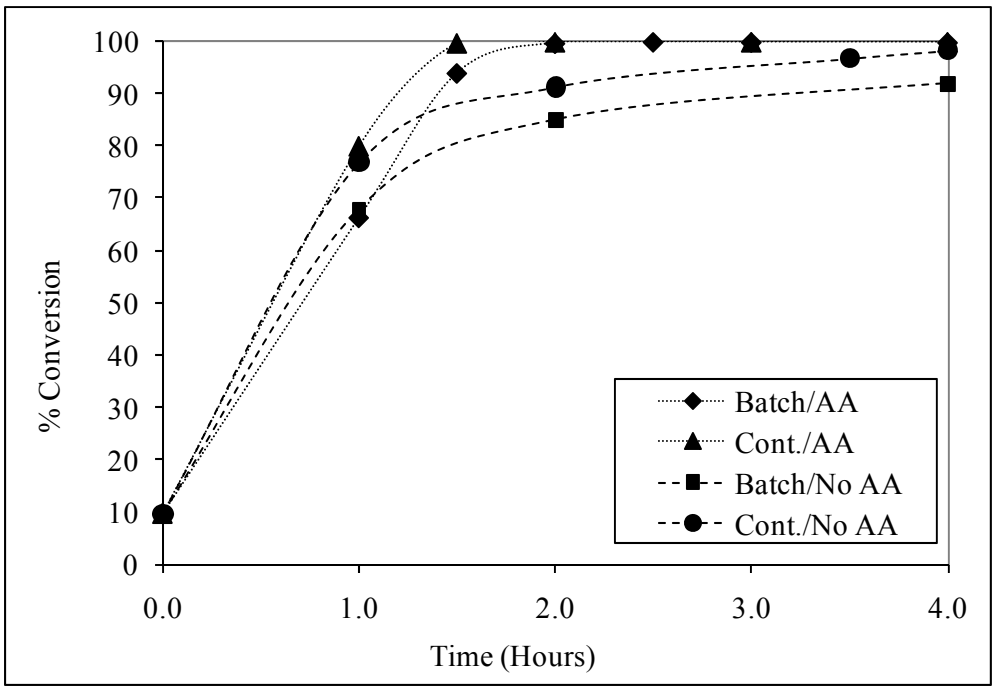

Figure 4-6. Batch versus Continuous NMP Miniemulsion. Effect of Ascorbic Acid on Conversion. Three Homogenizer Passes.

Reaction rate was significantly faster when ascorbic acid was present in the formulation. The rate enhancing behavior of ascorbic acid was described earlier, so this was an expected result.

Reaction rate seemed to be slightly faster in the continuous reactor during these reactions. This is likely due to the 'time-zero' assumption that was used for the batch reactor. That is, the heating rate was slow as described earlier, and time zero was taken to be at 110°C. The reactor took approximately one hour to heat between 110°C and 135°C, during which time the reactants were polymerizing at lower temperature than the reactants in the tubular reactor. The continuous reactor also seemed to give slightly better control of the NMP reaction, as evidenced by the slightly narrower molecular weight polydispersities that were achieved.

Molecular weight PDI was relatively low and indicated controlled NMP conditions in all cases except the batch reaction without ascorbic acid (Experiment 6). This was unexpected, and it suggested that the continuous reactor has some benefit over the batch reactor in maintaining control of the NMP mechanism. The reason for the loss of NMP control turned out to be the slow temperature ramp in the batch reactor, and this is discussed in Section 4.6.3.

Significant reactor fouling was observed in both of the batch reactors. Solids loading for the product from the continuous reactors was significantly lower than expected (theoretical solids loading at full conversion should be 19.9%), and this suggested that material was also being lost to fouling on the tube walls. It was theorized that the latex may have been unstable because the particle size was too small. These were the first experiments that used three homogenizer passes to prepare the latex, and the particle size was well below the usual 100-120 nm range that was observed previously. To test this hypothesis, a set of experiments was done using only two homogenizer passes to create larger particle size latex.

4.6.2 Two Homogenizer Passes

The above set of experiments was repeated using only two passes through the piston homogenizer. In this set of experiments, the step one bulk prepolymer reaction went to 12.2 % conversion. Molecular weight characteristics of the polymer (Mn = 3186, Mw = 3637, and PDI = 1.14) indicated that the NMP reaction was controlled due to the narrow PDI. Analysis of the final miniemulsion product is shown in Table 4-3 and conversion versus time data is shown Figure 4-7.

Table 4-3. Batch versus Continuous NMP Miniemulsion. Effect of Ascorbic Acid. Two Homogenizer Passes.

Experiment Number	% Solids	GPC Analysis			GC Analysis		Particle Size	
		MN	MW	PDI	ppm Styrene (Residual)	% Conversion (Calculated)	Vol. Mean (nm)	Num. Mean (nm)
8 (Batch; AA)	19.9%	38427	49210	1.28	<100	>99.9	122.6	84.6
9 (Cont.; AA)	19.9%	37244	47313	1.27	<100	>99.9	120.0	80.1
10 (Cont.; AA)	19.9%	36932	46228	1.25	<100	>99.9	118.3	78.0
11 (Batch; No AA)	19.1%	29717	64376	2.17	4893	96.9	100.1	62.9
12 (Cont.; No AA)	18.1%	27304	31808	1.16	12348	92.2	117.1	70.6

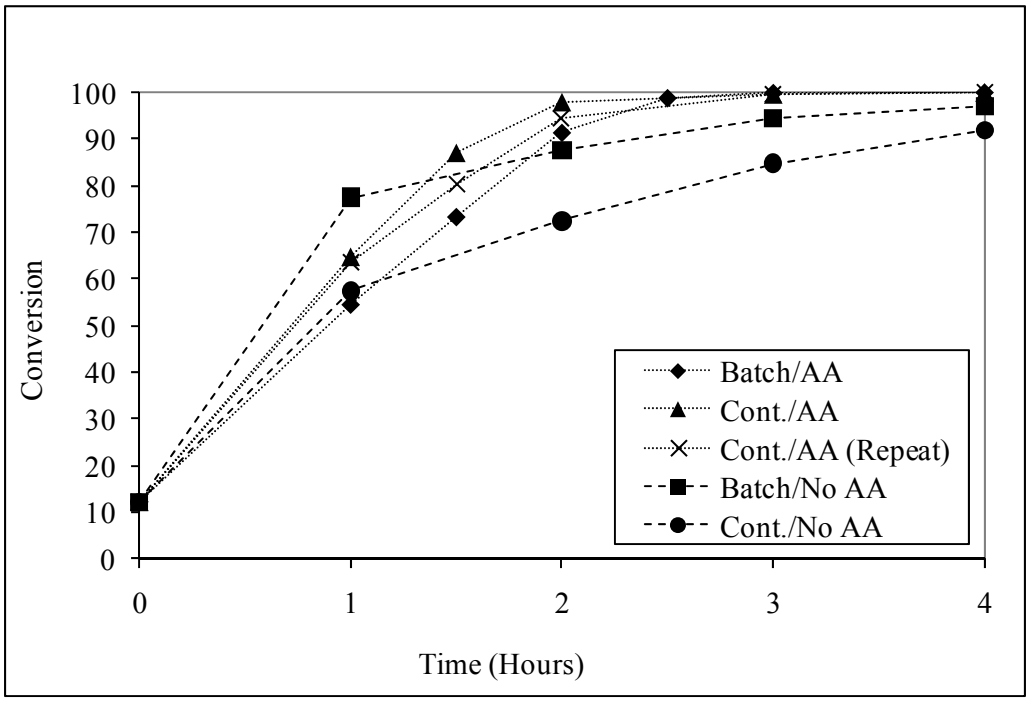

Figure 4-7. Batch versus Continuous NMP Miniemulsion. Effect of Ascorbic Acid on Conversion. Two Homogenizer Passes.

Minimal fouling was observed in all batch experiments in this set, and solids analysis of the final product for all experiments indicated that the latex did not lose any polymer to fouling. Volume average particle size was approximately twice the size as in the previous experiments that used three homogenizer passes. This suggests that the small particle size in the previous experiments destabilized the latex, and this set of conditions is more appropriate for running these NMP miniemulsion experiments.

Ascorbic acid increased the reaction rate significantly as expected. However once again the conditions of batch reaction without ascorbic acid (Experiment 11) resulted in high polydispersity, indicating loss of NMP mechanism control. The reactions without ascorbic acid (Experiments 11 and 12) were repeated and results are shown in Table 4-4 and Figure 4-8. These results verified that something about the batch reaction procedure was causing the NMP reaction to lose control.

Table 4-4. Repeat Experiments: Batch and Continuous without Ascorbic Acid.

Experiment Number	% Solids	GPC Analysis			GC Analysis		Particle Size	
		MN	MW	PDI	ppm Styrene (Residual)	% Conversion (Calculated)	Vol. Mean (nm)	Num. Mean (nm)
15 (Batch; No AA)	19.4%	26400	63904	2.42	1000	99.3	113.3	68.9
16 (Cont.; No AA)	18.2%	25472	32325	1.27	9200	93.7	127	76.5

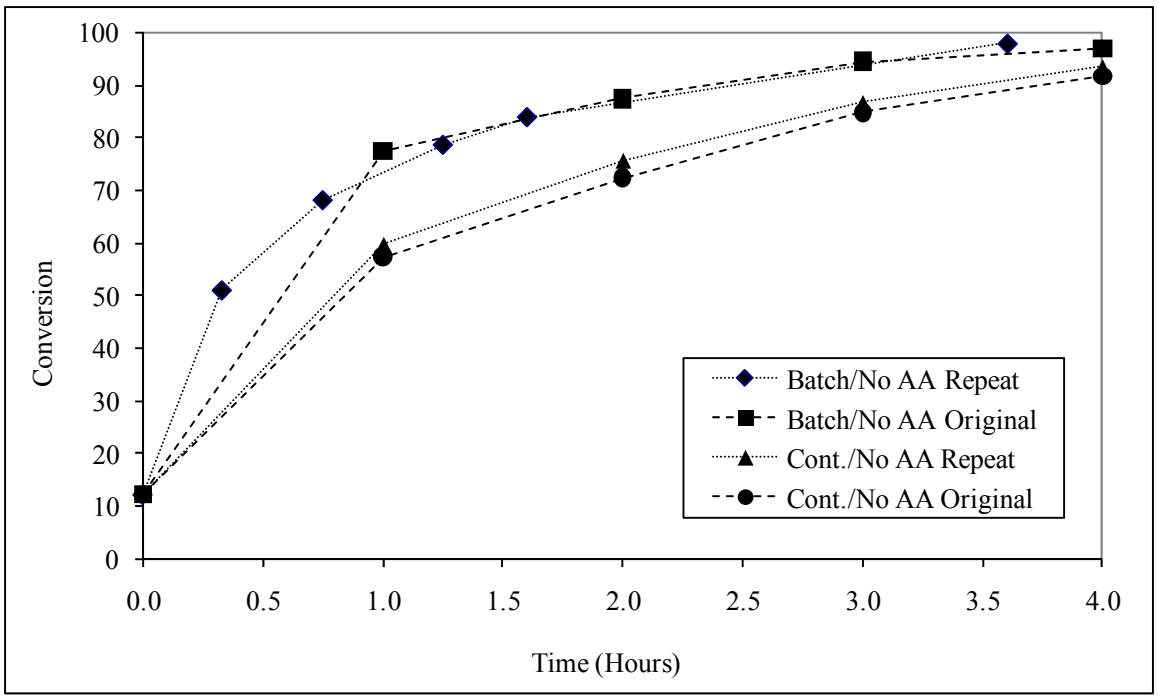

Figure 4-8. Repeat Experiments. Batch and Continuous without Ascorbic Acid.

4.6.3 Effect of Batch Reactor Heating Profile

The loss of NMP control in the batch reactor was unexpected based on earlier experiments that had been done in this lab in a smaller Parr reactor system under similar conditions. The only significant difference between the two batch reactors, besides scale, appeared to be the temperature heating profile in that the Parr reactor heated much faster than the Buchi reactor. Therefore, the batch reactions with no ascorbic acid from the previous section (Experiments 11 and 15) were repeated in a 300 mL Parr reactor under two different heating profiles. In the first experiment, the slow heating profile of the 2-L Buchi reactor was used and the reactor reached 135°C in approximately 2.5 hours. In the second experiment, the Parr reactor was heated as fast as possible and it reached 135°C in approximately 15 minutes. For these experiments, only the molecular weight information

was analyzed to determine if the NMP reaction was under control in either case, and the results are summarized in Table 4-1.

Table 4-5. Batch Reaction without Ascorbic Acid in Parr reactor. Effect of Heating Profile.

Experiment Number	Heating Profile	GPC Analysis		
		MN	MW	PDI
17	Slow	21589	52030	2.41
18	Fast	23054	31353	1.36

The slow reactor heat up causes loss of control of the NMP reaction when ascorbic acid is not present, as seen by the higher than expected weight average molecular weight and polydispersity. This result is reproducible as described below, so it is a real effect. The data suggests that a significant number of polymer chains undergo a termination reaction during the slow temperature ramp, resulting in increased population of higher molecular weight material. Clearly an unexpected side reaction occurs within a certain temperature range below the reaction temperature, but the exact nature of this side reaction is currently unclear and further study is required. Until this is better understood, it is important to maximize the heating rate to reaction temperature for this system to ensure good control of the polymerization.

To address this issue with the 2 L Buchi batch system, a bypass line was added to the glycol bath/reactor jacket system to allow preheating of the bath. The glycol bath is isolated from the Buchi reactor jacket and preheated to the desired reaction temperature and then the glycol stream is diverted to the Buchi jacket. This enables a much faster heating profile, and a typical time temperature profile is shown in Figure 4-9.

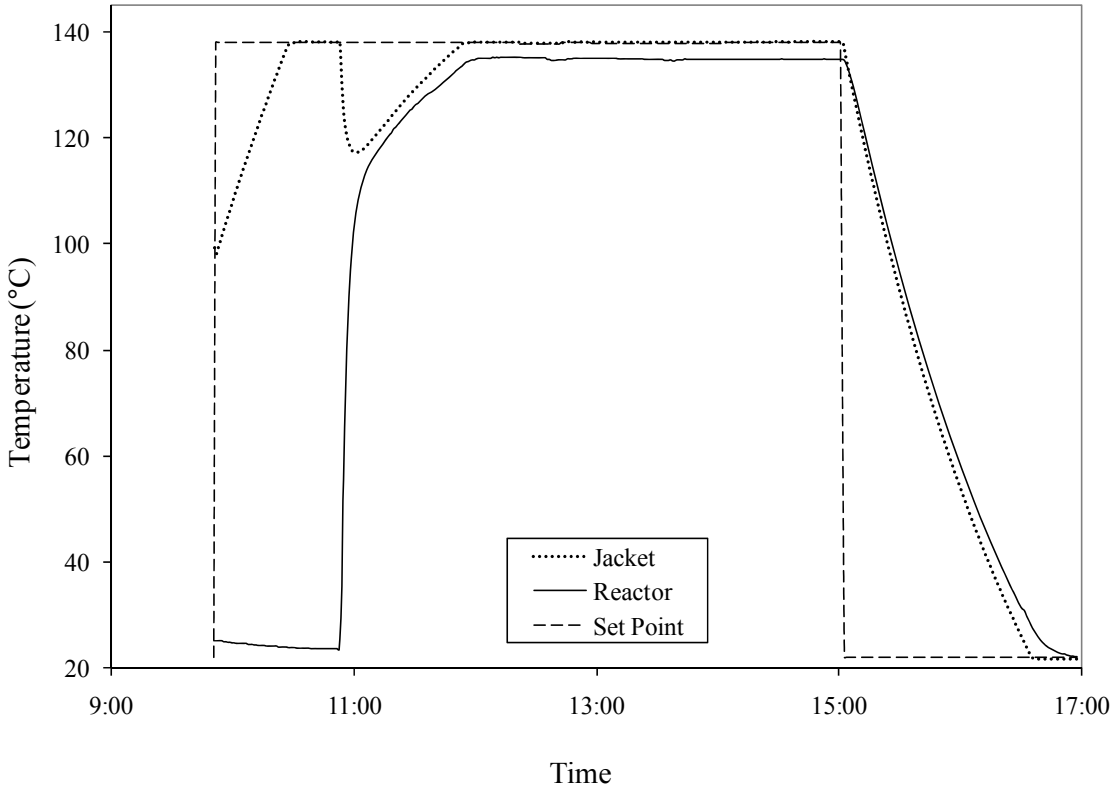

Figure 4-9. Batch Time Temperature Profile for Modified Buchi Reactor.

The modified Buchi reactor heats up to 115°C in approximately 15 minutes using this apparatus, compared to about 1.75 hours in the earlier experiments. It then takes approximately 1 hour to increase from 115°C to the 135°C setpoint. To test this apparatus, another batch NMP miniemulsion polymerization was done without using ascorbic acid (Experiment 19). This was for comparison with the analogous experiments that were previously done using the slowly heated Buchi reactor (Experiments 11 and 15; NMP not controlled), slowly heated Parr reactor (Experiment 17; NMP not controlled), and fast heated Parr reactor (Experiment 18; NMP controlled). The results of all these experiments are tabulated in Table 4-6, and it is clear that the NMP was brought back under control with the improved heating.

Table 4-6. NMP Miniemulsion without Ascorbic Acid. Effect of Slow versus Fast Heating Profile.

Experiment Number	Reactor	Heating Profile	GPC Analysis		
			MN	MW	PDI
11	2 L Buchi	Slow	29717	64376	2.17
15	2 L Buchi	Slow	26400	63904	2.42
17	300 mL Parr	Slow	21589	52030	2.41
18	300 mL Parr	Fast	23054	31353	1.36
19	2 L Buchi	Fast	23719	29539	1.25

4.6.4 Ascorbic Acid – Room Temperature Initiation

At this point in the study, there were some unusual observations when using ascorbic acid in the NMP miniemulsion formulation. During several experiments, the homogenizer became clogged during the homogenization step when ascorbic acid was present in the formulation. Troubleshooting indicated that the latex was actually polymerizing in the homogenizer, and this did not occur when ascorbic acid was not present. As a workaround, ascorbic acid was added to the unreacted latex after the homogenization step. In this case, it was observed that a large amount of heat was generated in the latex when the ascorbic acid was added at room temperature, indicating that polymerization was occurring. A small set of experiments was done to probe this phenomenon where latex samples were dried directly after the homogenization step and the results are shown in Table 4-7.

Table 4-7. Effect of Ascorbic Acid at Room Temperature.

Experiment Number	Ascorbic Acid Added	Sample Detail	Latex % Solids	GPC Analysis		
				MN	MW	PDI
20	No	Unreacted Latex	4.2%	2117	2434	1.15
21	No	Polymerized Latex (from Expt 20)	19.0%	26836	35263	1.31
22	Yes - Before homogenization	Unreacted Latex	19.5%	138203	565352	4.09
23	Yes - After Homogenization	Unreacted Latex	19.5%	136063	565942	4.16

This set of experiments demonstrates that polymerization was being induced by ascorbic acid at room temperature to the point that full conversion was achieved without any external heating. The reaction proceeded similar to a conventional free radical polymerization process, so molecular weight and PDI was significantly higher than a controlled NMP reaction. By comparison, the latex that was made without ascorbic acid showed no sign of polymerization in the unreacted latex. The latex without ascorbic acid was further polymerized to completion in the 2 L Buchi batch reactor as usual, and the product had low PDI that is indicative of a well controlled NMP reaction.

A substantial amount of troubleshooting was done to determine why ascorbic acid had worked in earlier scoping experiments and then started to demonstrate this room temperature polymerization phenomenon. It is possible that the phenomenon was present in the earlier experiments to a smaller degree but was not noticed. It is also possible that a new lot of one of the raw materials induced this change, but nothing could be identified to explain the phenomenon. At this point in time during the study, it was decided to focus primarily on reactions without ascorbic acid for simplicity and to pass this

phenomenon on to someone else for further study. Osti et al. proceeded with this work and it turns out that there is an interaction between ascorbic acid and the SDBS surfactant that forms a redox initiation system.[4] Further study is required to fully explain this phenomenon in the current miniemulsion system so that it can be understood why some reactions proceeded in a controlled manner in the presence of ascorbic acid while some polymerized in an uncontrolled manner at room temperature.

4.7 Conclusions

A continuous tubular reactor was designed and built for producing controlled NMP miniemulsion reactions. The optimum design required pressurized sample cylinders at the reactor inlet to serve as reactant holding vessels, and reactant flow was controlled by a high pressure peristaltic pump at the reactor outlet. Piston pumps were found to be unsuitable for this application because the small particles of the latex product seized and damaged the pistons.

Initial scoping experiments demonstrated that controlled NMP reactions could be completed to full conversion in the continuous reactor in the presence of ascorbic acid. It was shown that latexes became unstable and reactor fouling occurred below a certain particle size (< 100 nm). Preliminary comparison between batch and continuous reactors showed that the batch apparatus was not suitable for a direct comparison. Notably, the slow temperature ramping rate of the batch reactor caused loss of NMP control. The batch reactor was modified to increase the temperature ramping rate, and NMP control was achieved. Anomalous experimental results were observed when using ascorbic acid in the NMP formulation, and it was determined that it was causing polymerization initiation at room temperature.

At this point in the study it was felt that reaction conditions without ascorbic acid were suitable to enable a well controlled NMP reaction, and the batch reactor and tubular reactor operating conditions were suitably understood. Therefore the next step of the study was to do a more detailed comparison of the reaction kinetics between the continuous and batch reactors, and this is described in the next chapter.

.

4.8 References

1. Keoshkerian, B.; MacLeod, P. J.; Georges, M. K. *Macromolecules*, **2001**, *34*, 3594.

2. Keoshkerian, B.; MacLeod, P. J.; Odell, P. G.; Georges, M. K. US Patent 6,469,094 **2002**, assigned to Xerox Corporation.

3. Muller, M.; Cunningham, M. F.; Hutchinson, R. A. *Macromol. React. Eng.* **2008**, *2*, 31.

4. Osti, M.; Cunningham, M. F.; Whitney, R.; Keoshkerian, B. *J. Polym. Sci., Part A: Polym. Chem.* **2007**, *45*, 69.

Chapter 5

Nitroxide-Mediated Polymerization of Styrene in a Continuous Tubular Reactor

published in Macromolecular Rapid Communications 2005, 26, 221-225.

5.1 Preface

The previous chapter described the successful development of a continuous tubular reactor for producing polymer latex using a controlled NMP miniemulsion process. Also, scoping experiments helped to develop and good basic understanding of the reaction conditions that were appropriate for the system. This chapter expands the earlier work by presenting a more detailed comparison of the differences between running the NMP miniemulsion polymerization in a batch reactor versus the continuous reactor. More detailed kinetic analysis is shown, and further validation of the controlled nature of the polymerization is demonstrated by chain extension of the polymer latex.

5.2 Abstract

Nitroxide-mediated polymerization of styrene has been demonstrated for the first time in a continuous tubular reactor. The polymerization kinetics in the tubular reactor are similar to those in a batch reactor. Number average molecular weight increases linearly with conversion and chain extension experiments were successful, indicating that the living nature of the polymerization is maintained in the tubular reactor.

5.3 Introduction

Interest in free radical polymerization has been reinvigorated since the development in the 1990's of several techniques that allow for unprecedented reaction control. Three methods of controlled radical polymerization (CRP) have been the focus of numerous studies over the past decade: nitroxide-mediated polymerization (NMP),[1,2] atom transfer radical polymerization (ATRP)[3] or metal-catalyzed radical polymerization,[4] and reversible addition-fragmentation transfer polymerization (RAFT).[5] These processes enable narrow molecular weight polydispersity, block copolymers, and other complex architectures that were previously difficult or impossible to achieve using conventional free radical polymerization techniques.

Most early CRP studies were done using homogenous bulk or solution polymerization processes, while more commercially attractive aqueous-based heterogeneous techniques such as emulsion and miniemulsion have recently been investigated.[6-12] Batch reactors have been used for most of these studies, but it would be of great value to demonstrate these processes in a continuous reactor. The improved economics of a continuous reactor may be a significant incentive towards commercialization of CRP processes.

There are few references in the literature regarding controlled free radical polymerization in a continuous reactor. Homogeneous bulk ATRP of methyl methacrylate in a continuous packed bed has been demonstrated successfully by Zhu et al..[13,14] They demonstrated the potential for molecular weight control through adjustment of reactant feed rate, along with the feasibility of easily preparing block copolymers in a continuous reactor system.[15] Durant discussed miniemulsion

polymerization using a "double" surfactant technique to improve latex stability.[16] Schork and Smulder[17] have discussed the theoretical aspects of CRP in continuous reactors for reversible addition-fragmentation transfer (RAFT) polymerization and reversible termination polymerization (NMP and ATRP) mechanisms. It is predicted that molecular weight distribution polydispersity index approaches two for a homogeneous CSTR instead of the value of unity predicted for a batch reactor. For a segregated CSTR, used to emulate a miniemulsion polymerization process, the polydispersity is predicted to always exceed that of the homogeneous CSTR. Russum et al. have recently described RAFT miniemulsion experiments in a tubular reactor.[18] Stable latexes were produced in the tubular reactor and the polymerization exhibited living nature. However, the tubular reactor produced polymer with higher polydispersity than comparable samples that were produced in a batch reactor. This was attributed to back-mixing or axial dispersion.

There are several potential benefits of using a continuous tubular reactor in miniemulsion SFRP. The ease of synthesizing polymers with controlled microstructure (e.g., diblocks, triblocks) will be simplified, because feed streams situated along the reactor can be used to introduce additional monomers (or mixtures of monomers). Furthermore, manipulation of the flow rate allows control of the conversion at which the additional monomer(s) are added. A tubular reactor also permits better control of the temperature profile, including the heating up period and temperature changes during polymerization, both of which influence polymer properties. Furthermore, operating a stirred tank-type reactor under pressure poses operating and technical concerns, while running a tubular reactor under the same pressure is a routine practice easily done in at scales ranging from the laboratory (e.g. HPLC/GPC equipment) to industrial scale. Even

the adaptation of our approach to continuous microreactors (including polymerizations in microfluidic channels) is feasible.

There have been no reports on nitroxide-mediated polymerization in a continuous reactor. This paper describes initial results using a continuous tubular reactor to produce stable polystyrene latexes by nitroxide-mediated miniemulsion polymerization.

5.4 Experimental

5.4.1 Apparatus

Continuous reactions were done in a stainless steel tube (167 m length; 3.2 mm outer diameter; 2.05 mm inner diameter) immersed in an oil bath at 135°C. Flow was controlled by a Masterflex high-pressure peristaltic pump situated at the outlet of the reactor tube. A schematic of the apparatus is shown in Figure 5-1.

Simultaneous batch reactions were also done as a comparison to the continuous reactions. These were done in a 2 L stainless steel Buchi reactor fitted with a four bladed pitch blade impeller.

5.4.2 Materials

Styrene (Apco), benzoyl peroxide (BPO; Aldrich; Luperox A75FP), TEMPO (Z.D. Chemipan), dodecylbenzene sulphonic acid sodium salt (SDBS; Aldrich; tech.) were all used as received. Deionized water was used for all experiments.

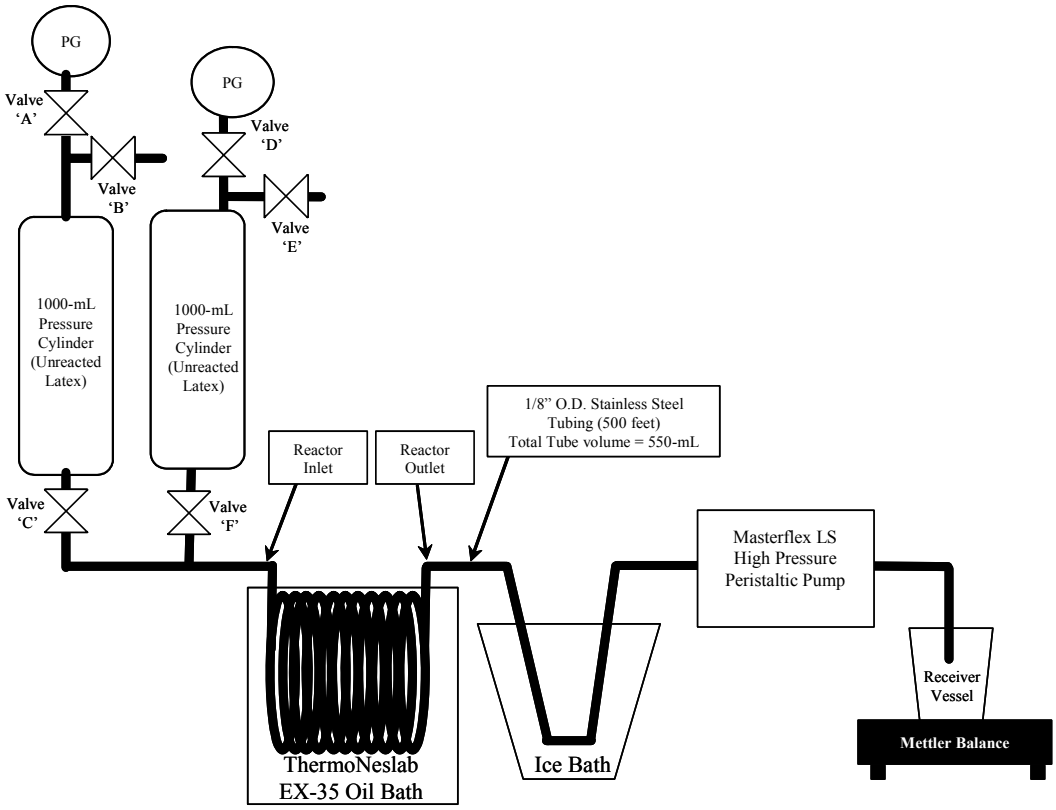

Figure 5-1. Schematic of continuous tubular reactor apparatus for nitroxide-mediated miniemulsion polymerization.

5.4.3 Analysis

Molecular weight and polydispersity index (PDI) were measured by gel permeation chromatography (GPC) using a Waters/Millipore liquid chromatograph equipped with a Waters model 510 pump, Ultrastyragel columns of pore size 10^5 Å, 10^4 Å, and 10^3 Å in series with a Styragel HR0.5 column, a Waters model 410 differential refractometer (RI), and a Waters model 486 tunable absorbance detector (UV). Polystyrene standards were used for calibration. Tetrahydrofuran was used as the eluant at a flow rate of 1.0 mL min^{-1}. Conversion was analyzed gravimetrically by drying latex samples overnight at room temperature, then vacuum drying at 50°C for eight hours.

Particle size analysis was done by dynamic light scattering using a NICOMP model 370 submicron particle sizer.

5.4.4 Procedure

A modified miniemulsion polymerization was used for the experiments.[19,20] Styrene was first bulk polymerized to low conversion in the presence of TEMPO, the nitroxide mediating agent. This monomer-polymer mixture was dispersed in the aqueous phase to form the miniemulsion which was then polymerized in the tubular reactor. There are two reasons why this approach was used. First, miniemulsion polymerization methods require the use of a costabilizer to ensure latex stability. Typically this costabilizer is a hydrophobic additive such as hexadecane. In our modified miniemulsion procedure, the low conversion polystyrene oligomer acts as the costabilizer, thus eliminating the need for an extra additive. The second reason for using the modified miniemulsion process is that the polymer chains are initiated prior to formation of the miniemulsion. Thus when the miniemulsion latex is formed, all of the particles are nucleated and complex nucleation and partitioning issues are eliminated. Note that we chose to do the bulk prepolymerization step in batch during these initial scoping experiments, as we wanted to focus initially on the more challenging miniemulsion step in continuous mode. It is our intent, however, to develop a fully continuous process which integrates both the bulk prepolymerization and miniemulsification steps.

The bulk polymerization step was done in batch using the 2 L Buchi reactor described above. 1473.6 g styrene, 16.2 g BPO, and 10.2 g TEMPO were dissolved in 1473.6 g styrene by mixing at 450 rpm in the Buchi reactor. The reactor was heated to

135°C over a period of 30 minutes, held at 135°C for one hour, and then cooled to room temperature. 696 g of the resulting monomer-polymer mixture (SFRP-BULK prepolymer) was then mixed with an aqueous phase that consisted of 61 g SDBS dissolved in 3076 g deionized water. Miniemulsion latex was prepared by passing this mixture once through a Niro Soavi piston homogenizer (400-600 bar pressure). The miniemulsion latex was then split between the continuous and batch reactors where reactions were done at 135°C.

To begin the continuous reactions, the reactor tube was quickly filled from Cylinder#1 with latex that was prepared in the previous step. The peristaltic pump was then started at the desired feed rate to begin latex feed from Cylinder #2. The mass feed rate was calculated by monitoring the collected latex on a balance at the reactor outlet. At this point, Cylinder #1 was refilled with more latex for use later in the reaction when Cylinder #2 was emptied.

Kinetic analysis is more difficult in a continuous reactor compared to a batch reactor, since it is not possible to remove batch samples at specific time intervals during the reaction. One possible solution for this problem would be to add 'T-junctions' at various intervals along the reactor for sample removal. However, it was felt that this would disrupt the flow pattern significantly in our reactor and have a negative effect on the kinetic results. This option may be explored in future experiments, but a different method was used for the experiments described in this report.

In this work, samples were removed for analysis at intervals during the start-up of the continuous reactor. When the experiment is first started, the polymer that exits the reactor has not yet started to react. The material that is then collected from the reactor

outlet over time has reacted to an integrally higher conversion until the initial startup plug of latex has flowed out of the reactor. During start-up, samples were collected at an 8-minute interval around the desired point of interest. For example, if a sample was desired after 60-minutes of reaction, latex was collected from the reactor outlet between 56 minutes and 64 minutes after startup. When one full residence time has been completed, the collected polymer should be consistently reacted to the same conversion. At this point, larger samples were collected and steady state was assumed. (Note: typically steady state is not achieved in a continuous reactor until several residence times have been completed,[21] this issue will be explored in future work).

5.5 Results and Discussion

Batch and continuous reactions both produced stable latexes, and minimal coagulum was observed in the reactors. Coagulum was quantified by soaking the reactors in THF at 60°C, then measuring the amount of dissolved coagulum gravimetrically. Back-calculation showed that the coagulum accounted for less than 0.5 wt% of the overall polymer in both the batch and continuous reactors. Volume mean particle size was 164 nm in the batch reactor with a standard deviation of 61 nm. In the continuous reactor, volume mean particle size was measured to be 170 nm with a standard deviation of 59 nm.

Figure 5-2 shows a comparison of kinetic results between batch and continuous tubular reactions. Note that the conversion starts at ~20% at time zero as a reflection of the partial polymerization that occurred in the initial partial bulk polymerization step. The reaction rate is almost identical between the batch and continuous reactors throughout most of the reaction. Conversion is slightly lower in the continuous reactor at

the end of the reaction. This may be caused by axial mixing within the tube during the experiment. Under perfect plug flow conditions, a tubular reactor should give the same conversion as a batch reactor within the same reaction time conditions. However, a dispersion model has been developed[22-24] which shows that conversion for a first-order reaction will decrease in a tubular reactor when axial mixing is present. Future work will include a residence time distribution analysis of the tubular reactor apparatus, and this will enable quantification of the axial mixing effect.

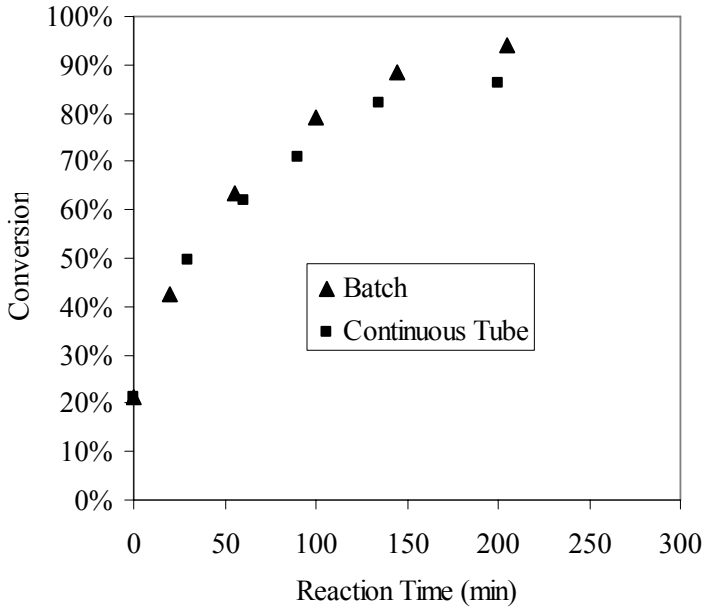

Figure 5-2. Conversion as a function of time for nitroxide mediated miniemulsion polymerization of styrene in batch (▲) and continuous tubular (■) reactors.

Figure 5-3 shows a plot of number average molecular weight (Mn) and polydispersity index (PDI) versus conversion. Number average molecular weight grows in a linear fashion, and polydispersity index is below 1.5 for batch and continuous reactions, indicating that the controlled nature of the polymerization mechanism has been maintained. Note that the experimental number average molecular weight lies slightly

above the theoretical Mn line, and this is indicative of some loss of chains due to termination.

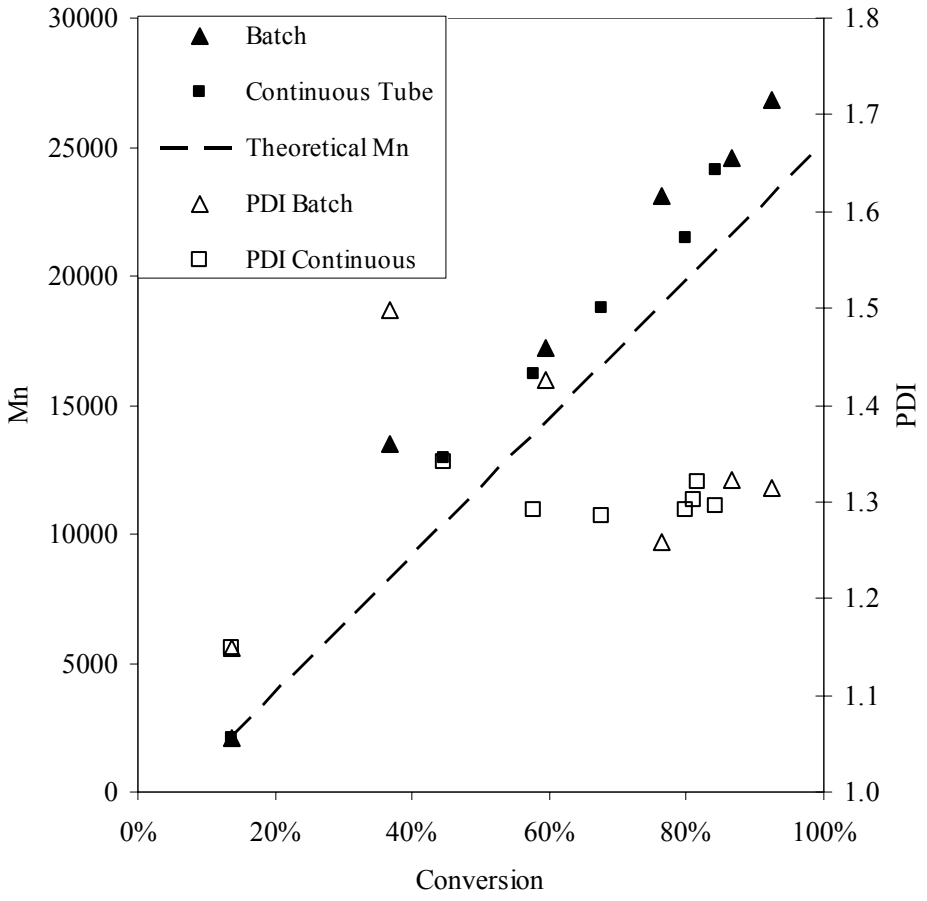

Figure 5-3. Number average molecular weight (filled symbols) and PDI (open symbols) as a function of conversion for nitroxide mediated miniemulsion polymerization of styrene in batch (▲) and continuous tubular (■) reactors. Dotted line (---) indicates theoretical.

Chain extension was performed on the polymer produced in the continuous tubular reactor to verify that the polymer chains were still active by demonstrating that they could react further. 95 g styrene was mixed into 650 g latex that was produced in the continuous tubular reactor. The mixture was stirred overnight to allow swelling of styrene into the polystyrene miniemulsion particles. This mixture was then fed through

the continuous tubular reactor at 135°C using a two hour average residence time. Figure 5-4 shows the evolution of molecular weight over time for the chain extension experiment. One can see that the original polymer chains continued to grow and maintained a relatively narrow PDI, indicating that the original miniemulsion polymer had living characteristics.

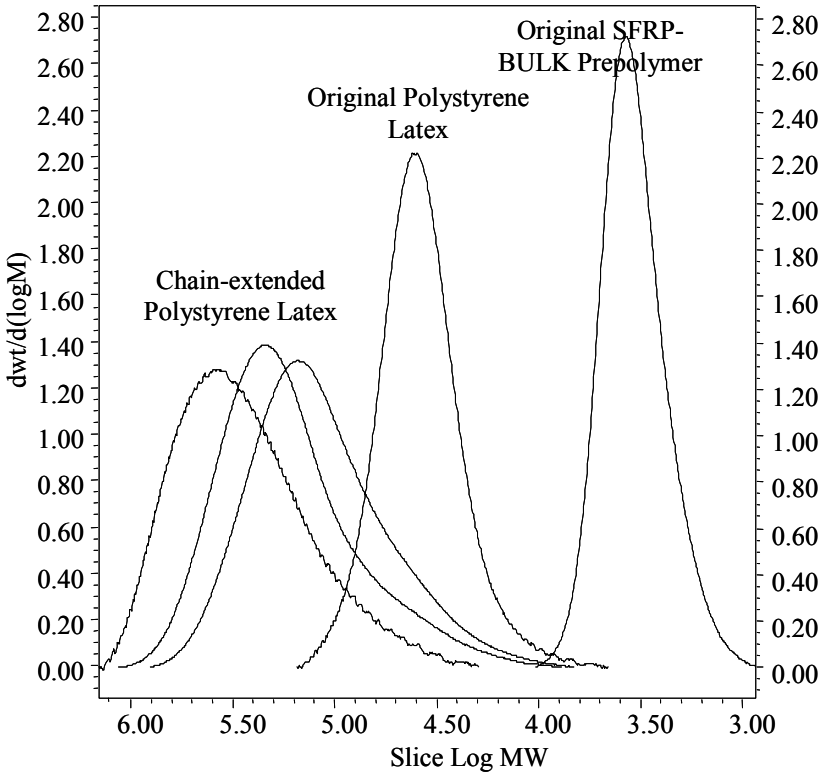

Figure 5-4. Evolution of molecular weight as measured by GPC for chain-extended latex in continuous tubular reactor. Molecular weight increases from right to left, with samples taken after 60, 90, and 120 minutes respectively.

5.6 Conclusions

Nitroxide-mediated miniemulsion polymerization of styrene was demonstrated for the first time in a continuous tubular reactor, resulting in stable latexes with minimal

coagulum formation. Kinetics were similar between batch and continuous reactors. Final conversion was slightly lower in the tubular reactor compared to the batch reactor, and this is attributed to axial mixing effects. Polymerization was controlled and the final product maintained living characteristics as indicated by narrow PDI and chain extension experiments. This initial work was done to determine the feasibility of this technology, and further detailed studies are now in progress based on the successful results. Full details of this work will be published in a future paper.

5.7 References

1. Georges, M. K.; Veregin, R. P. N.; Kazmaier, P. M.; Hamer, G. K. *Macromolecules*, **1993**, *26*, 2987.
2. Hawker, C. J.; Bosman, A. W.; Harth, E. *Chem. Rev*., **2001**, *101*, 3661.
3. Wang, J.-S.; Matyjaszewski, K. *J. Am Chem Soc.* **1995,** *117*, 5614.
4. Kato, M.; Kamigaito, M.; Sawamoto, M.; Higashimura, T. *Macromolecules*, **1995**, *28*, 1721.
5. Chiefari, J.; Chong, Y. K.; Ercole, F.; Krstina, J.; Jeffrey, J.; Le, T. P. T.; Mayadunne, R. T. A.; Meijs, G. F.; Moad, C. L.; Moad, G.; Rizzardo, E.; Thang, S. H. *Macromolecules* **1998,** *31*, 5559.
6. MacLeod, P. J.; Barber, R.; Odell, P. G.; Keoshkerian, B.; Georges, M. K. *Macromol. Symp*., **2000**, *155*, 31.
7. Charmot, D.; Corpart, P.; Adam, H.; Zard, S. Z.; Biadatti, T.; Bouhadir, G. *Macromol. Symp*., **2000**, *150*, 23.
8. Charleux, B. *Macromolecules*, **2000**, *33*, 5358.

9. Cunningham, M. F. *Prog. Polym. Sci*., **2002**, *27*, 1039.

10. Qiu, J.; Charleux, B.; Matyjaszewski, K. *Prog. Polym. Sci.*, **2001**, *26*, 2083.

11. Cunningham, M. F. *C. R. Chimie,* **2003**, *6*, 1351.

12. Uzulina, I.; Gaillard, N.; Guyot, A.; Claverie, J. *C. R. Chimie,* **2003**, *6*, 1375.

13. Shen, Y.; Zhu, S.; Pelton, R. *Macromol. Rapid Commun*., **2000**, *21*, 956.

14. Shen, Y.; Zhu, S.; Zeng, F.; Pelton, R. H. *Macromolecules*, **2000**, *33*, 5427.

15. Shen, Y. ; Zhu, S. *AIChE J.,* **2002**, *48*, 2609.

16. Durant, Y. G. *Polym. Mater. Sci. and Eng*., **1999**, *80*, 538.

17. Schork, F. J.; Smulders, W. *J. Appl. Polym. Sci*., **2004**, *92*, 539.

18. Russum, J. P.; Jones, C. W.; Schork, F. J. *Macromol. Rapid Commun*., **2004**, 25, 1064.

19. Keoshkerian, B.; MacLeod, P. J.; Georges, M. K. *Macromolecules*, **2001**, *34*, 3594.

20. Keoshkerian, B.; MacLeod, P. J.; Odell, P. G.; Georges, M. K. *US Patent 6,469,094* **2002**, assigned to Xerox Corporation.

21. Ouzineb, K.; Graillat, C.; McKenna, T. *J. Appl. Polym. Sci*., **2004**, *91*, 2195.

22. Danckwerts, P. V. *Chem. Eng. Sci*., **1953**, *2*, 1.

23. Fogler, H. S. *Elements of Chemical Engineering, 1st Edition*; Prentice-Hall: New Jersey, 1986, pp.697-706.

24. Levenspiel, O. *Chemical Reaction Engineering, 3rd Edition*; Wiley: New York, 1999.

Chapter 6

Nitroxide-Mediated Bulk and Miniemulsion Polymerization in a Continuous Tubular Reactor: Synthesis of Homo-, Di-, and Tri-block Copolymers

published in Macromolecular Reaction Engineering 2010, 4, 186-196.

6.1 Preface

This chapter describes further advancement of the NMP miniemulsion system that has been described so far in this work. The step one prepolymerization reaction is demonstrated for the first time in the continuous reactor followed by the miniemulsion step using this material. Copolymerization in the tubular reactor is also demonstrated for the first time with production of diblock and triblock copolymers.

6.2 Abstract

In previous work, a modified nitroxide-mediated miniemulsion polymerization was demonstrated in a continuous tubular reactor to prepare a latex of polystyrene homopolymer dispersed in water. There, the initial reaction step (low conversion bulk polymerization to prepare macroinitiator) was done in a batch reactor while the miniemulsion polymerization step was done in a continuous tubular reactor. The present paper describes an extension of that work in which all the reaction steps have been achieved in the continuous tubular reactor. Chain extension of the polystyrene latex to give poly(styrene-block-n-butyl acrylate) diblock copolymers and poly(styrene-block-n-butyl acrylate-block-styrene) triblock copolymers by miniemulsion polymerization in the tubular reactor is also described.

6.3 Introduction

Controlled or "living" radical polymerization is a relatively new technology that has been the subject of much recent study. These techniques improve control over polymer growth during polymerization reactions which enables the preparation of unique structures that cannot be made using conventional free radical polymerization methods. For example, structures that have been produced using controlled radical polymerization processes include block copolymers, surface grafted polymers, brush/comb polymers, and star polymers.[1]

The three most studied methods of controlled radical polymerization are nitroxide-mediated polymerization (NMP),[2-5] atom transfer radical polymerization (ATRP),[6-8] and reversible addition-fragmentation chain transfer polymerization (RAFT).[9-11]

The attribute that differentiates controlled radical polymerization processes from conventional free radical polymerization processes is the inclusion of a reversible activation-deactivation step within the reaction mechanism. This reduces the probability of polymer termination reactions, thus allowing polymer chains to remain "living" for much longer than was previously possible. Ideal living polymerization processes are defined by complete elimination of termination reactions, such that every polymer chain can continue to grow indefinitely given a monomer source. This ideal state cannot be achieved using current controlled radical polymerization processes, but termination processes are minimized to a degree that living conditions are approached.

The various controlled radical polymerization techniques were initially demonstrated using bulk and solution polymerization processes, while more recently,

aqueous-based processes have been studied and several detailed reviews have been published.[12-16] Aqueous-based NMP reactions using TEMPO as the nitroxide mediator have been most successful to date using miniemulsion techniques. Miniemulsion polymerization shares some features of emulsion polymerization, but there are differences in the particle nucleation process and the resulting polymer particles can be significantly larger, ranging from ~50 to 500 nm.[17] TEMPO-based homopolymerization by miniemulsion has been studied in some detail for homopolymers, but there have been relatively few copolymerization studies.[18-21]

As these processes progress towards commercialization, some effort has been directed towards exploring continuous reactor technologies that may have economic benefit. An ideal continuous system would minimize costly shutdown and startup procedures that are inherent in batch processes. It would also allow for online parameter adjustment which could enable changeover to production of a different material without shutting down the system. For example, it is conceivable that one could switch over to a different molecular weight product or adjust the constituent ratios in a block copolymer without shutting down production.

ATRP solution polymerization of homopolymer and diblock copolymer has been demonstrated in packed bed tubular reactors[22-24] and continuous flow tubular reactors.[25-27] RAFT miniemulsion polymerization of homopolymer and diblock copolymer[28,29] has also been demonstrated in tubular reactors. Initial studies have also been done in continuous microreactors that are of smaller dimension than the aforementioned tubular reactors.[30] Homopolymers[31] as well as block[32] and graft[33] copolymers have been synthesized via ATRP within a microtube reactor. Preparation of homopolymers and diblock copolymers

has also been demonstrated in continuous flow microtube reactors via NMP solution polymerization.[34,35]

In an earlier paper, we described the use of a continuous tubular reactor for NMP miniemulsion processes for the preparation of polystyrene homopolymer latexes.[36] It was shown that kinetics were similar for reactions in the continuous tubular reactor compared to analogous batch reactions. The reaction procedure involved a two step process that included an initial bulk polymerization step, performed in batch, to make TEMPO-terminated polystyrene macroinitiator. The macroinitiator, which was dissolved in styrene, was dispersed using high shear in aqueous media and polymerized as miniemulsion in the tubular reactor. While this earlier work demonstrated the feasibility of using a tubular reactor for conducting nitroxide-mediated miniemulsions, it suffered from the limitation of not being a true complete continuous process. The experiments described in this study expand the scope of our earlier work to include running the bulk reaction step in the continuous reactor and also conducting chain extension experiments in the continuous reactor to create diblock and triblock copolymers. The purpose of this study was to determine the overall feasibility and practicality of conducting the entire NMP miniemulsion process polymerizations in a continuous tubular reactor.

6.4 Experimental Part

6.4.1 Materials

Styrene (Apco), benzoyl peroxide (BPO; Aldrich; Luperox A75FP), 2,2,6,6-tetramethylpiperidine 1-oxyl (TEMPO; Z.D. Chemipan), and dodecylbenzene sulfonic acid sodium salt (SDBS; Aldrich; tech.) were all used as received. Deionized water was used for all experiments.

6.4.2 Analysis

Molecular weight and polydispersity (PDI) were measured by gel permeation chromatography (GPC) using a Waters/Millipore liquid chromatograph equipped with a Waters model 510 pump, Ultrastyragel columns of pore size 10^5 Å, 10^4 Å, and 10^3 Å in series with a Styragel HR0.5 column, a Waters model 410 differential refractometer (RI), and a Waters model 486 tunable absorbance detector (UV). Polystyrene standards were used for calibration. Tetrahydrofuran was used as the eluant at a flow rate of 1.0 mL min^{-1}. Conversion for bulk polymerization experiments was analyzed gravimetrically by drying samples overnight at room temperature, then vacuum drying at 50°C for eight hours. Conversion for miniemulsion polymerization experiments was analyzed by gas chromatography (GC) using a Perkin-Elmer XL Autosystem GC equipped with a flame ionization detector and Supelcowax 10 column (15m x 0.53 mm ID; 0.5 μm film). Particle size analysis was done by dynamic light scattering using a Microtrac S3500 particle sizer. Reported particle size values are Mean Volume diameter (MV) and Graphical Standard Deviation (GSD) which is descriptive of the particle size distribution. GSD is the typical standard deviation and is calculated in the Microtrac software using the formula (84% - 16%)/2, where 84 % and 16% refer to the 84% and 16% cumulative frequency values that have been counted by the device.

Theoretical number of chains (N_c) was calculated based on the initial concentration of initiator ([I]), assuming two polymer chains per initiator molecule:

$$N_c = 2[I] \qquad (6\text{-}1)$$

Theoretical number average molecular weight (Mn (theoretical)) was calculated based on experimentally measured conversion (x) of monomer ([M]) versus the theoretical number of chains (N_c):

$$Mn\ (theoretical) = (x[M]/N_c)MW_{styrene} \qquad (6\text{-}2)$$

6.4.3 Apparatus

Continuous reactions were done in a stainless steel tube (167 m length; 3.2 mm outer diameter; 2.05 mm inner diameter) that was immersed in a heated oil bath. For bulk polymerization reactions, reactant flow was controlled by an FMI piston pump (1/4" piston) attached to a Masterflex console drive (6-600 RPM variable speed motor). For miniemulsion polymerizations, reactant flow was controlled by a Masterflex high-pressure peristaltic pump situated at the outlet of the reactor tube. The piston pump could not be used for miniemulsion polymerization experiments because the piston was prone to seizing in the presence of latex. A schematic of the apparatus is shown in Figure 6-1.

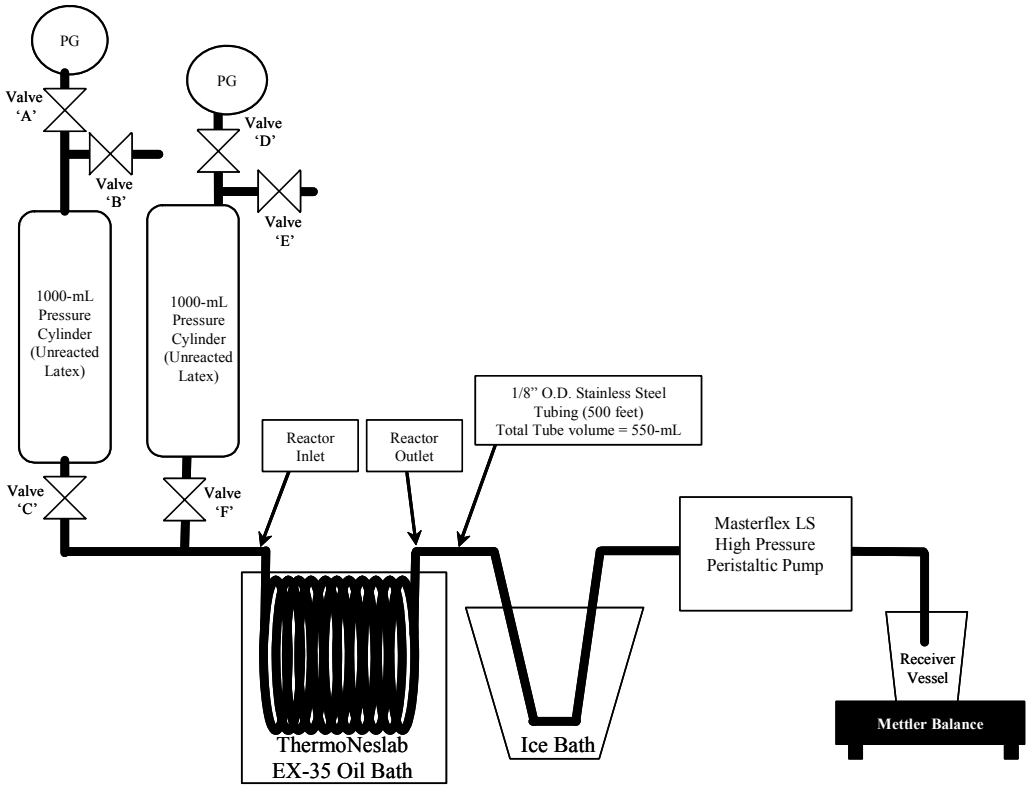

Figure 6-1. Schematic of continuous tubular reactor apparatus for nitroxide-mediated miniemulsion polymerization.

Batch reactions were also done as a comparison to some of the continuous reactions. These were done in a jacketed 2 L stainless steel Buchi reactor fitted with a four bladed pitch blade impeller.

6.4.4 Procedure

A modified miniemulsion polymerization was used in these experiments, involving an initial bulk polymerization (to low conversion) followed by dispersion of the resulting styrene/polystyrene mixture in water and then miniemulsion polymerization.[37,38]

Low conversion bulk polymerization of styrene was first done in the presence of 2,2,6,6-tetramethylpiperidene-1-oxyl (TEMPO). The product of this step was a solution

of low conversion 'living' polystyrene terminated with TEMPO, typically between 5 to 10% conversion, dissolved in styrene monomer.

The monomer-polymer mixture from the bulk polymerization step was dispersed in an aqueous phase consisting of water and surfactant to form miniemulsion latex which was then polymerized to high conversion. The low molecular weight polymer that formed during the partial bulk polymerization step acted as a costabilizer in the subsequent miniemulsion step, thus eliminating the need for a separate costabilizer such as hexadecane. The low conversion bulk polymerization step also ensured that all of the polymer chains were initiated before dispersion in water, so all of the particles were nucleated when the miniemulsion was formed. (A small number of additional chains will be generated due to thermal initiation.) This eliminated complex nucleation and partitioning issues that would arise if the polymerization reaction was initiated during the miniemulsion step.[14] Bulk polymerization experiments were done concurrently in the batch and continuous reactors to allow comparison of reaction kinetics. Miniemulsion polymerization experiments were only done in the continuous reactor for this study because kinetics were compared to batch reactor cases in a previous paper.[36]

6.4.5 Experiment Set #1

6.4.5.1 Bulk Polymerization in Continuous Reactor

In a 4 L stainless steel beaker, 2456 g styrene, 17 g TEMPO, and 27 g BPO were mixed for 10 minutes with a pitch blade impeller at 400 rpm to dissolve the TEMPO and BPO. Approximately 800 g of this monomer solution was charged by vacuum into each of the two sample cylinders indicated in the apparatus (Figure 6-1). These cylinders were refilled with reactants as required throughout the reaction. The cylinders were

deoxygenated by five cycles of vacuum followed by nitrogen pressurization (500 kPa). The cylinders were then pressurized to 600 kPa with nitrogen and held at this pressure throughout the reaction. The oil bath was heated to 135°C and the reactor tube was quickly filled with monomer solution from Cylinder #1 by pushing the monomer solution through with nitrogen pressure. The reactor filling step took about two minutes in all experiments. The piston pump was then started at a rate of 7.3 g/minute to begin feeding monomer solution through the reactor from Cylinder #2, and Cylinder #1 was refilled with fresh monomer solution. This feed rate corresponds to a mean residence time of 75 minutes within the tubular reactor for comparison to the batch reactor reaction time. The mass feed rate was calculated by monitoring monomer solution mass on a balance at the reactor outlet. Samples were removed at intervals after the first 550 mL plug of solution had passed through the reactor (i.e., after one theoretical pass of the reactor). This was done to determine when steady state was achieved in the system. Product collection was started thirty minutes after sampling was started, and a total of 2250 g product was collected (Product ID: BULK-1). This monomer/polymer solution was used in all of the miniemulsion experiment sets that are described in the following sections.

BULK-1 was also repeated to test the reproducibility of this process. The process was repeated as described above, and 526 g product was collected (Product ID: BULK-2).

Two low conversion bulk polymerization experiments were also run in a batch reactor for comparison with the continuous reactor (Product IDs: BULK-3, BULK-4). The formulation described above was scaled back to a total of 1800 g. The monomer solution was prepared in the same manner described above and was charged into a

jacketed 2 L stainless steel Buchi reaction kettle. Mixing was started at 375 rpm using a four bladed pitch blade impeller and the reactor was deoxygenated by purging for 15 minutes with nitrogen. Nitrogen blanket was maintained in the reactor for the remainder of the reaction. The reactor was heated to 135°C and held for 75 minutes, then cooled down and discharged. A transparent amber coloured solution was formed in all of the above bulk polymerization experiments.

6.4.6 Experiment Set #2 (Homopolymer and Diblock Copolymer)

6.4.6.1 Miniemulsion Homopolymerization in Continuous Reactor

In the next set of experiments, the above bulk polymerized monomer-polymer solution (BULK-1) was dispersed into an aqueous phase for miniemulsion polymerization. This created latex consisting of monomer droplets that were stabilized in water, and "living" polymer chains dissolved in the monomer droplets. 250 g of the monomer-polymer solution (BULK-1; 7.1% conversion; 17.8 g polystyrene, 232.2 g styrene) from the previous step was mixed with an aqueous phase that consisted of 43.7 g SDBS dissolved in 2205 g deionized water. The miniemulsion latex was prepared by passing this mixture once through a Niro Soavi piston homogenizer at a pressure between 400 to 600 bar. The miniemulsion latex was then reacted in the continuous tubular reactor at 135°C using the same procedure described above for the BULK-1 experiment. In this case, a Masterflex high pressure peristaltic pump was used instead of the piston pump, and the feed rate was controlled at 3.1 g/minute which corresponds to a mean residence time of 180 minutes within the reactor. Product collection was started after 600 mL of latex had passed through the reactor to ensure that the original reactor fill was not

included in the final product, and a total of 2320 g polystyrene latex product was collected (Product ID: STY-1).

The next experiment was an attempt to create a diblock copolymer from the above "living" polymer by swelling the polymer particles with a different monomer, *n*-butyl acrylate, followed by a chain extension reaction.

6.4.6.2 Diblock Copolymerization in Continuous Reactor

In a 2 L stainless steel beaker, 700 g polystyrene miniemulsion from the previous reaction step (STY1; 82.6 % conversion; 57.8 g polystyrene, 12.2 g styrene) was mixed overnight with 50 g n-butyl acrylate using a magnetic stirrer. The resulting miniemulsion latex was then reacted in the continuous tubular reactor at 135°C using the same procedure described for the previous STY-1 miniemulsion polymerization. Mean residence time within the reactor was 180 minutes for this reaction. Product collection was started after 600 mL of latex had passed through the reactor to ensure that the initial reactor fill was not included in the product, and a total of 100 g latex product was collected (Product ID: STY-nBA-1).

6.4.7 Experiment Set #3 (Homopolymer and Diblock Copolymer with added Ascorbic Acid)

6.4.7.1 Miniemulsion Homopolymerization in Continuous Reactor

The STY-1 reaction process was repeated in this reaction, except 1.8 g ascorbic acid was added to the STY-1 formulation as a reaction accelerant to increase reaction rate and conversion.[39] The ascorbic acid was mixed into the miniemulsion mixture after latex dispersion in the Niro Soavi homogenizer and ten minutes before the latex was charged

into the storage cylinders in the apparatus. As in the previous STY-1 reaction, the feed rate was controlled at 3.1 g/minute which corresponds to a mean residence time of 180 minutes, and a total of 2300 g polystyrene latex product was collected during this experiment (Product ID: STY-2).

6.4.7.2 Diblock Copolymerization in Continuous Reactor

The above STY-2 homopolymer latex was swollen with *n*-butyl acrylate monomer and further reacted in an attempt to produce block copolymer. The same procedure was used as described for STY-nBA-1 in Experiment Set #2 with the following formulation changes. 700 g polystyrene miniemulsion latex (STY2; 97.7 % conversion; 68.4 g polystyrene, 1.6 g styrene) was mixed overnight with 50 g *n*-butyl acrylate using a magnetic stirrer. 0.5 g ascorbic acid was added to the miniemulsion latex and mixed with a magnetic stirrer for 10 minutes before the mixture was added to the reaction apparatus. Mean residence time in the reactor was 180 minutes for this reaction. Product collection was started after 600 mL of latex had passed through the reactor to ensure that the initial reactor fill was not included in the product, and a total of 100 g latex product was collected (Product ID: STY-nBA-2).

The next stage of experimentation was to attempt further chain extension of this diblock copolymer. This was done by swelling the latex particles with styrene monomer with the intention of performing chain extension to form an A-B-A block triblock copolymer.

6.4.8 Experiment Set #4 (A-B-A Triblock Copolymer with Ascorbic Acid)

Experiment Set #3 was repeated to provide sufficient polystyrene homopolymer and polystyrene-block-*n*-butyl acrylate diblock copolymer latexes for the following triblock copolymerization experiments. 4000 g of polystyrene homopolymer latex was produced (Product ID: STY-3) by repeating the STY-2 reaction procedure with a scaled up formulation. 1300 g of poly(styrene-*block*-*n*-butyl acrylate) latex was produced (Product ID: STY-nBA-3) by repeating the STY-nBA-2 reaction procedure with a scaled up formulation using STY-3 as the latex that was swollen with *n*-butyl acrylate.

At this point, the latex consisted of poly(styrene-*block*-*n*-butyl acrylate) particles suspended in water. The intention of the next step was to swell the polymer particles with more styrene monomer to determine if further chain extension was possible to produce triblock copolymer. 1300 g of the copolymer latex (STY-nBA-3; containing approximately 201.3 g block copolymer, 0.001 g styrene, 6.7 g n-butyl acrylate), was mixed overnight with 100 g styrene monomer using a magnetic stirrer. The next day, 1 g ascorbic acid was added and the latex mixture was stirred for ten minutes. The latex was then added to the reactor storage cylinders, and reaction was done using the same general procedure as the previously described reactions. Reaction temperature was 135°C and feed rate was 3.1 g/minute corresponding to an average residence time of 180 minutes, and a total of 500 g latex product was collected during the experiment (Product ID: STY-nBA-STY-1).

6.4.9 Experiment Set #5 (A-B-A Triblock Copolymer with Ascorbic Acid/Reduced Time)

The latex feed rate was increased in the next set of experiments to reduce the average residence time in the tubular reactor. The purpose was to reduce overall reaction time and determine the effect on livingness of the product. Note that all of the miniemulsion experiments done to this point in the study had a 180 minute average reaction time.

The styrene homopolymer latex from Experiment Set #4 (STY-3) was used as the starting block for this set of experiments. Using the STY-3 homopolymer, 1800 g of poly(styrene-*block*-*n*-butyl acrylate) latex was produced (Product ID: STY-nBA-4) using the same procedure described for STY-nBA-3 except the reactant feed rate was increased to 4.6 mL/minute which corresponds to an average residence time of 120 minutes. STY-nBA-4 was used to produce 700 g of poly(styrene-*block*-*n*-butyl acrylate-*block*-styrene) latex (Product ID: STY-nBA-STY-2) using the same procedures described above for STY-nBA-STY-1 except the reactant feed rate was increased to 4.6 mL/minute which corresponds to an average residence time of 120 minutes.

6.5 Results and Discussion

6.5.1 Experiment Set #1

6.5.1.1 Bulk Polymerization in Continuous Reactor

Molecular weight distribution and conversion data for the first bulk polymerization in the continuous tubular reactor are shown in Table 6-1. Molecular weight and conversion both decreased slightly over the thirty minute period after the first

theoretical pass through the reactor was completed. After this thirty minute period, the molecular weight and conversion became stable, indicating that steady state was achieved within the reactor. Theoretical Mn and number of chains (N_c) data are also shown in Table 6-1. In all cases, the actual molecular weight was higher than theoretical and number of chains was lower than theoretical. This is expected because some initiator radicals do not initiate polymers because they are lost to various side reactions. The results here indicate an initiator efficiency between 60 to 70%.

All of the samples from BULK-1B to BULK-1F were combined for use in the subsequent miniemulsion polymerization experiments, and this combined batch was labeled BULK-1.

The analytical characteristics for the combined product of the first continuous bulk polymerization reaction (BULK-1) and the repeat experiment (BULK-2) are shown in Table 6-2. Note that the narrow PDI ~1.2 indicates that this was a well-controlled polymerization.

Table 6-1. Experiment Set #1a.–Bulk polymerization of styrene in continuous reactor. Mean residence time = 75 minutes.

Sample ID	Sampling Time (min)	% Conversion	Mn (Theoretical) (g/mol)	Mn (GPC) (g/mol)	PDI (GPC)	Theoretical Number of Chains, N_c (mol/L)
BULK-1A	75	9.0%	1322	2285	1.18	3.58×10^{-2}
BULK-1B	90	7.5%	1102	1557	1.17	4.38×10^{-2}
BULK-1C	105	7.1%	1043	1498	1.17	4.31×10^{-2}
BULK-1D	130	6.9%	1014	1501	1.17	4.18×10^{-2}
BULK-1E	145	7.0%	1028	1505	1.17	4.23×10^{-2}
BULK-1F	345	7.0%	1028	1490	1.17	4.27×10^{-2}

Table 6-2. Experiment Set #1b – Partial bulk polymerization of styrene in continuous and batch reactors.

Sample ID	Reaction Time[a)] (min)	% Conversion	Mn (Theoretical) (g/mol)	Mn (GPC) (g/mol)	PDI (GPC)	Theoretical Number of Chains, N_c (mol/L)	Reactor Mode
BULK-1	75	7.1%	1043	1496	1.17	4.31×10^{-2}	Continuous
BULK-2	75	10.3%	1513	2061	1.20	4.54×10^{-2}	Continuous
BULK-3	75	17.0%	2497	3126	1.17	4.94×10^{-2}	Batch
BULK-4	75	17.8%	2615	3186	1.14	5.08×10^{-2}	Batch

[a)] Reaction time for continuous reactor = mean residence time. Reaction time for batch reactor = time at 135°C

Reaction conversion, and therefore molecular weight, was somewhat higher in the second bulk polymerization experiment, indicating slight variability in the process. The concentration of polymer chains observed in the BULK-2 reaction is very similar (within ~5%) to that of BULK-1, signifying the main reason for the higher Mn in BULK-2 was its higher conversion. These results are not surprising, and reflect small differences in the induction period early in the polymerization. It is more important to have a reproducible number of chains produced, as was observed experimentally, since this will determine the final Mn.

Analytical characteristics for the analogous bulk polymerizations in batch reactor are also tabulated in Table 6-2 (BULK-3, 4). Polydispersity was comparable between batch and continuous reactors, indicating that living polymers were produced in both types of reactor. Molecular weight and number of polymer chains for the batch polymerized materials was significantly higher than the analogous continuous reaction product. This is possibly due to the heat up and cool down time associated with the batch reactors. It typically takes the reactants in the batch reactor approximately 40 minutes to heat up to the reaction temperature of 135°C, and it takes approximately 20 minutes to cool down. Polymerization occurs at varying rates during these heating and cooling steps depending on the temperature in the reactor at any given point. The continuous reactor does not have this extended heat up and cool down time since the reactor is preheated to 135°C before the reactants are added and the surface-to-volume ratio is much larger. This likely accounts for the higher molecular weight in the batch reactor, and batch reaction times would have to be adjusted accordingly to match the kinetics in the continuous reactor. This would also account for the increased number of polymer chains,

as styrene autopolymerization would be ongoing for a longer period of time in the batch reactor.[40] This is an advantage of the continuous reactor in that the heat up and cool down rates are not an issue as the process moves to larger scales (i.e., longer tubes and/or tube bundles), while it is an issue that must be considered carefully for batch reactors that become more difficult to heat and cool at reasonable rates as the scale increases.

6.5.2 Experiment Set #2 (Homopolymer and Diblock Copolymer)

6.5.2.1 Miniemulsion Homopolymerization in Continuous Reactor

Analytical characteristics for the first miniemulsion reaction of polystyrene homopolymer latex (STY-1) are summarized in Table 6-3. The gel permeation chromatography trace for this material is shown in Figure 6-2, along with the original BULK-1 polymer from which this polymer was grown. In the STY-1 trace, there is no observable indication of the original BULK-1 polymer. This indicates that the majority of BULK-1 was chain extended to produce the STY-1 latex polymer. The polydispersity of the STY-1 latex polymer was relatively narrow (1.19), indicating that the living nature of the polymer was maintained. Experimental Mn was lower than theoretical Mn which indicates that new chains were initiated during the reaction, likely due to styrene autopolymerization. This also suggests that termination reactions were minimal, which is another indication that a significant portion of the polymer remained living.

Table 6-3. Experiment Sets #2 to 5 – Miniemulsion polymerization of homopolymer, diblock copolymer, and triblock copolymer in continuous tubular reactor.

Expt. Set	Sample ID	Mean Residence Time (min)	% Conversion Styrene (GC)	% Conversion nBA (GC)	Mn (Theoretical) (g/mol)	Mn (GPC) (g/mol)	PDI (GPC)	Mean Volume Diameter (MV) (nm)	Particle Size GSD (nm)
2	STY-1	180	82.6%	n/a	17211	15500	1.19	148	57
2	STY-nBA-1	180	85.6%	63.1%	24902	20500	1.25	160	52
3	STY-2	180	97.7%	n/a	19124	24300	1.34	175	67
3	STY-nBA-2	180	97.8%	91.6%	28366	37200	1.92	196	71
4	STY-3	180	99.1%	n/a	19398	25227	1.32	188	53
4	STY-nBA-3	180	99.9%	92.3%	28541	39300	2.02	200	70
4	STY-nBA-STY-1	180	91.5%	98.6%	34491	58600	2.95	213	69
5	STY-3	180	99.1%	n/a	19398	25227	1.32	188	53
5	STY-nBA-4	120	99.4%	79.5%	27312	38817	1.78	198	69
5	STY-nBA-STY-2	120	89.9%	96.0%	33983	57876	2.30	204	64

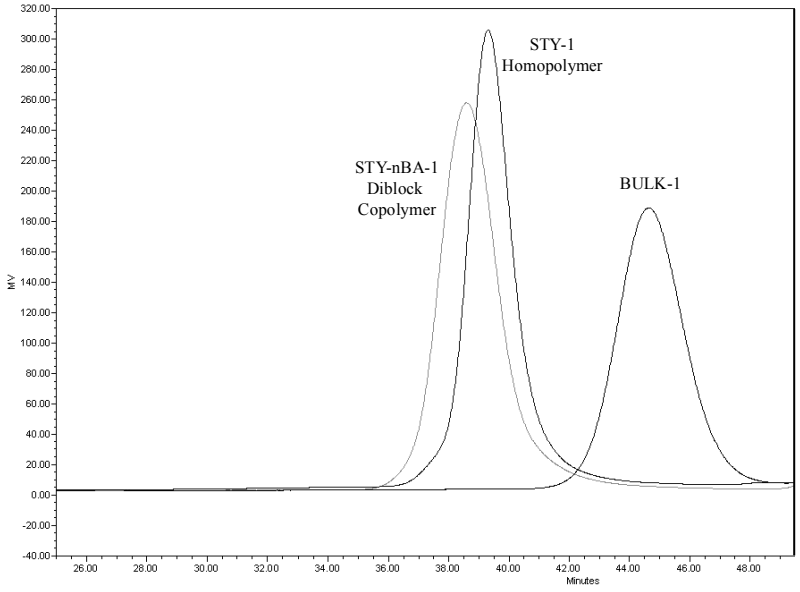

Figure 6-2. GPC trace for Experiment Set #2 – Bulk prepolymer, polystyrene homopolymer, and poly(styrene-block-n-butyl acrylate) diblock copolymer. Continuous reactor with no ascorbic acid in formulation.

6.5.2.2 Diblock Copolymerization in Continuous Reactor

Analytical characteristics for the first diblock copolymer latex (STY-nBA-1) are summarized in Table 6-3. GC analysis shows that additional styrene conversion in the second stage was relatively low (indicating minimal reaction of the residual styrene from the STY-1 homopolymer) while moderate conversion (63%) of n-butyl acrylate was achieved.

GPC analysis shows a moderate increase in molecular weight compared to the initial STY-1 homopolymer. Polydispersity remained relatively low (1.25), indicating that the living nature of the reaction was maintained. The GPC trace shown in Figure 2 shows that the entire polymer molecular weight distribution shifted to higher molecular weight compared to the original STY-1 homopolymer. This indicates that diblock copolymer was formed via chain extension and supports the contention that the original

STY-1 contained significant living polymer. If *n*-butyl acrylate polymerized to form homopolymer, one would expect a new peak to appear on the GPC trace and the original STY-1 polystyrene peak would remain in its original position. Experimental Mn was lower than theoretical Mn which indicates that new chains were initiated during the reaction, likely due to styrene autopolymerization. This also suggests that termination reactions were minimal, which is another indication that a significant portion of the polymer remained living.

Since the *n*-butyl acrylate conversion in this experiment was lower than desired for practical applications, ascorbic acid was used in the next set of experiments to increase reaction rate and conversion.

6.5.3 Experiment Set #3 (Homopolymer and Diblock Copolymer with Ascorbic Acid)

6.5.3.1 Miniemulsion Homopolymerization in Continuous Reactor

Analytical characteristics for the first polystyrene homopolymer latex produced with ascorbic acid (STY-2) are summarized in Table 6-3. The GPC trace for this material is shown in Figure 6-3, along with the original BULK-1 material from which this polymer was grown. In the STY-2 trace, there is no remaining indication of the original BULK-1 polymer. This indicates that the majority of BULK-1 was chain extended to produce the STY-2 latex polymer. Also, the polydispersity of STY-2 is relatively narrow (1.34) which indicates that the living nature of the polymer was maintained. The conversion and molecular weight of STY-2 are significantly higher than STY-1 which indicates that the ascorbic had the desired effect of increasing the reaction rate. However, polydispersity of STY-2 is higher than STY-1 which indicates that some loss in

polymerization control has occurred. The experimental Mn is higher than theoretical in this reaction, which indicates that termination reactions occurred to a larger extent than in the STY-1 experiment. This trend was observed for all of the subsequent experiments that are described below. Thus, higher conversion is achieved at the price of lower concentration of living polymer in the product.

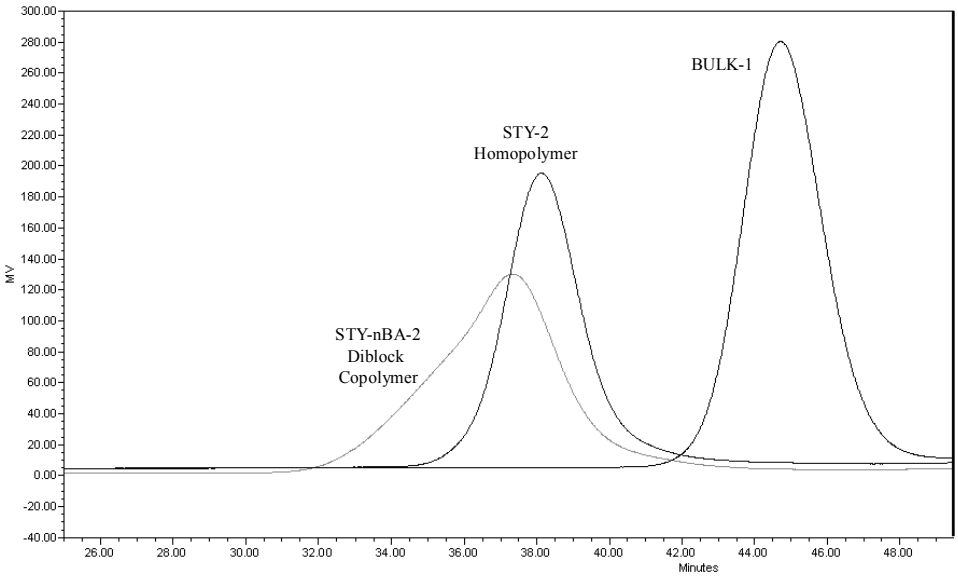

Figure 6-3. GPC trace for Experiment Set #3 – Bulk prepolymer, polystyrene homopolymer, and poly(styrene-block-n-butyl acrylate) diblock copolymer. Continuous reactor with ascorbic acid added to formulation.

6.5.4 Diblock Copolymerization in Continuous Reactor

Analytical characteristics of the first poly(styrene-*block*-*n*-butyl acrylate) diblock copolymer produced with ascorbic acid (STY-nBA-2) are summarized in Table 6-3. There was a significant increase in molecular weight, *n*-butyl acrylate went to very high conversion, and there was a significant increase in particle size. The polydispersity is quite high (1.92) compared to the analogous experiment that did not use ascorbic acid. One can see in the GPC trace (Figure 6-3) that the entire molecular weight distribution

increased as expected from STY-2, but it is also significantly broader. Specifically, a high molecular weight shoulder is observed in the trace. There are a few possible reasons for this broadening, namely chain termination, side reactions such as backbiting, and also the fact that n-butyl acrylate has a significantly higher reaction rate than styrene. The faster reaction rate leads to some loss of molecular weight growth control, as the living chains have the potential to add significantly more monomer units during their short active growing cycles. This leads to molecular weight distribution broadening, while the polymer chains can still maintain their living nature. This is particularly an issue for TEMPO-based NMP reactions as they typically need to be run at significantly higher temperature than other systems (e.g., SG1), thus further increasing the reaction rate of n-butyl acrylate. Reducing the reaction rate of n-butyl acrylate would result in narrower molecular weight distribution, and this could be achieved by finding the optimum balance of lower temperature and concentration/type of reaction rate accelerant that gives high conversion in a relatively short time frame while maintaining maximum livingness of the final polymer. This will be a topic for future study.

6.5.5 Experiment Set #4 (A-B-A Triblock Copolymer with Ascorbic Acid)

Analytical characteristics for the repeat homopolymer (STY-3) and diblock copolymer (STY-nBA-3) experiments are tabulated in Table 3 and GPC traces are shown in Figure 6-4. Conversion, molecular weight, and particle size results of these experiments closely match the analogous experiments that were done in Experiment Set #3.

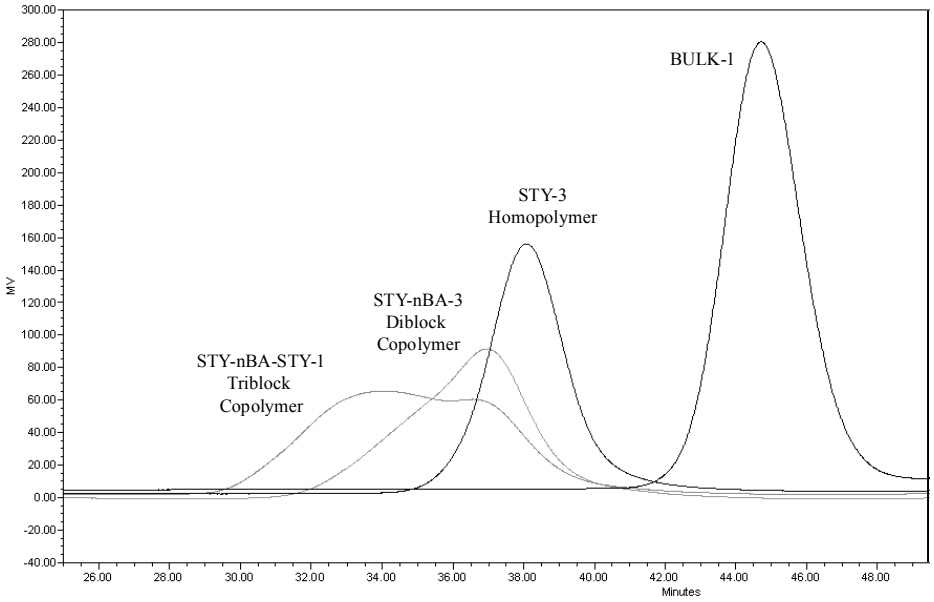

Figure 6-4. GPC trace for Experiment Set #4 – Bulk prepolymer, polystyrene homopolymer, poly(styrene-block-n-butyl acrylate) diblock copolymer, and poly(styrene-block-n-butyl acrylate-block-styrene) triblock copolymer. Continuous reactor with ascorbic acid added to formulation.

Analytical characteristics for the first poly(styrene-*block*-*n*-butyl acrylate-block-styrene) triblock copolymer (STY-nBA-STY-1) are shown in Table 6-3 and the GPC trace is shown in Figure 6-4. Styrene and butyl acrylate conversion were both relatively high in this experiment at 91.5% and 98.6% respectively. Molecular weight increased significantly, but the high polydispersity suggests much of the living nature was lost through termination reactions. However, the GPC trace suggests that significant chain extension occurred. The initial homopolymerization exhibited a high degree of livingness, as evidenced by low polydispersity and growth of most of the chains during the subsequent block copolymerization step with n-butyl acrylate. During the second reaction step with *n*-butyl acrylate, it appears that a significant portion of the chains terminated, since we were not able to subsequently re-initiate them. However a

significant portion of the chains did re-initiate, exhibiting substantial chain extension. The resulting molecular weight distribution is bimodal, with a high polydispersity index.

6.5.6 Experiment Set #5 (A-B-A Triblock Copolymer with Ascorbic Acid/Reduced Time)

It is known that loss of livingness is unavoidable in NMP processes and the probability of dead chain formation increases significantly at longer reaction times for two reasons. Termination continues throughout the polymerization, resulting in a gradual increase in dead chains. However disproportionation of the TEMPO-terminated PS to give hydroxylamine and unsaturated dead polymer is also important at these temperatures.[41,42] It has been demonstrated that dead chain formation is minimized if the reaction can be done in a shorter time frame.[43] Therefore, reaction time was reduced in the next set of experiments.

Analytical results for the diblock copolymer (STY-nBA-4) and triblock copolymer (STY-nBA-STY-2) experiments are shown in Table 6-3 and GPC traces are shown in Figure 6-5. There was a minor improvement in this set of experiments in that the monomer conversion was approximately the same the same as the previous experiments even though the overall reaction time was reduced by two hours. Also, polydispersity was reduced slightly. However, it is clear from the GPC traces that the same general problems occurred in this set of reactions as previously. That is, it appears that a portion of the polymer chains terminated during the *n*-butyl acrylate polymerization step resulting in a low molecular weight shoulder, while the remaining living chains continued to grow during the styrene triblock copolymerization step. The end result is a

bimodal molecular weight distribution, so the final product is likely a mixture of various diblock and triblock copolymers.

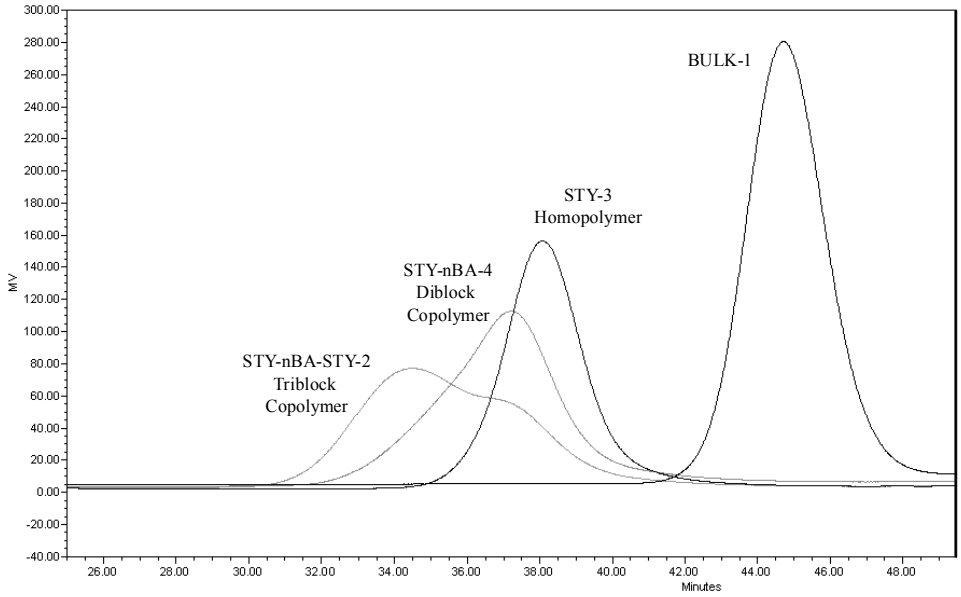

Figure 6-5. GPC trace for Experiment Set #5 – Bulk prepolymer, polystyrene homopolymer, poly(styrene-block-n-butyl acrylate) diblock copolymer, and poly(styrene-block-n-butyl acrylate-block-styrene) triblock copolymer. Continuous reactor with ascorbic acid added to formulation. Reduced reaction time.

6.6 Conclusion

Nitroxide-mediated bulk styrene homopolymerization (to low conversions) was demonstrated in a continuous tubular reactor and was compared to similar reactions done in a batch reactor. Higher molecular weight and conversion was observed in the batch reactor compared to analogous reactions in the continuous reactor; this is attributed to polymerization that occurs during heat up and cool down cycles in the batch reactor. The bulk polymerization product mixture was then further reacted via miniemulsion polymerization within a continuous flow tubular reactor to form polystyrene homopolymer latex. Stable latexes were produced containing polymer particles that

showed living characteristics. Chain extension of this polymer was demonstrated using *n*-butyl acrylate to produce diblock copolymer in the tubular reactor. The chain extended copolymer showed broadened molecular weight distribution, and this is attributed to chain termination, side reactions such as backbiting, and the high reactivity of *n*-butyl acrylate which creates less controlled polymerization conditions than with styrene. The diblock copolymer miniemulsion latex was further swollen with more styrene monomer to produce triblock copolymer in the tubular reactor by a second chain extension reaction. Further molecular weight broadening was observed to the point of a bimodal distribution. Results indicate that some triblock copolymer was formed while some of the initial diblock copolymer terminated early in the reaction. The continuous tubular reactor appears to be a viable approach to producing diblock and triblock copolymers, although there is potential for product improvement through process optimization.

6.7 References

1. Braunecker, W. A; Matyjaszewski, K. *Prog. Polym. Sci.* **2007**, *32*, 93.
2. Solomon, D. H.; Rizzardo, E.; Cacioli, P. *US Patent 4,581,429*, **1986**, assigned to Commonwealth Scientific and Industrial Research Organization.
3. Georges, M. K.; Veregin, R. P. N.; Kazmaier, P. M.; Hamer, G. K. *Macromolecules* **1993**, *26*, 2987.
4. Hawker, C. J.; Bosman, A. W.; Harth, E. *Chem. Rev.* **2001**, *101*, 3661.
5. Sciannamea, V.; Jerome, R.; Detrembleur, C. *Chem. Rev.* **2008**, *108*, 1104.
6. Kato, M.; Kamigaito, M.; Sawamoto, M.; Higashimura, T. *Macromolecules* **1995**, *28*, 1721.

7. Matyjaszewski, K.; Xia, J. *Chem. Rev.* **2001**, *101*, 2921.

8. Kamigaito, M.; Ando, T.; Sawamoto, M. *Chem. Rev.* **2001**, *101*, 3689.

9. Chiefari, J.; Chong, Y. K.; Ercole, F.; Krstina, J.; Jeffery, J.; Le, T. P. T.; Mayadunne, R.T.A.; Meijs, G. F.; Moad, C. L.; Moad, G.; Rizzardo, E.; Thang, S. H. *Macromolecules* **1998**, *31*, 5559.

10. Moad, G.; Rizzardo, E.; Thang, S. H. *Aust. J. Chem.* **2005**, *58*, 379.

11. Moad, G.; Rizzardo, E.; Thang, S. H. *Aust. J. Chem.* **2006**, *59*, 669.

12. Qiu, J.; Charleux, B.; Matyjaszewski, K. *Prog. Polym. Sci.* **2001**, *26*, 2083.

13. Cunningham, M.F. *Prog. Polym. Sci.* **2002**, 27, 1039.

14. Cunningham, M. F. *C. R. Chimie* **2003**, *6*, 1351.

15. Cunningham, M. F. *Prog. Polym. Sci.* **2008**, *33*, 365.

16. Zetterlund, P. B.; Kagawa, Y.; Okubo, M. *Chem. Rev.* **2008**, *108*, 3747.

17. Schork, F. J.; Luo, Y.; Smulders, W.; Russum, J. P.; Butté, A.; Fontenot, K. *Adv. Polym. Sci.* **2005**, *175*, 129.

18. Alam, M. N.; Zetterlund, P.B.; Okubo, M. *Macromol. Chem. Phys.* **2006**, *207*, 1732.

19. Saka, Y.; Zetterlund, P.B.; Okubo, M. *Polymer* **2007**, *48*, 1229.

20. Zetterlund, P.B.; Alam, M. N.; Minami, H.; Okubo, M. *Macromol. Rapid Commun.* **2005**, *26*, 955.

21. Keoshkerian, B.; MacLeod, P. J.; Georges, M. K. *Macromolecules* **2001**, *34*, 3594.

22. Shen, Y.; Zhu, S.; Pelton, R. *Macromol. Rapid Commun.* **2000**, *21*, 956.

23. Shen, Y.; Zhu, S.; Zeng, F.; Pelton, R. H. *Macromolecules* **2000**, *33*, 5427.

24. Shen, Y.; Zhu, S. *AIChE J.* **2002**, *48*, 2609.

25. Noda, T.; Grice, A. J.; Levere, M. E.; Haddleton, D. M. *Eur. Polym. J.* **2007**, *43*, 2321.

26. Müller, M.; Cunningham, M. F.; Hutchinson, R. A. *Macromol. React. Eng.* **2008**, *2*, 31.

27. Chan, N.; Boutti, S.; Cunningham, M. F.; Hutchinson, R. A. *Macromol. React. Eng.* **2009**, *3*, 222.

28. Russum, J. P.; Jones, C. W.; Schork, F. J. *Macromol. Rapid Commun.* **2004**, *25*, 1064.

29. Russum, J. P.; Jones, C. W.; Schork, F. J. *Ind. Eng. Chem. Res.* **2006**, *44*, 2484.

30. Enright, T. *Living Radical Polymerization*, in: *Micro Process Engineering*, *Vol. 2*, V. Hessel, A. Renken, J. C. Schouten, J.-I. Yoshida, Eds.; Wiley-VHC Verlag GmbH & Co. KgaA: Weinheim 2009, p. 199.

31. Wu, T.; Mei, Y.; Cabral, J. T.; Xu, C.; Beers, K. L. *J. Am. Chem. Soc.* **2004**, *126*, 9880.

32. Wu, T.; Mei, Y.; Xu, C.; Byrd, H. C. M.; Beers, K. L. *Macromol. Rapid Commun.* **2005**, *26*, 1037.

33. Xu., C.; Wu, T.; Drain, C. M.; Batteas, J. D.; Beers, K. L. *Macromolecules* **2005**, *38*, 6.

34. Rosenfeld, C.; Serra, C.; Brochon, C.; Hadziioannou, G. *Chem. Eng. Sci.* **2007**, 62, 5245.

35. Rosenfeld, C.; Serra, C.; Brochon, C.; Hessel, V.; Hadziioannou, G. *Chem. Eng. J.* **2008**, 135S, S242.

36. Enright, T. E.; Cunningham, M. F.; Keoshkerian, B. *Macromol. Rapid Commun*. **2005**, *26*, 221.

37. Keoshkerian, B.; MacLeod, P. J.; Georges, M. K. *Macromolecules* **2001**, *34*, 3594.

38. Keoshkerian, B.; MacLeod, P. J.; Odell, P. G.; Georges, M. K. *US Patent 6,469,094* **2002**, assigned to Xerox Corporation.

39. Lin, M.; Cunningham, M.F.; Keoshkerian, B. *Macromol. Symp.* **2004**, *206*, 263.

40. Mayo, F.R. *Polym. Prepr. (Am. Chem. Soc., Div. Polym. Chem.)* **1961**, *2*, 55

41. Ma, J. W.; Smith, J. A.; McAuley, K. B.; Cunningham, M. F.; Keoshkerian, B.; Georges, M. K. *Chem. Eng. Sci.* **2003**, *58*, 1163.

42. Ma, J. W.; Cunningham, M. F.; McAuley, K. B.; Keoshkerian, B.; Georges, M. K. *Chem. Eng. Sci.* **2003**, *58*, 1177-1190.

43. Cunningham, M. F.; Lin, M.; Milton, S.; Ng, D.; Hsu, C. C.; Keoshkerian, B. *Polymer* **2005**, *46*, 1025.

Chapter 7

Residence Time Distribution Study of a Living/Controlled Radical Miniemulsion Polymerization System in a Continuous Tubular Reactor

for submission to Macromolecular Reaction Engineering

7.1 Preface

At this point in the study, a continuous tubular reactor had been developed for the controlled production of polymers via a NMP miniemulsion process, and there were some differences observed between this and a typical batch polymerization process. To help understand these differences, a residence time distribution tracer study was done for the tubular reactor. Initial tests were done with a simple aqueous salt solution, and this was followed by tests that used the unreacted latex (monomer droplets in water) and the final product latex (polymer particles in water). Significant differences were observed between the various systems, and the results help to explain some of the differences that were seen with batch reactions. The results also highlight the importance of experimental understanding of the RTD of specific systems such that the proper operating conditions are used for a given experiment.

7.2 Abstract

Residence time distribution (RTD) studies were done to determine the flow characteristics for a controlled free radical miniemulsion polymerization system in a continuous tubular reactor. The specific reaction system was a nitroxide-mediated controlled free radical miniemulsion polymerization to produce polystyrene latex. Pulse tracer experiments were done at different flow rates and temperatures, and a comparison was made between a homogeneous aqueous salt mixture versus the heterogeneous miniemulsion mixture in the tubular reactor. The heterogeneous system was studied under two different conditions, one with a monomer-in-water droplet dispersion and one with fully formed polymer particles dispersed in water. This was done to determine the difference in flow characteristics between the unreacted monomer droplet dispersion versus the corresponding fully reacted product versus a simple aqueous solution. There were differences observed between all of the different systems tested, and none of them matched an ideal plug flow condition. The reactor contains stagnant zones of varying volume and tracer spreading was observed in all cases. The dispersion model was found to model the system quite well in most cases.

7.3 Introduction

Living/controlled radical polymerization (L/CRP) processes were first demonstrated successfully in the early 1990's.[1] These discoveries were a breakthrough for free radical polymerization processes because they significantly improved control over polymer architecture and molecular weight distribution of the end product compared to conventional free radical polymerization processes.[2] There have been a number of different L/CRP methods developed in the ensuing years but three specific processes have received the most attention to date, namely nitroxide mediated polymerization (NMP),[3,4] atom transfer radical polymerization (ATRP),[5,6] and reversible addition-fragmentation transfer polymerization (RAFT).[7,8] Each of these processes has unique attributes that make them useful for a variety of applications, and they have all been introduced commercially to some degree.[9]

Initial L/CRP studies were primarily done using bulk or solution polymerization conditions, while more recent research activities have been directed towards dispersed-phase reactions in aqueous media such as emulsion and miniemulsion polymerization.[10,11] The reason for the interest in aqueous based systems is that they have potential economic and environmental benefits over solvent and bulk based systems.

Early studies of L/CRP reactions were done using batch reactors, while recently there has been interest in studying these reactions in continuous reactors.[12] There are a number of potential benefits to using continuous reactors instead of batch from both economic and technical standpoints. For example, reduced downtime (e.g., minimal heating, cooling, discharge cycles) and less capital investment are attractive economic benefits. From a technical standpoint, the ability to do on-the-fly formulation

adjustments could enable quicker changeover to different products, such as block copolymers with different molecular weight or different functional blocks.

We have done a series of studies to demonstrate the feasibility of aqueous miniemulsion-based NMP reactions in a continuous tubular reactor.[13,14] As the studies have progressed, there has been interest in characterizing the residence time distribution (RTD) within the reactor. Due to the kinetics of controlled radical polymerization processes, the RTD in a continuous reactor could have a significant impact on the final product. In an ideal L/CRP process, all of the polymer chains should grow at the same rate and the resulting polymer mixture should contain polymer chains that are all of the same length and molecular weight. Current L/CRP processes do not achieve this ideal scheme, but it is approached and the molecular weight distribution is quite narrow for the polymers that are produced in real systems. A broad RTD in a continuous reactor would have a clear impact on this result because the polymer chains that exit the reactor would have reacted for different lengths of time, and this would broaden the molecular weight distribution. This concept has been studied demonstrated by Russum et. al. for a RAFT miniemulsion polymerization system in a tubular reactor.[15]

Initial NMP miniemulsion studies have shown that there is minimal difference in molecular weight distribution between materials prepared in a batch reactor versus continuous tubular reactor.[14] This suggests that the RTD is likely quite narrow within the reactor. However, it was also shown that conversion was slightly lower in the continuous tubular reactor compared to batch, and this was attributed to axial mixing effects. This indicates that the flow pattern likely deviates from the ideal plug-flow profile that is desired for this type of reaction, and it is therefore of interest to understand the RTD

properties of this system in some detail. This will be particularly important for long term operation of the reactor, a critical consideration for commercial operations.

In straight tube systems, flow patterns have been well defined theoretically and experimentally. Laminar flow with a parabolic flow pattern is expected at low Reynolds number ($Re < 2300$), there is a transitionary flow pattern when $2300 < Re < 4000$, and turbulent conditions that approach plug flow behavior occur when $Re > 4000$. Ideal plug flow is typically not seen in real systems where broadening of the RTD is usually observed due to axial mixing or dispersion in the direction of fluid flow, thus creating a flow pattern termed dispersed plug flow which can be described using the dispersion model. This flow pattern is also observed even under laminar flow conditions in long small diameter tubes due to the Taylor-Aris dispersion[16,17] effect where radial diffusion is sufficient to blur out the expected parabolic profile. The extent of dispersion is characterized by the dimensionless number $\mathbf{D}/uL$ which is termed the vessel dispersion number. **D** is the axial dispersion coefficient, while u (linear velocity of liquid) and L (length of tube) are fixed experimental properties.

Straight tubes are often bent into helical coils to produce a more compact configuration. It is known that this can have a significant effect on the RTD because centrifugal forces are induced by the coiled shape and this creates secondary circulating flow streamlines on the material that is flowing within the tube. Figure 7-1 shows a cross-sectional view of a tube with the secondary flow circulation pattern that is created by the coiled configuration. In a straight tube, all of the flow streamlines would be aligned perpendicular to the tube cross-section (i.e., straight into the page in Figure 7-1),

so it is clear that the helical tube's overall flow profile will deviate from the previously described straight tube flow patterns.

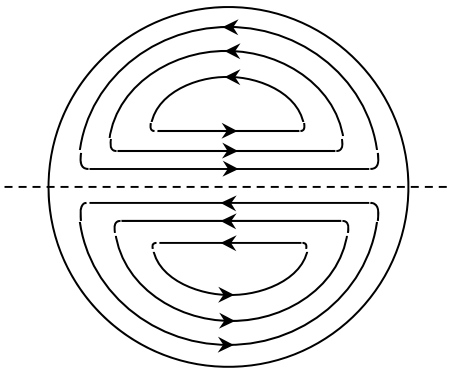

Figure 7-1. Secondary flow circulation pattern caused by helical tube configuration.

Dean first developed a detailed analytical description of these flow patterns for incompressible viscous fluids in a helically coiled tube, and approximated the fluid velocity as a function of position within the tube.[18,19] This analysis is valid at low Reynolds number and coil curvature, and it has been extended to encompass a larger range of values.[20] A dimensionless number, the Dean number ($De=Re*\lambda$, where λ is the ratio of tube diameter to coil diameter) was proposed to help characterize this type of flow.

Theoretical residence time distributions have been derived using Dean's flow equations for laminar flow in helical tubes,[21,22] and there have been numerous experimental studies that describe RTD details for diffusion-free laminar flow[23] and axial dispersion in laminar flow[24,25] for Newtonian and non-Newtonian[26] systems, including polymer solutions.[27] Most of these studies have been done using step tracer experiments, as opposed to the pulse tracer method that was used in the study.

In general, the main effect of the helical tube flow pattern is that it typically reduces axial dispersion compared to what is observed in straight tubes. This in turn improves heat and mass transfer, and is thus considered an improvement in most situations. Typically, RTD becomes narrower as the Dean number increases in the system.

The purpose of this study was to elucidate the RTD characteristics of our tubular reactor system, specifically for the miniemulsion NMP latex system that is being investigated. Tracer studies were done for this purpose. Initial tracer tests were done using an aqueous salt solution for simplicity. Further testing was then done using a dye tracer in latex to determine if the initial aqueous experiments gave an accurate reflection of the true RTD for the latex system of interest. Two distinct latex systems were studied to determine the extremes of the RTD: 1) unreacted latex consisting of monomer droplets dispersed in water (i.e., the starting material), and 2) fully reacted latex consisting of polymer particles suspended in water (i.e., the final product).

7.4 Experimental

7.4.1 Tubular Reactor Apparatus

The continuous tubular reactor consisted of a series of stainless steel tubes (183 m total length; 3.20 mm outer diameter; 2.05 mm inner diameter) immersed in an oil bath (Figure 7-2). Twelve stainless steel tubes were wrapped into coils (coil diameter = 10 cm) and connected in series. The volume of the reactor was measured by filling with water eight times between the 'inlet' and 'outlet' points noted in Figure 7-2, measuring the mass of water each time, and taking the average (V = 604 ± 4 mL). Two 1 L stainless steel cylinders were used as reactant holding vessels at the inlet of the reactor. Tracer

solution was held in one of the vessels while the other vessel held the baseline mixture that was being studied. Flow started with the baseline mixture, switched over to the tracer vessel for a short period of time to introduce the tracer pulse, and then switched back to the baseline solution vessel. Flow through the reactor was controlled by a Masterflex high-pressure peristaltic pump situated at the outlet of the reactor tube. Mass flow rate was monitored using a Mettler Toledo balance situated at the outlet of the reactor, and the pump was adjusted accordingly to achieve the desired mass flow rate. A series of volumetric flow rates were selected for this study, and the corresponding mass flow rate was calculated based on density (ρ) of the media for the given experiment ($\rho_{water,\ 25°C}$ = 0.997.0 g/mL, $\rho_{latex\ droplets,\ 25°C}$ = 0.985 g/mL, $\rho_{latex\ particles,\ 25°C}$ = 1.005 g/mL). For all experiments at 135°C, the density of water was assumed for all media ($\rho_{135°C}$ = 0.930 g/mL). A continuous backpressure of 650 kPa nitrogen was maintained in the reactor holding vessels throughout the experiments, which was necessary to prevent boiling during high temperature experiments.

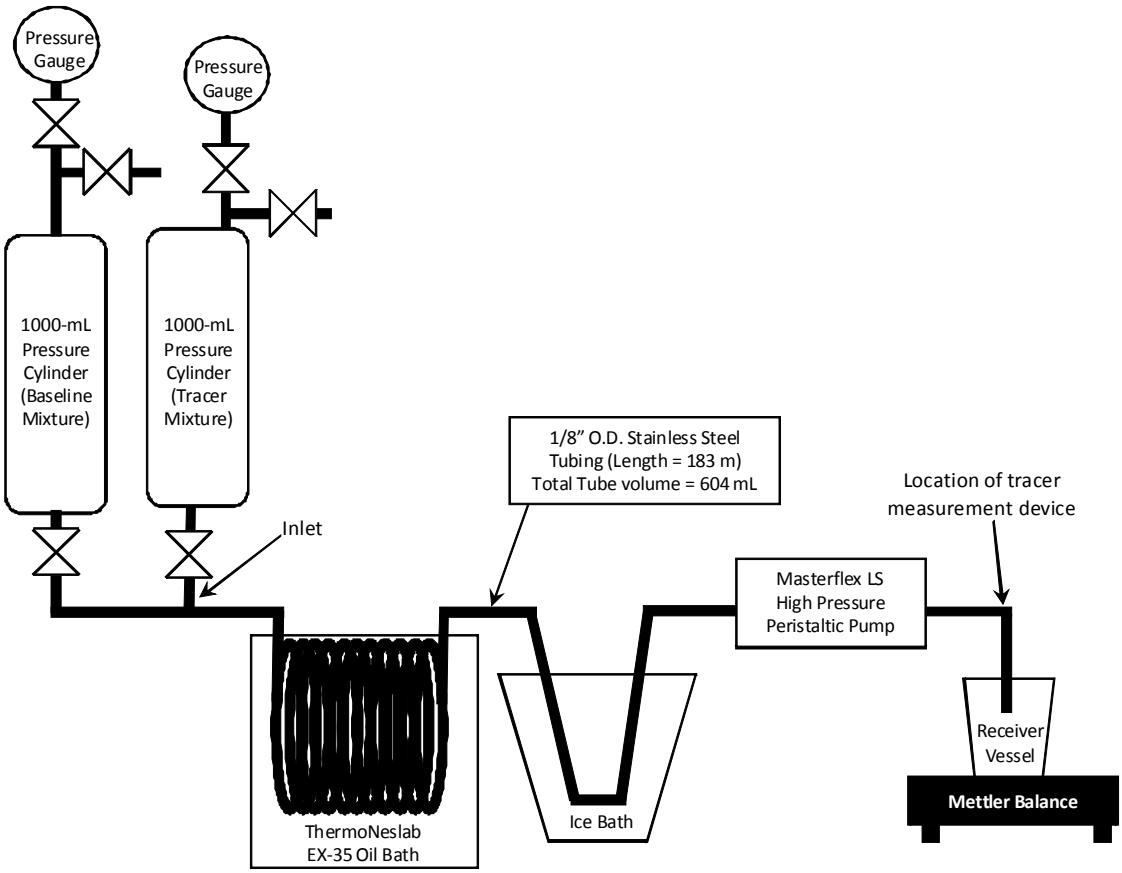

Figure 7-2. Continuous tubular reactor schematic.

7.4.2 Materials

Styrene (Apco), benzoyl peroxide (BPO; Sigma Aldrich; Luperox A75FP), 2,2,6,6-tetramethylpiperidine 1-oxyl (TEMPO; Z.D. Chemipan), dodecylbenzene sulfonic acid sodium salt (SDBS; Aldrich; tech.), sodium chloride (Sigma Aldrich, reagent), and water soluble Quinoline Yellow (Sigma Aldrich) were all used as received. Deionized water was used for all experiments.

7.4.3 RTD Measurement of Homogeneous Aqueous NaCl Salt Solution

Initial RTD experiments were done using a homogeneous mixture of NaCl salt tracer in water, and the tracer was detected by conductivity. A Fisherbrand flow-through

conductivity probe cell with an Accumet AP65 conductivity meter was installed at the reactor outlet between the pump and receiver vessel.

One holding vessel was filled with deionized water and the second holding vessel was filled with tracer, a 3 g/L tracer solution of NaCl in deionized water. The continuous reactor was filled with deionized water, and flow was started from the deionized water holding vessel at the desired flowrate. Once a consistent feedrate was established, a 6 gram pulse of the NaCl solution was introduced into the inlet stream of the reactor at the same feedrate as the water. The feed stream was switched back to deionized water after the NaCl pulse was added, and flow was continued at the same feed rate. Conductivity of the exit stream was monitored to detect the NaCl pulse. Once an increase in conductivity was observed, readings were taken every 30 seconds until the pulse had passed and conductivity returned to the baseline value for deionized water. A calibration of NaCl concentration versus conductivity was prepared, and this was used to convert the conductivity measurements from the RTD experiment to concentration values. These calculated concentration values were used to calculate the RTD curves as described below in the calculations section. RTD experiments were done at various temperatures and feedrates as shown in Table 7-1.

Following the initial salt solution experiments, RTD measurements were made on the actual miniemulsion latex mixture in both its unreacted and reacted state. The following procedure describes the preparation of the miniemulsion latex, and this is followed by the RTD measurement procedure.

7.4.4 Miniemulsion Polymerization Procedure

A three step modified miniemulsion polymerization was required to enable a successful controlled radical polymerization process:

Step 1. Bulk polymerization of monomer to low conversion.

Step 2. Dispersion of the resulting styrene/polystyrene mixture in water in the presence of surfactant to produce a monomer/polymer droplet dispersion.

Step 3. Miniemulsion polymerization of the above dispersion to produce latex consisting of polymer particles dispersed in water.

Step 1 low conversion bulk polymerization was done in a batch reactor for convenience. 16.2 g BPO and 10.2 g TEMPO were dissolved in 1473.6 g styrene by mixing with a pitch blade impeller at 450 rpm in a 2 litre stainless steel Buchi reactor. The reactor was heated to 135°C over a period of 30 minutes, held at 135°C for one hour, and then cooled to room temperature. The product of this reaction was a low viscosity transparent orange colored liquid containing approximately 10 wt% polystyrene dissolved in 90 wt% styrene monomer. The polymer in this mixture functions as a hydrophobe, thereby eliminating the need for an additional hydrophobe (e.g., hexadecane) that is commonly required to maintain droplet stability in miniemulsion polymerization.[28] This monomer polymer mixture was dispersed in water in the next step to form the miniemulsion latex dispersion.

Step 2 dispersion of the above monomer-polymer mixture to create the miniemulsion latex was done as follows. 61 g SDBS surfactant was dissolved in 3076 g deionized water by mixing in a 4 L beaker for 30 minutes at 350 rpm with a pitch blade impeller attached to an overhead mixer. 696 g of the ‘step 1’ monomer-polymer mixture

was mixed into this surfactant solution by mixing with the pitch blade impeller at 550 rpm for 5 minutes. This mixture was passed twice through a Niro Soavi piston homogenizer that was set between 400-600 bar pressure. The product from this step was a milky white low viscosity liquid consisting of monomer-polymer droplets suspended in water. One set of RTD tracer experiments was done using this unreacted latex, while a separate set of tracer experiments was done using the reacted latex that is described in the next step.

Step 3 miniemulsion polymerization to produce polymer particles suspended in water was done as follows. Latex from the 'step 2' dispersion step was charged into the two holding vessels in the continuous reactor apparatus. The reactor oil bath was heated to 135°C and the reactor tube was quickly filled by pushing the latex from the holding vessel through the reactor tube using nitrogen pressure. The reactor filling step took about two minutes in all experiments. The peristaltic pump was then started at the desired feed rate to begin feeding latex through the reactor. The mass feed rate was calculated by monitoring latex mass on a balance at the reactor outlet. Product collection was started after 1.1 L of latex had passed through the tubular reactor (i.e., after two theoretical passes of latex through the reactor), and a total of 2500 g latex product was collected. The final product was a milky white low viscosity liquid consisting of polymer particles suspended in water. A set of RTD experiments was done using this fully reacted latex product for comparison with the RTD experiments that were done with the unreacted latex droplets produced in step 2 above.

7.4.5 RTD Measurement of Heterogeneous Miniemulsion Mixtures using Dye Tracer

As previously mentioned, two distinct sets of RTD experiments were done with the heterogeneous miniemulsion system:

1) RTD of the unreacted monomer-polymer droplet latex. This mixture consisted of monomer (90%)/polymer (10%) droplets suspended in water.
2) RTD of the fully reacted polymer particle latex. This mixture consisted of polymer particles suspended in water.

In both cases, a water soluble tracer dye (Quinoline Yellow, water soluble) was used as the tracer and was monitored by UV-Vis spectroscopy. An Ocean Optics UV-Vis spectrometer flow through cell was attached to the outlet of the continuous tubular reactor between the pump and the receiver vessel, and this was used in conjunction with an Ocean Optics S2000 spectrometer to detect the dye tracer. The spectrometer measurements were transmitted to computer via an ADC1000-USB analog-digital converter, and spectra were analyzed using Ocean Optics OOIBase 32 software. The following settings were used while collection spectral data points: Integration time = 400ms, Spectra Average = 5, Boxcar smoothing = 5. Data points were collected every 15 seconds at 380 nm, 410 nm, 417 nm, 480 nm, 500 nm, and 600 nm. Maximum reflectance was observed at 417 nm, so this wavelength was chosen as the primary reference wavelength.

For all experiments, a large quantity of stock latex was prepared as described in the previous section, and this was used as the baseline undyed latex. 200 g of this stock mixture was removed and mixed with 0.1 g quinoline yellow dye by stirring with a

magnetic stirrer, and this was used as the tracer. Several mixtures were then prepared using various ratios of undyed and dyed latex, and these were used to calibrate concentration of dye versus reflectance measured by the UV-Vis spectrometer at 417 nm.

To perform the RTD experiment, one holding vessel was filled with latex (unreacted monomer droplets or polymer particle product) and the second holding vessel was filled with the corresponding dyed tracer mixture. The continuous reactor was filled with latex, and flow was started from the latex holding vessel at the desired flowrate. Once a consistent feedrate was established, a 6 g pulse of dyed tracer was introduced into the inlet stream of the reactor at the same feedrate as the undyed latex. The feed stream was switched back to undyed latex after the tracer pulse was added, and flow was continued at the same feed rate. Reflectance of the exit stream was monitored as described above, continuously throughout the entire experiment. Reflectance measurements were converted to concentration measurements as previously described, and these values were used to calculate the RTD curves. RTD experiments were done at various temperatures and feedrates as shown in Table 7-1.

For the unreacted monomer droplet experiments at high temperature, 2 g excess TEMPO was mixed into the latex to inhibit the polymerization reaction from occurring. The purpose of this was to observe the extreme of unreacted materials flowing through the entire length of the reactor compared to the opposite extreme of final product flowing through the entire length. Samples were tested gravimetrically to ensure that reaction did not occur during these experiments.

7.4.6 Calculations

Residence-time distribution (E) was calculated using equation 7-1 with the experimentally measured concentration data:

$$\mathbf{E} = E(t) = \frac{C(t)}{\int_0^\infty C(t)dt} \tag{7-1}$$

Experimental mean residence time, t_m, was calculated using equation 7-2.

$$t_{m,\exp t} = \frac{\int_0^\infty tC(t)dt}{\int_0^\infty C(t)dt} \tag{7-2}$$

Theoretical mean residence time for plug flow, $t_{m,pf}$, was calculated using the equation 7-3, where V is reactor volume (604 mL) and v is volumetric flow rate (mL/min) for the particular experiment:

$$t_{m,pf} = \mathrm{V/v} \tag{7-3}$$

In all of the experiments, there were differences between experimental and theoretical mean residence time. Specifically, the experimental mean residence time was always shorter than theoretical plug flow. This is indicative of stagnant regions within the reactor that reduce the effective volume of the reactor. To characterize this observation, the effective active reactor volume (V_{active}) was calculated using equation 7-4 for each experiment. This was then used in equation 7-5 to quantify the effective deadspace volume ($V_{deadspace}$) that characterizes the volume of stagnant regions within the reactor:

$$V_{active} = t_{m,expt} * \mathrm{v} \tag{7-4}$$

$$V_{deadspace} = \mathrm{V} - V_{active} = 604\ \mathrm{mL} - V_{active} \tag{7-5}$$

Variance (σ), which is an indication of spread of the residence time distribution, was calculated using equation 7-6.

$$\sigma^2 = \frac{\int_0^\infty (t - t_{m,\exp t})^2 C(t) dt}{\int_0^\infty C(t) dt} \tag{7-6}$$

For testing the dispersed plug flow or axial flow model against experimental RTD, the effective vessel dispersion number (**D**/*uL*) was calculated by substituting the above experimental values of $t_{m,expt}$ and σ^2 into van der Laan's equation[29] (equation 7-7).

$$\frac{\sigma^2}{t_{m,\exp t}^2} = 2\left(\frac{\mathbf{D}}{uL}\right) - 2\left(\frac{\mathbf{D}}{uL}\right)^2 \left[1 - e^{-uL/\mathbf{D}}\right] \tag{7-7}$$

It was found that all of the vessel dispersion values were quite low (<0.01), so the values were compared against the simplification of van der Laan's equation described by Levenspiel[30] (equation 7-8).

$$\frac{\sigma^2}{t_{m,\exp t}^2} = 2\left(\frac{\mathbf{D}}{uL}\right) \tag{7-8}$$

The van der Laan and simplified equations for effective dispersion number gave equal values in all cases.

Once the value for **D**/*uL* was established using the above equation, the experimental effective dispersion coefficient, $\mathbf{D_{eff}}$, was calculated by substituting in the tube length (L = 183 m) and linear velocity of fluid (u) for each experiment.

Dimensionless time was calculated using equation 7-9 for calculation of normalized RTD.

$$\theta = \frac{t}{t_{m,\exp t}} \tag{7-9}$$

Normalized RTD curves were calculated by equation 7-10 using the experimental values of dimensionless time and residence time distribution that were calculated above in equations 7-9 and 7-1.

$$\mathbf{E}_{\theta,\text{expt}} = t_{m,\text{exp}t} \cdot \mathbf{E} \tag{7-10}$$

Theoretical RTD curves based on the dispersion model were calculated using the experimentally determined values of dimensionless time (θ) and effective dispersion number (**D**/uL) from above in equation 7-11.

$$\mathbf{E}_{\theta,\text{model}} = \frac{1}{\sqrt{4\pi(\mathbf{D}/uL)}} \exp\left[-\frac{(1-\theta)^2}{4(\mathbf{D}/uL)}\right] \tag{7-11}$$

7.5 Results and Discussion

Mean residence time and variance results are tabulated in Table 7-1, and the residence time distribution curves at room temperature and 135°C are shown in Figure 7-3 and Figure 7-4 respectively.

A few general trends can be observed in the basic RTD curves shown in Figure 7-3 and Figure 7-4. The first primary RTD characteristic that will be discussed is the mean residence time. In all of the experiments, the observed mean residence time in the reactor ($t_{m,expt}$) was lower than the value calculated for theoretical plug flow ($t_{m,pf}$). In other words, the tracer was observed to move more quickly through the reactor than expected in all cases. This typically indicates that there are stagnant regions within the reactor that the tracer is bypassing, hence the shorter than expected residence time. The

difference between experimental and theoretical plug flow mean residence time ($t_{m,pf}$ - $t_{m,expt}$) for the different liquid systems at varying flow rate and temperature are shown in Figure 7-5 and Figure 7-6. From these figures, it is clear that the difference between experimental and theoretical plug flow mean residence time was affected by the type of liquid system, temperature and flow rate.

In terms of the different liquid systems, tracer moved fastest through the reactor with unreacted latex droplets, slightly slower with the aqueous salt solution, and slowest with the latex particles. In other words, mean residence time for the fully reacted latex particles gave the closest match to the theoretical mean residence time, while the aqueous salt solution and unreacted latex droplets deviated further from the theoretical value. In terms of temperature, tracer moved faster through the reactor at 135°C compared to the corresponding experiment at 25°C. This suggests that the stagnant regions in the reactor become more pronounced at higher temperature.

In terms of flow rate, the difference between experimental and theoretical mean residence time decreased as the flow rate increased. Notably, at the experimental conditions with the fastest flow rate (6.5 mL/min) and lower temperature (25°C), the experimental mean residence time matched very closely with the theoretical plug flow value for all three of the liquid systems.

Since the difference between experimental and theoretical plug flow mean residence time appears to be caused by stagnant zones in the reactor, it is of interest to know the volume that is being lost in these zones. This can be characterized by the effective active volume and effective deadspace volume within the reactor as described earlier. Deadspace volume values are shown in Figure 7-7 and Figure 7-8, where higher

deadspace volume indicates increased deviation from the expected mean residence time for plug flow.

Analogous to the mean residence time observations, the deadspace volume was lowest for latex particles, and it increased for aqueous salt solution and unreacted latex droplets respectively. It is possible that the deadspace observed in these experiments was caused by air pockets that form in the top portions of the reactor coils. The flow from the peristaltic pump is pulsatile by nature, and it is possible that air pockets form as liquid drains to the lower portion of the coils when the flow stops momentarily during the pulse. This would explain why the deadspace decreases as flow rate increases, as the faster flow is better able to fill in the air pockets. This effect may be exacerbated by the slightly lower viscosity of the monomer droplet mixture (~0.8 cP) compared to water, thus causing slightly higher deadspace as more liquid can drain to the lower portion of the coil when flow stops during the pulse. Likewise, the higher viscosity of the polymer particle mixture (~2 cP) could have the opposite effect which may explain the lower observed deadspace.

Table 7-1. Residence Time Distribution Data

Liquid System	Reactor Temp. (°C)	Flow Rate (mL/min)	Mean Residence Time (min)		V_{active}	$V_{deadspace}$	σ^2	D/uL	D_{expt} (m^2/s)
			Theoretical Plug Flow $t_{m,pf}$	Experimental $t_{m,expt}$					
NaCl Solution	25	6.50	92.9	91.5	594.8	9.2	8.9	0.00053	0.0032
		3.97	152.1	147.0	583.8	20.2	16.9	0.00039	0.0014
		2.31	261.5	248.5	574.0	30.2	25.3	0.00021	0.0004
	135	6.50	92.9	86.3	561.0	43.0	2.4	0.00016	0.0010
		3.97	152.1	140.2	556.5	47.5	3.9	0.00010	0.0004
		2.31	261.5	236.8	547.1	56.9	15.5	0.00014	0.0003
Latex Particle	25	6.50	92.9	92.5	601.4	2.6	18.1	0.00106	0.0064
		3.97	152.1	150.7	598.5	5.5	30.7	0.00068	0.0025
		2.31	261.5	258.7	597.5	6.5	42.8	0.00032	0.0007
	135	6.50	92.9	89.5	581.6	22.4	4.9	0.00031	0.0019
		3.97	152.1	145.9	579.3	24.7	9.1	0.00021	0.0008
		2.31	261.5	249.9	577.4	26.6	17.2	0.00014	0.0003
Latex Droplet	25	6.50	92.9	88.5	575.5	28.5	7.8	0.00050	0.0030
		3.97	152.1	142.9	567.1	36.9	33.2	0.00081	0.0030
		2.31	261.5	244.0	563.7	40.3	47.9	0.00040	0.0009
	135	6.50	92.9	85.6	556.6	47.4	4.8	0.00033	0.0020
		3.97	152.1	139.4	553.6	50.4	13.3	0.00034	0.0013
		2.31	261.5	235.2	543.4	60.6	17.1	0.00016	0.0003

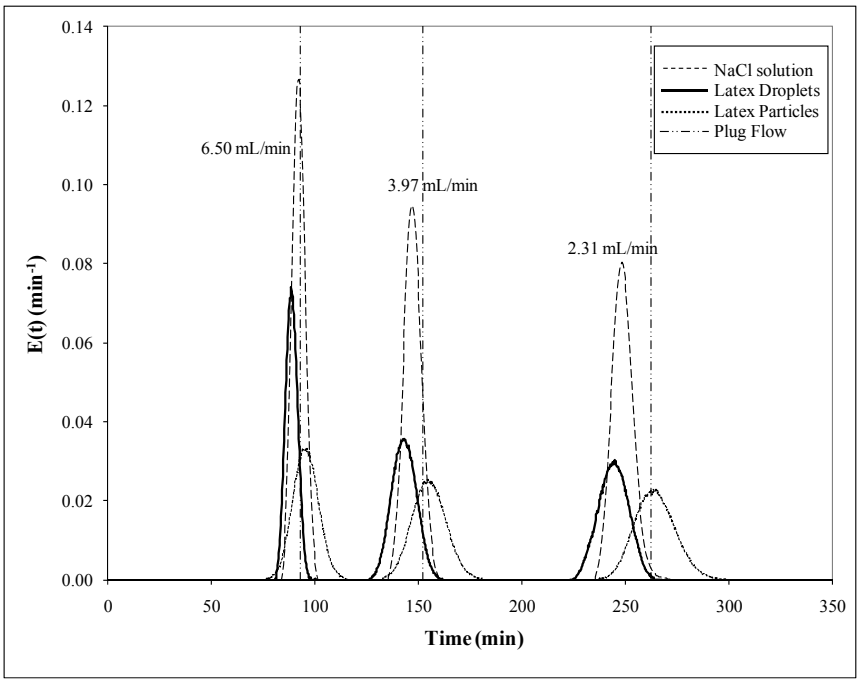

Figure 7-3. Residence Time Distribution at 25°C.

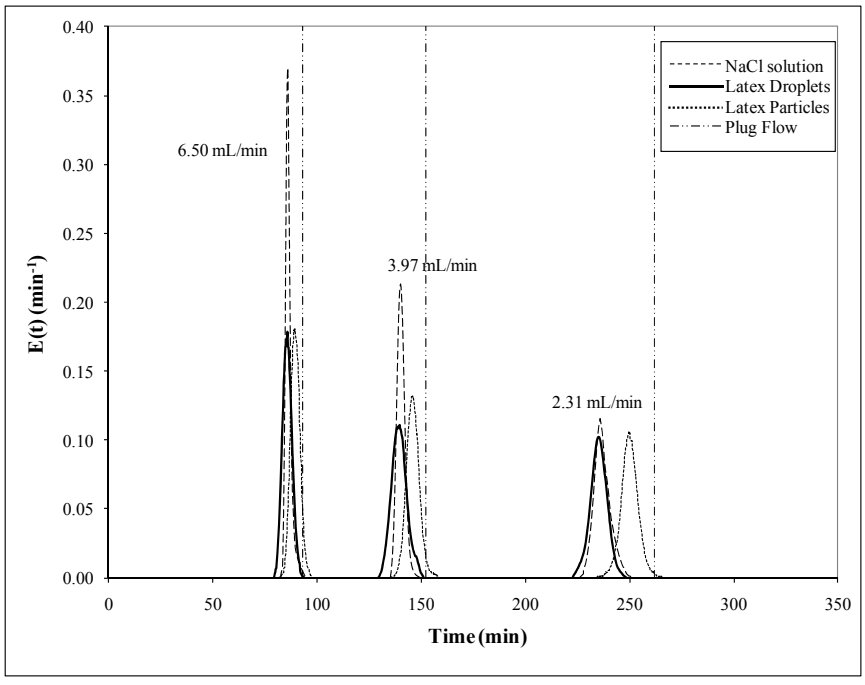

Figure 7-4. Residence Time Distribution at 135°C.

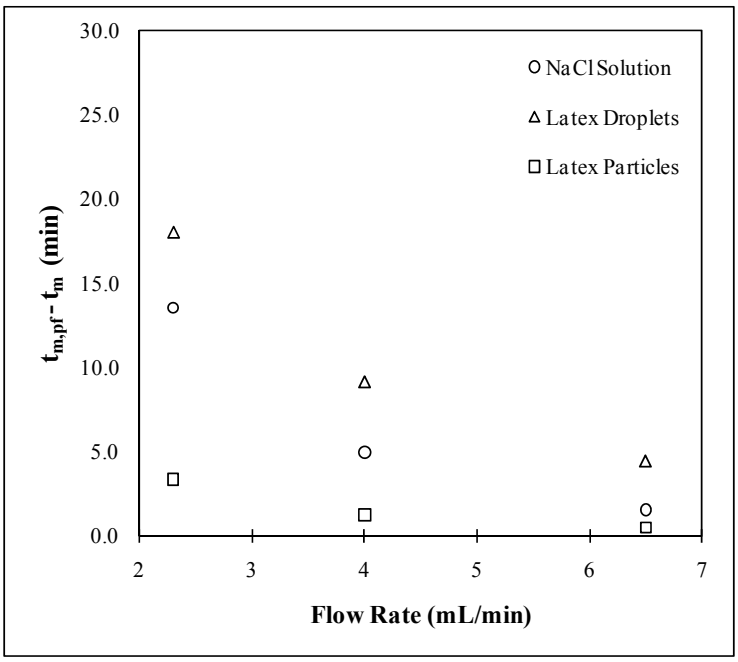

Figure 7-5. Difference between experimental (t_m) and theoretical plug flow ($t_{m,pf}$) mean residence time at 25°C.

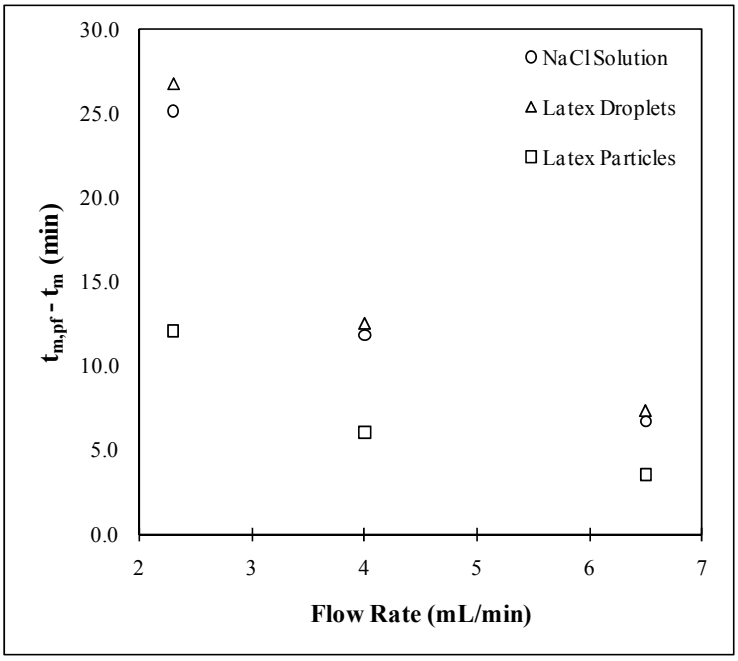

Figure 7-6. Difference between experimental (t_m) and theoretical plug flow ($t_{m,pf}$) mean residence time at 135°C.

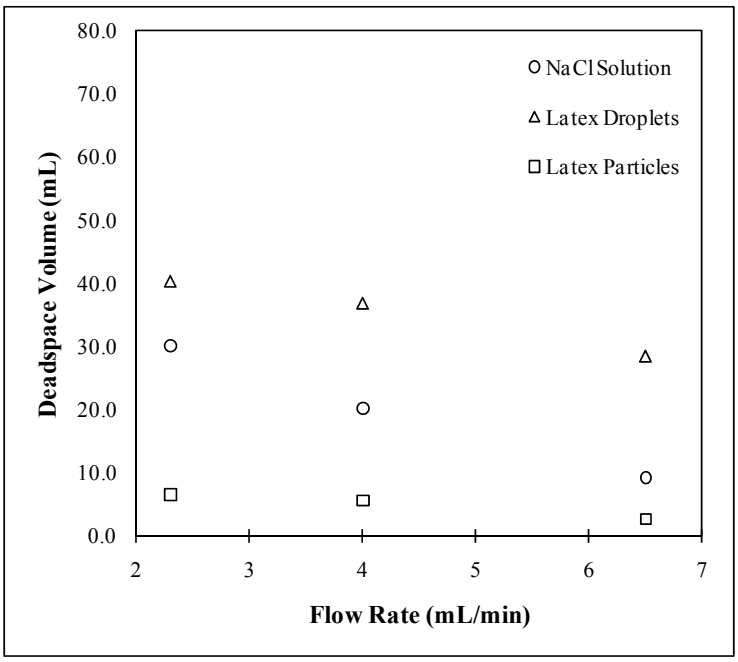

Figure 7-7. Deadspace volume versus flow rate at 25°C.

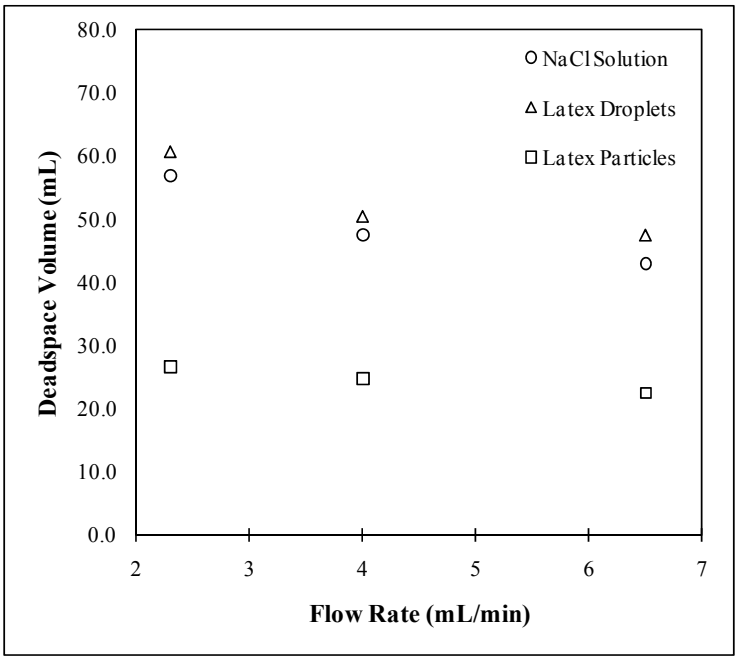

Figure 7-8. Deadspace volume versus flow rate at 135°C.

Deadspace volume increased approximately twofold for all systems when the reactor temperature was increased from 25°C to 135°C. The increase in deadspace due to

temperature increase is possibly due to liberation of nitrogen gas within the heated reactor causing gas pockets in the upper sections of the reactor coils. The reactant holding vessels at the inlet of the reactor are at room temperature and are pressurized to 650 kPa throughout the experiment. The following calculation assumes 650 kPa pressure throughout the reactor, although it should be noted that this will represent the upper limit as there will be a slight pressure drop along the reactor. Figure 7-9 indicates that the solubility of nitrogen in water is approximately 0.12 g N_2 per kg water at this condition.[31] When the water is exposed to 135°C in the reactor tube, the solubility of N_2 drops to approximately 0.05 g per kg water. Assuming that the ideal gas law is a reasonable approximation (compressibility factor for nitrogen is close to unity under these conditions),[32] then the density of nitrogen at 650 kPa and 135°C is approximately 5.4 g/L. If one assumes that two reactor volumes of liquid are used during each experiment (one volume for initial reactor fill plus one volume for the tracer to pass through the reactor), then approximately 1.2 L of liquid pass through the reactor during one tracer experiment. This is a conservative estimate, because usually excess material was passed through the reactor during the initial filling step. Based on these solubility, density and liquid volume values, it is calculated that at least 16 mL of nitrogen would be released from the water as it moves through the heated reactor. This corresponds reasonably with the increase in deadspace volume that is observed in all of the systems as they move from room temperature to 135°C.

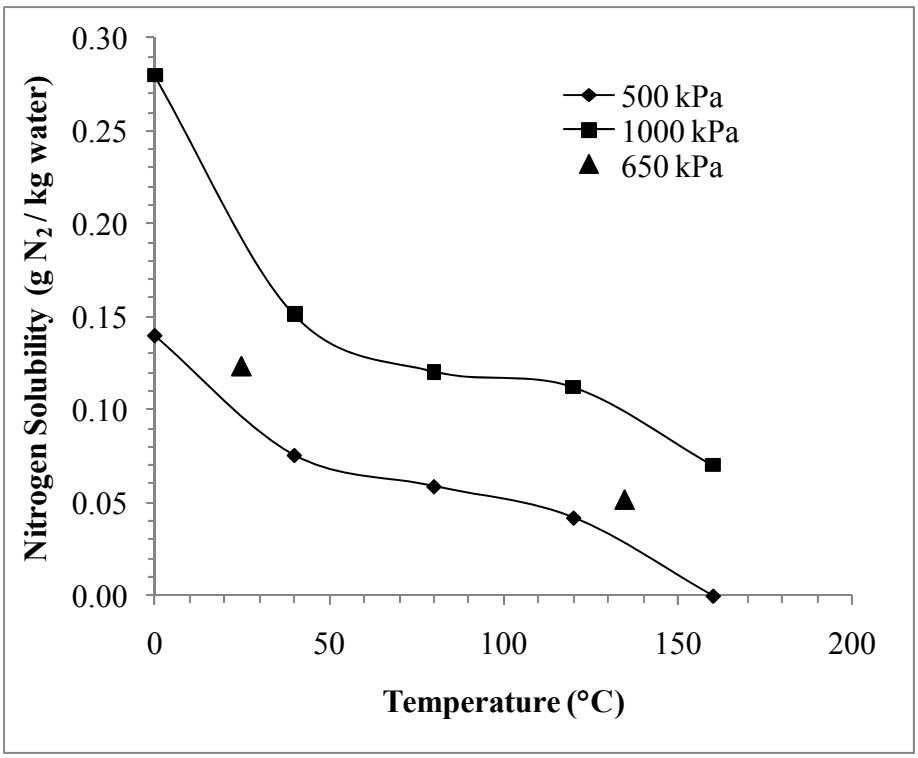

Figure 7-9. Solubility of nitrogen in water. Values at 650 kPa are interpolated from values at 500 and 100 kPa.

The smallest observed deadspace volume was for the latex particle experiments at room temperature. In this case, deadspace volume was only approximately 3 mL for the fastest flowrate, and this is less than 1% of the total reactor volume. Mean residence times in these experiments were very close to the theoretical plug flow value.

On the other end of the spectrum, the highest deadspace volume values were observed for unreacted latex droplets at 135°C and the lowest flowrate. In this case, the observed deadspace volume was 60.6 mL which is almost 10% of the total reactor volume. Corresponding to this, the experimental mean residence time for the unreacted latex droplets at this condition is approximately 27 minutes faster than the mean residence time for theoretical plug flow. This set of experimental conditions represents the actual conditions that would be used for a typical NMP experiment, and this shows

that the initial reactants will be in the reactor for a shorter time than the theoretically calculated value. Fully reacted latex particles at these conditions are closer to the theoretical plug flow than the unreacted latex droplets, but there is still a significant deviation. Deadspace volume was approximately 17.4 mL, and experimental mean residence time was about 8 minutes faster than theoretical plug flow. Since the unreacted latex droplets are polymerizing and turning into latex particles in a real reactor, one would expect the deadspace volume and experimental mean residence time to fall somewhere between the values described above. Since the reactants and product of this reaction spend less time than expected in the tubular reactor, this helps to explain why conversion results were lower than corresponding batch reactions in initial experiments with this system.[14]

The previous discussion focused on mean residence time, particularly the observed difference between the values for experimental data ($t_{m,expt}$) and theoretical plug flow ($t_{m,pf}$). The other primary descriptive characteristic for RTD is variance (σ) which indicates the broadness of the RTD. There were some general trends in RTD broadness between the various liquid systems that can be observed in the general RTD curves in Figure 7-3 and Figure 7-4. The specific RTD variance values are shown in Figure 7-10 and Figure 7-11. The smallest variance and narrowest distributions were observed for the aqueous salt solution, followed by unreacted latex droplets which showed slightly broader distribution, then latex particles which showed significantly broader distribution. At higher temperature, the variance was much lower giving a significantly narrower distribution in all cases. Variance decreased as the flow rate increased, and this is the same general trend observed in historical studies with helically coiled tubes where the

variance decreased with increased Dean number. In this set of experiments, the coil-to-tube diameter aspect ratio was constant, so increased flow rate is directly proportional to increased Dean number. Reduced variance should also be expected at higher flow rate because the tracer is resident in the reactor for a shorter period of time and therefore has a less time in which to spread.

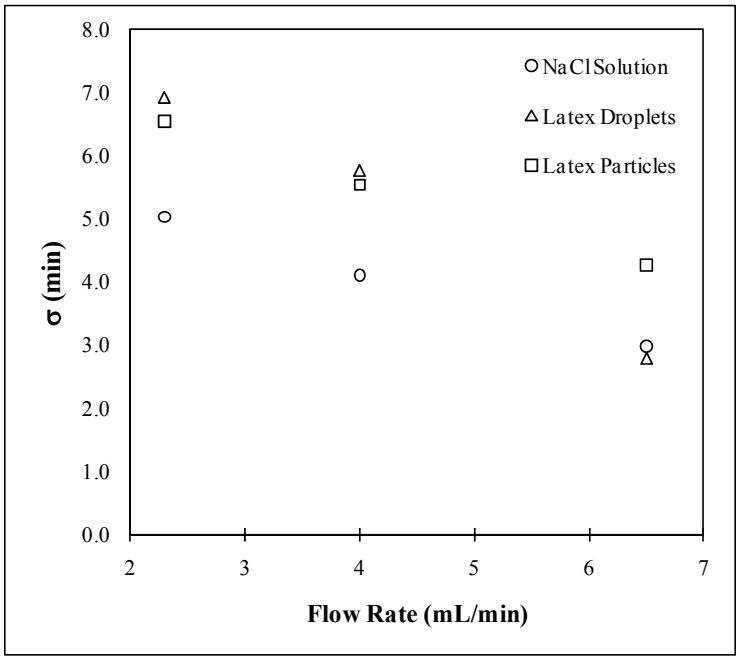

Figure 7-10. Experimental RTD variance versus flow rate at 25°C.

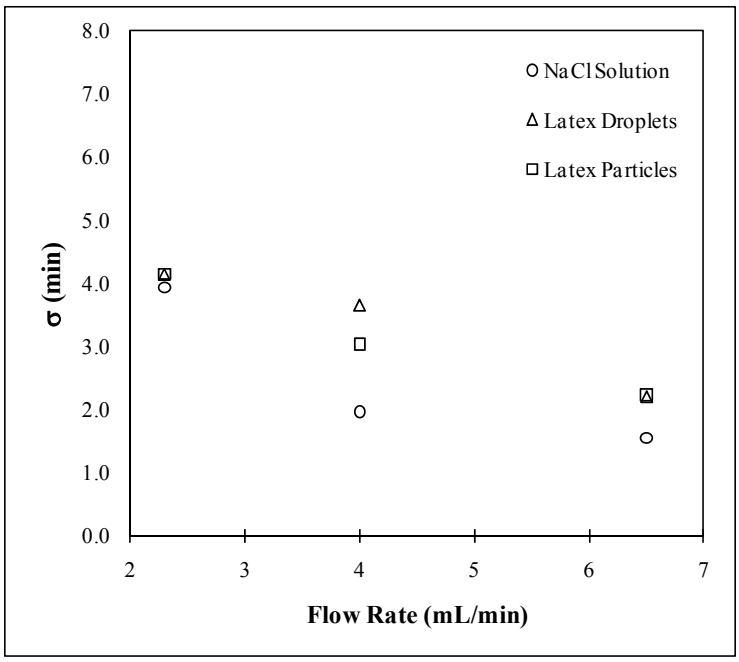

Figure 7-11. Experimental RTD variance versus flow rate at 135°C.

Another interesting piece of information is the effective dispersion which accounts for both the variance and the mean residence time. Experimental variance and mean residence time values were used to calculate effective vessel dispersion number ($\mathbf{D}/uL$) for each experimental condition, and then this was used to calculated effective dispersion coefficient ($\mathbf{D}_{eff}$) using the reactor length (L) along with the linear flow rate (u) at each condition. Results are shown in Figure 7-12 and Figure 7-13.

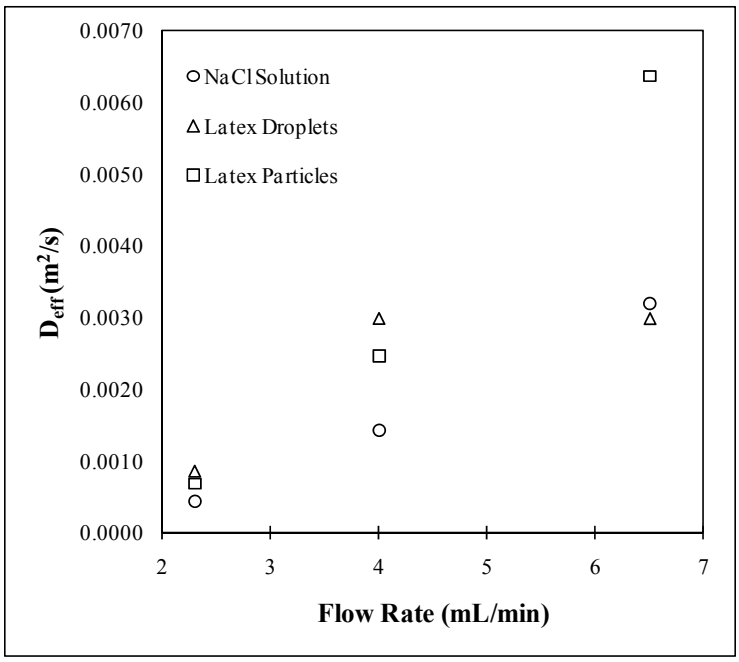

Figure 7-12. Effective dispersion coefficient versus flow rate at 25°C.

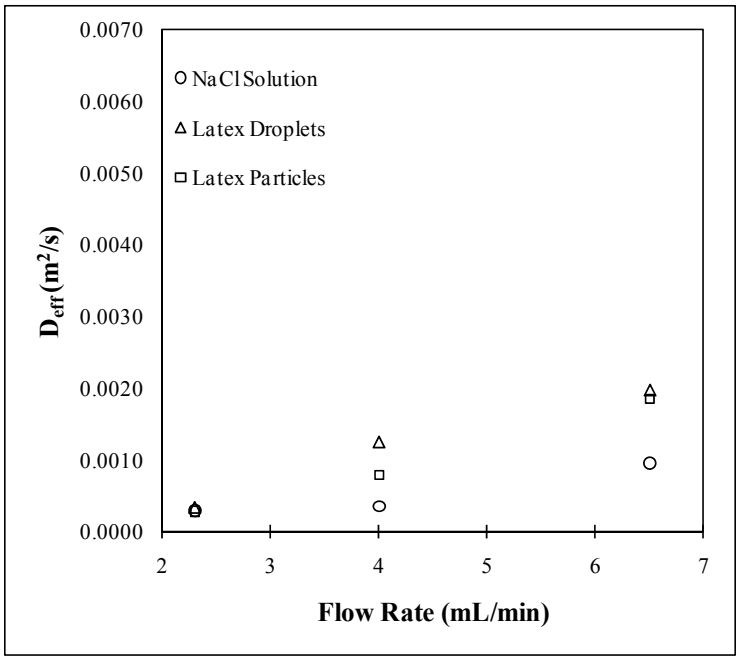

Figure 7-13. Effective dispersion coefficient versus flow rate at 135°C.

In general, the effective dispersion coefficient increased as flow rate increased and as temperature decreased. At room temperature, $\mathbf{D_{eff}}$ was essentially equal for all

three liquid systems at the lowest feed rate (2.3 mL/min). As flow rate increased, $\mathbf{D_{eff}}$ increased linearly for the NaCl salt solution and latex particles, and the latex particles had significantly higher $\mathbf{D_{eff}}$ at the fastest flowrate. Unreacted latex droplets increased initially as flowrate increased, but seemed to plateau as the flowrate increased further. At high temperature, $\mathbf{D_{eff}}$ was also approximately equal for all three liquid systems at the lowest flowrate, and the value was slightly lower than at room temperature. There was a modest linear increase in $\mathbf{D_{eff}}$ for all three liquid systems as flow rate increased, and the values were substantially lower than the corresponding values at room temperature. The lowest $\mathbf{D_{eff}}$ values were observed at high temperature (135°C) and the lowest flowrate (2.3 mL/min), which corresponds to conditions that would be used for a real polymerization reaction with this system. At this set of conditions, the $\mathbf{D_{eff}}$ values were essentially equal for aqueous salt solution, unreacted latex droplets and latex particles. This indicates that at real polymerization conditions, the "tightness" of the experimental RTD approaches ideal plug flow conditions more than any of the other experimental conditions that were tested.

The observed increase in $\mathbf{D_{eff}}$ as flow rate increases would be expected for flow in straight circular pipes (i.e., as Reynolds number increases due to increased flow rate).[33] Similarly, higher $\mathbf{D_{eff}}$ is expected for higher viscosity materials (i.e., as Reynolds number decreases due to increased viscosity), so the differences in $\mathbf{D_{eff}}$ between the three mixtures can potentially be explained by the viscosity differences.

It is possible that $\mathbf{D_{eff}}$ does not increase as fast for the aqueous NaCl system because secondary flow patterns due to the coiled configuration are more pronounced compared to the latex systems and therefore the dispersion is dampened. The density

differences between phases in the latex systems (i.e., $d_{styrene}$ = 0.909 g/cm^3; $d_{polystyrene}$ = 1.05 g/cm^3) could shift the monomer droplets and particles into different regimes of the secondary flow, thus causing the faster increase in dispersion as flow rate increases.

In many real experimental systems, the RTD can be approximated using the dispersion model. Comparisons of the experimental data versus the dispersion model are shown in Figure 7-14 through Figure 7-19.

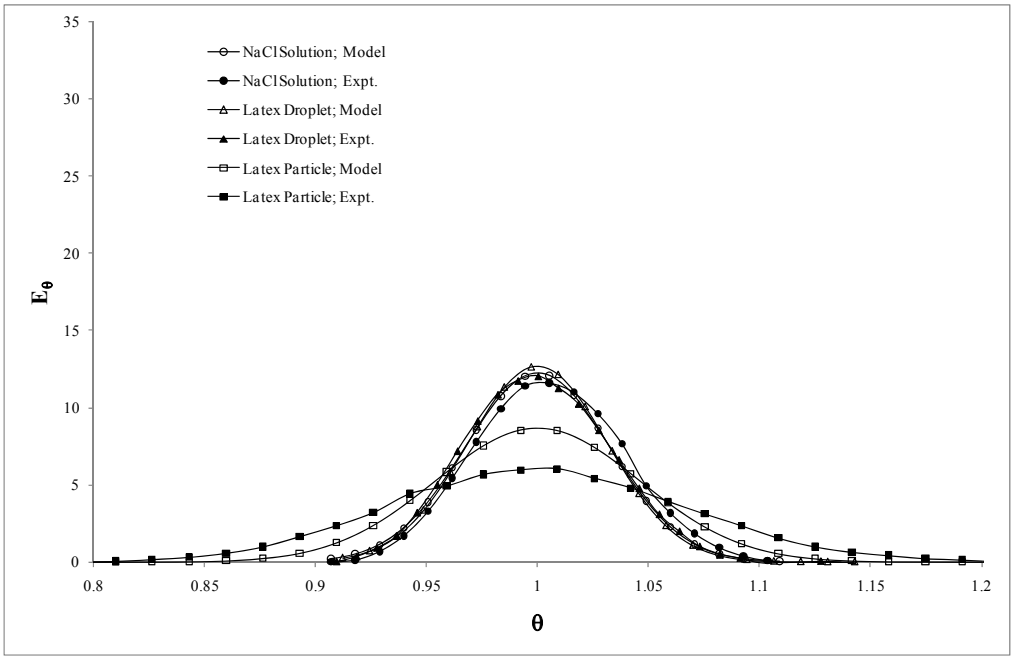

Figure 7-14. Dispersion model versus experimental RTD: 6.5 mL/min at 25°C.

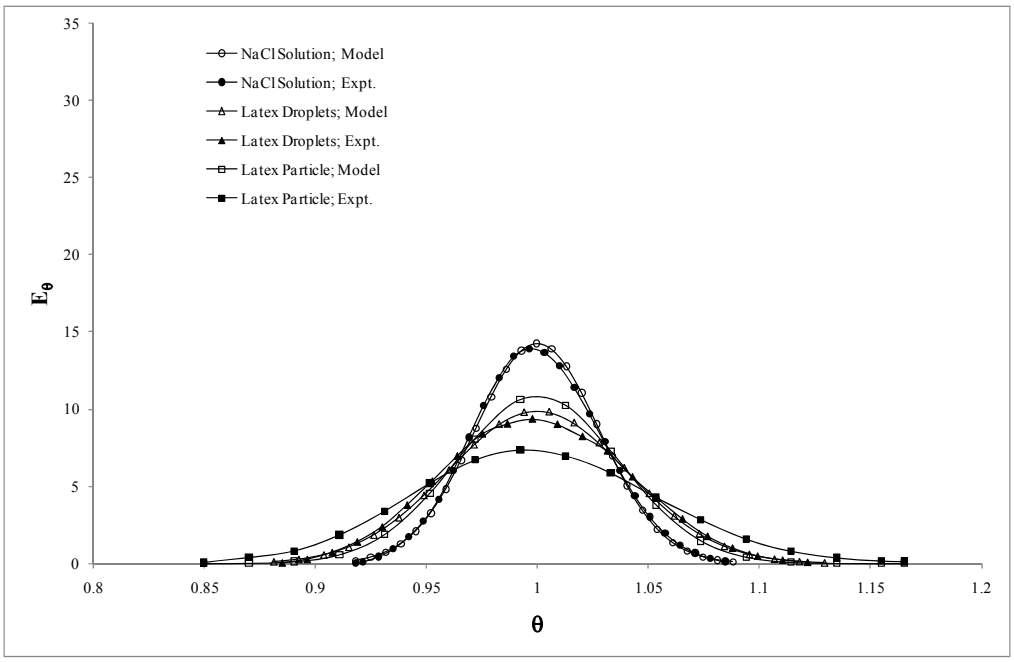

Figure 7-15. Dispersion model versus experimental RTD: 4.0 mL/min at 25°C.

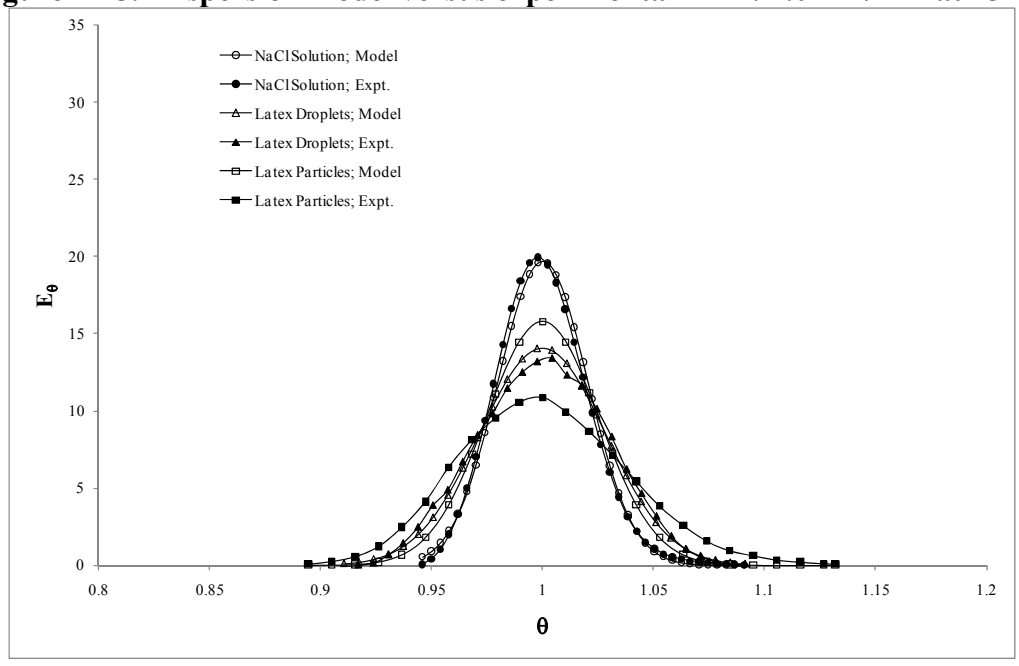

Figure 7-16. Dispersion model versus experimental RTD: 2.3 mL/min at 25°C.

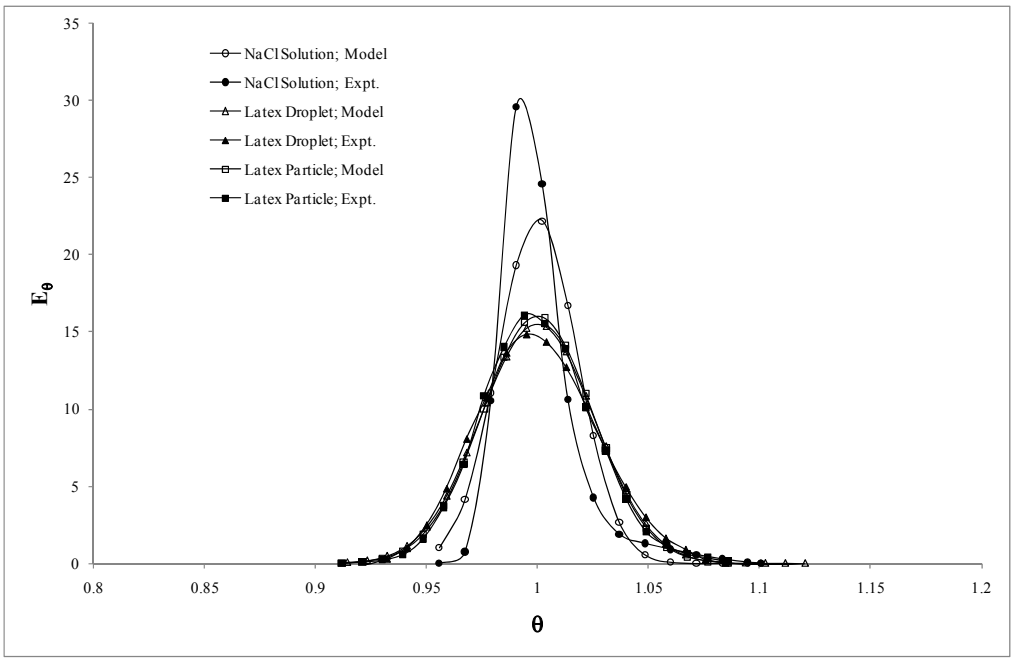

Figure 7-17. Dispersion model versus experimental RTD: 6.5 mL/min at 135°C.

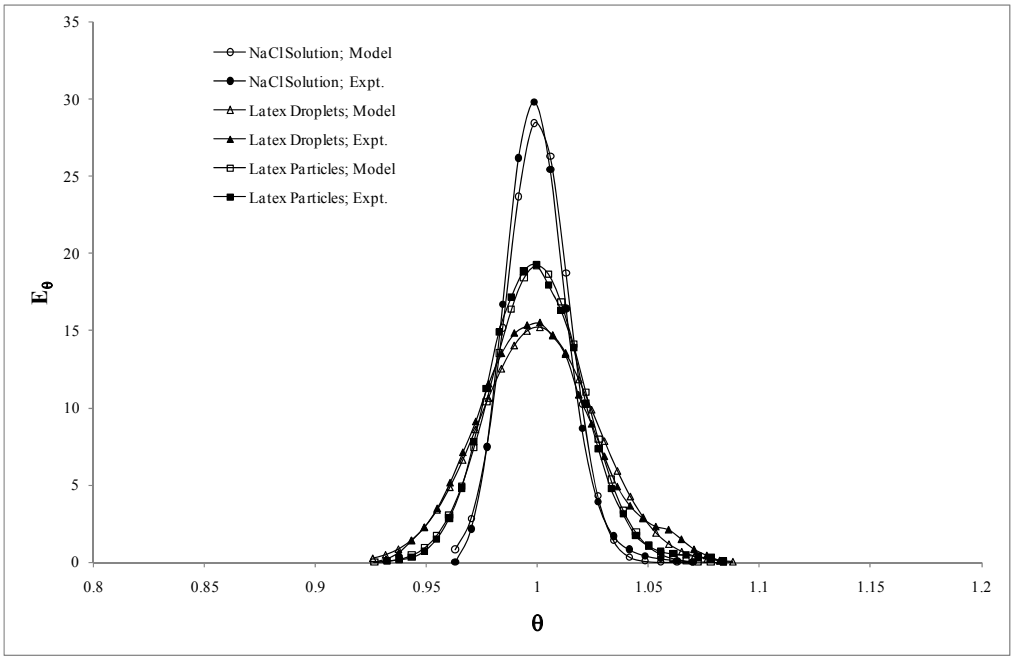

Figure 7-18. Dispersion model versus experimental RTD: 4.0 mL/min at 135°C.

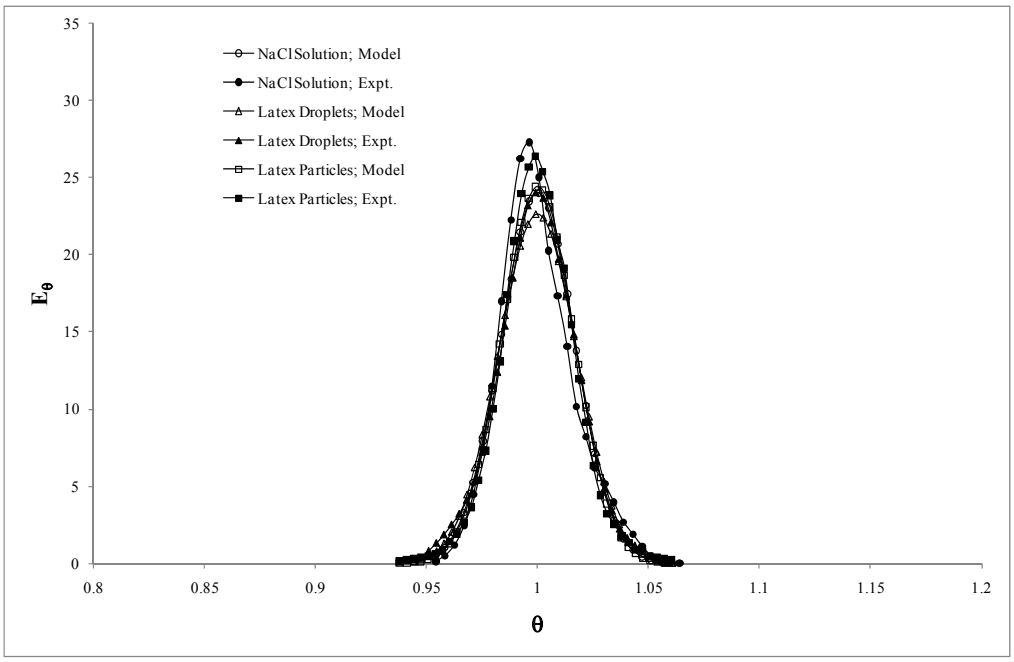

Figure 7-19. Dispersion model versus experimental RTD: 2.3 mL/min at 135°C.

For the aqueous salt solution experiments, the dispersion model (open circles) fits the experimental data (filled circles) very well for all cases except one. At high temperature (135°C) and the fastest flowrate (6.5 mL/min), the experimental data shows a slightly narrower distribution than the model and it is skewed with a tail on the right side of the curve (Figure 7-17). This behavior is known to occur when unstable flow conditions are imparted on a tubular system due to the experimental technique or apparatus, such as unstable tracer injection, non-ideal connections between pieces, changes in internal diameter, etc.[34] It is possible that a minor experimental deviation caused the effect in this case.

For the unreacted latex droplets, the dispersion model (open triangles) fits the experimental data (filled triangles) for all cases. There is a very close match between theory and experiment at all of the flow rates tested at high and low temperature.

For latex particles, the dispersion model (open squares) fits the experimental data (filled squares) very well for all of the experiments that were done at high temperature. However, the model does not fit the experimental data well for the room temperature experiments. In all of the room temperature experiments, the data is observed to have a significantly broader distribution than the predicted dispersion model. Some aspect of the latex particle mixture causes the RTD to assume a non-Gaussian distribution at room temperature, and this effect is eliminated at higher temperature where the normal Gaussian shape is observed.

It is interesting to note that at the high temperature and slowest flowrate condition, the normalized RTD curves for all of the liquid systems fall almost on top of each other and demonstrate a very good fit with the dispersion model prediction. These RTD curves showed the narrowest distributions, approaching the ideal plug flow case. This set of experimental conditions represents typical real reaction conditions for our NMP polymerization system. Since the RTD is very narrow for all of the liquid systems, this explains why molecular weight distribution remains narrow in the tubular reactor compared to batch reactor. As explained previously, the kinetic scheme of this system is such that broadening of the RTD would result in broadening of the molecular weight distribution of the final product.

7.6 Conclusions

Residence time distribution tracer studies were done to compare a homogeneous NaCl solution with heterogeneous monomer droplet and polymer particle latexes at room temperature and 135°C. All of the systems showed variation from the theoretical mean residence time for an ideal plug flow system. Mean residence time was shorter than

predicted in all cases, indicating that tracer was bypassing stagnant regions within the reactor. All of the liquid systems demonstrated broadening of the RTD curves to varying degree depending on the flow rate, temperature, and specific liquid system. Similar differences were observed for the effective vessel dispersion numbers (**D**/*uL*) and effective dispersion coefficients ($\mathbf{D_{eff}}$) under varying conditions. In most cases, the RTD could be modeled using the dispersion model, except in the case of polymer particles at room temperature which showed a broader distribution than the model.

At the standard polymerization conditions for this NMP system, the normalized RTD curves for all of the liquid systems were narrowest and approached the tightness of a plug flow system. This explains why molecular weight distribution remains narrow in our tubular reactor experiments and comparable to analogous experiments in batch reactors. However, at real polymerization conditions, the deadspace volume and deviation from theoretical mean residence time is greatest. That is, the material is in the reactor for a significantly shorter period of time than expected based on calculation. This explains why polymer conversion was lower than expected in earlier tubular reactor experiments compared to batch.

7.7 References

1. Georges, M. K.; Veregin, R. P. N.; Kazmaier, P. M.; Hamer, G. K. *Macromolecules*. **1993**, *26*, 2987.

2. Moad, G.; Solomon, D.H. *The Chemistry of Radical Polymerization, 2nd. Ed.* ; Elsevier Ltd.: UK, 2006.

3. Hawker, C. J.; Bosman, A. W.; Harth, E. *Chem. Rev*. **2001**, *101*, 3661.

4. Sciannamea, V.; Jerome, R.; Detrembleur, C. *Chem. Rev.* **2008**, *108*, 1104.

5. Matyjaszewski, K.; Xia, J. *Chem. Rev*. **2001**, *101*, 2921.

6. Kamigaito, M.; Ando, T.; Sawamoto, M. *Chem. Rev.* **2001**, *101*, 3689.

7. Moad, G.; Rizzardo, E.; Thang, S. H. *Aust. J. Chem*., **2005**, *58*, 379.

8. Moad, G.; Rizzardo, E.; Thang, S. H. *Aust. J. Chem*., **2006**, *59*, 669.

9. Destarac, M. *Macromol. React. Eng.* **2010**, *4*, 165.

10. Cunningham, M. F. *Prog. Poly. Sci.* **2008**, *33*, 365.

11. Zetterlund, P.B.; Kagawa, Y.; Okubo, M. *Chem. Rev.* **2008**, *108*, 3747.

12. Enright, T. E "*Living Radical Polymerization"*, in: *Micro Process Engineering, Vol. 2,* V. Hessel, A. Renken, J. C. Schouten, J.-I. Yoshida, Eds.; WILEY-VHC Verlag GmbH & Co. KgaA, Weinheim 2009, p. 199.

13. Enright, T. E.; Cunningham, M. F.; Keoshkerian, B. *Polym. React. Eng.* **2010**, *4*, 186.

14. Enright,T. E.; Cunningham, M. F.; Keoshkerian, B. Macromol. *Rapid Commun.* **2005**, *26*, 221.

15. Russum, J. P.; Jones, C. W.; Schork, F. J. *AIChE Journal* **2006**, *52*, 1566.

16. Taylor, G. I. *Proc. Roy. Soc.* **1953**, *A219*, 186.

17. Aris, R. *Proc. Roy. Soc.* **1956**, *A235*, 67.

18. Dean, W. R. *Phil. Mag.* **1927**, *4*, 208.

19. Dean, W. R. *Phil. Mag.* **1928**, *5*, 673.

20. Truesdell, L. C.; Adler, R. J. *AIChE J.* **1970**, *16*, 1010.

21. Ruthven, D. M. *Chem. Eng. Sci.* **1971**, *26*, 1113.

22. Nauman, E. B. *Chem. Eng. Sci.* **1977**, *32*, 287.

23. Trivedi, R. N.; Vasudeva, K. *Chem. Eng. Sci.* **1974**, *29*, 2291.

24. Trivedi, R. N.; Vasudeva, K. *Chem. Eng. Sci.* **1975**, *30*, 317.

25. Tijssen, R. *Analytica Chimica Acta* **1980**, *114*, 71.

26. Ranade, V. R.; Ulbrecht, J. J. *Chem. Eng. Commun.* **1981**, *8*, 165.

27. Saxena, A. K.; Nigam, K. D. P. *J. Appl. Polym. Sci.* **1981**, *26*, 3475.

28. MacLeod, P.J.; Barber, R.; Odell, P.G.; Keoshkerian, B.; Georges, M.K. *Macromol. Symp.* **2000**, *155*, 31.

29. Van der Laan, E. T. *Chem. Eng. Sci.* **1958**, *7*, 187.

30. Levenspiel, O. "*Chemical Reaction Engineering, Vol. 3"*; John Wiley and Sons, Inc., NJ 1999, p. 296.

31. Sun, R.; Hu, W.; Duan, Z. *J. Solution Chem.* **2001**, *30*, 561.

32. Alberty, R.A. "*Physical Chemistry, 7th Ed."*; John Wiley and Sons, Inc., NY 1987, p. 9.

33. Richardson, J. F.; Peacock, D. G. "*Coulson and Richardson's Chemical Engineering, Vol. 3, 3rd Ed., Chemical and Biochemical Reactors and Process Control"*; Elsevier Science Inc., NY 1994, p. 97.

34. Sternberg, J.C. *Adv. Chromatogr.* **1966**, *2*, 205.

Chapter 8

Summary and Conclusions

A continuous tubular reactor was designed and built that could be used to produce living polymers via nitroxide-mediated bulk and miniemulsion polymerization processes, and a comparison was made with analogous polymers made in a batch reactor. The main conclusions from this research are as follows.

A number of interesting observations were made during the initial scoping experiments. Temperature ramping rate is a critical factor in ensuring that polymerization is controlled during TEMPO-mediated miniemulsion polymerization of styrene. Slow temperature ramping can cause loss of control of the polymerization, and this must be considered when scaling up to larger reactors where fast temperature ramps may not be possible. In some cases, ascorbic acid could be used to mitigate this effect and controlled NMP reactions were possible with slow temperature ramps. However, it was also found that ascorbic acid can cause room temperature initiation of polymerization under in some cases. This seems to be a redox initiation reaction that occurs sometimes in the presence of SDBS surfactant.

It was demonstrated that TEMPO-mediated styrene miniemulsion polymerization can produce living polymer latexes that can be chain extended with more styrene. Initial experiments indicated that the reaction proceeded slightly slower in the continuous reactor compared to a batch reactor. It was further demonstrated that the miniemulsion latex can be chain extended with n-butyl acrylate to produce diblock copolymer, and then further chain extended with more styrene to create triblock copolymer. However, as the number of chain extension steps increased, the degree of livingness decreased in the system. This resulted in a mixture of living and dead diblock and triblock copolymers.

Residence time distribution tracer studies indicated that there is a significant difference in flow patterns between aqueous salt solution, unreacted latex (monomer droplets in water), and final product latex (polymer particles in water). In all cases there were dead zones present in the reactor which means that tracer flowed through the reactor faster than expected based on plug flow conditions. This explained why reaction rates appeared to be slightly slower in the continuous reactor compared to batch, since the material was in the reactor for a shorter time than assumed. Differences in RTD variance and dispersion were observed depending on the specific mixture, flow rate, and temperature. At the real NMP reaction conditions (high temperature and low flow rate), variance and dispersion was lowest and was approximately the same for all of the mixtures. At this condition, the RTD was very narrow, approaching plug flow, and this is why molecular weight distribution was similar for experiments that were done in the continuous tubular reactor compared to the batch reactor.

There are still some challenges that need to be overcome to bring this technology to a fully continuous state. The intermediate dispersion step to produce the unreacted latex is currently done using a homogenizer in batch-mode. However, this homogenizer could be used in continuous-mode given that the feed rates of the bulk and miniemulsion polymerization steps are coordinated appropriately. There is also potential for investigating alternative continuous dispersion methods such as inline mixers and rotor-stator devices that have shown some promise in this area. The idea of installing inlet ports along the length of the reactor for introducing new feed streams also needs further investigation to determine the feasibility of producing specialty materials such as block copolymers in a completely continuous mode.

Ultimately, this study has proven the feasibility and laid the groundwork for a continuous controlled radical miniemulsion polymerization system. More work needs to be done to refine the technology, but this study provides a framework for a method that provides a relatively inexpensive alternative to a typical batch autoclave system.

Chapter 9

Recommendations for Future Work

1. Investigation of inline homogenization should be done to make this a fully continuous process. It is possible that a rotor-stator homogenizer, micromixer, sonicator, or a combination of these could be added in-line between the step 1 bulk polymerization and step 3 miniemulsion polymerization steps.
2. Longer term reactions should be done to determine if the NMP reaction will remain stable over the long term. Also, this will show whether or not the miniemulsion remains stable over the long term such that fouling does not build up in the reactor.
3. Further examination of the effect of ascorbic acid with SDBS surfactant should be done. It is not yet fully understood why some reactions proceeded under controlled conditions at high temperature while others reacted in an uncontrolled manner at room temperature. This study could be done in a Design of Experiments fashion using factors such as reactant concentration in both the bulk and miniemulsion step (ascorbic acid, SDBS, initiator, TEMPO), conversion/molecular weight of the bulk prepolymer, excess TEMPO as a reactant, number of passes through homogenizer, addition of ascorbic acid before or after homogenizing, etc.
4. Further testing of the reaction conditions should be explored to determine if there is a more optimum operating condition for this particular reaction. For example, there should be experiments at a range of temperature, initiator concentration, TEMPO concentration, solids loading, etc.
5. This study focused specifically on a TEMPO-based NMP system with styrene, along with some initial scoping work with n-butyl acrylate copolymerization. Testing of other monomers and nitroxides should be done to determine the flexibility of this process to accommodate other materials.

6. Different geometry of the reactor should be investigated to determine the effect on residence time distribution. It may be possible that the dead zones could be reduced or eliminated by turning the reactor on its side or by ensuring that the material is flowing primarily upwards or downwards, etc. Different sized tubing could also be tested.
7. One extension of the residence time distribution study is that a similar tracer experiment could be done with a fully reacting system as opposed to the two extremes that were tested in this study (i.e., unreacted versus fully reacted system). In this case, excess TEMPO would not be added to the unreacted latex before the tracer study, and the reaction would be allowed to proceed throughout the test.
8. Another extension of the RTD study would be to use an oil soluble tracer (e.g., Sudan Black) instead of the water soluble tracer that was used in this study. This would show if there are any differences in RTD between the aqueous phase and organic phase.
9. Do a sequential tracer study to determine if gas buildup in the tubular reactor continues to change the RTD over time. That is, do an initial tracer pulse as described in this study, then continue the experiment and do a second tracer pulse later in the experiment and perhaps more pulses. This would be useful for demonstrating if the reactor reaches some type of steady state with respect to nitrogen gas being trapped in the reactor versus being expelled at the outlet.